AFWL-TR-87-112

AFWL-TR-
87-112

CHEMICAL GENERATION OF NITROGEN METASTABLES

R. D. Coombe

University of Denver
University Park
Denver, CO 80208-0179

September 1988

Final Report

AIR FORCE WEAPONS LABORATORY
Air Force Systems Command
Kirtland Air Force Base, NM 87117-6008

AFWL-TR-87-112

This final report was prepared by University of Denver, Denver, Colorado, under Contract F29601-84-C-0094, Job Order 33261W15 with the Air Force Weapons Laboratory, Kirtland Air Force Base, New Mexico. Mr. Leonard Hanko (ARBI) was the Laboratory Project Officer-in-Charge.

When Government drawings, specifications, or other data are used for any purpose other than in connection with a definitely Government-related procurement, the United States Government incurs no responsibility or any obligation whatsoever. The fact that the Government may have formulated or in any way supplied the said drawings, specifications, or other data, is not to be regarded by implication, or otherwise in any manner construed, as licensing the holder, or any other person or corporation; or as conveying any rights or permission to manufacture, use, or sell any patented invention that may in any way be related thereto.

This report has been authored by a contractor of the United States Government. Accordingly, the United States Government retains a nonexclusive, royalty-free license to publish or reproduce the material contained herein, or allow others to do so, for the United States Government purposes.

This report has been reviewed by the Public Affairs Office and is releasable to the National Technical Information Service (NTIS). At NTIS, it will be available to the general public, including foreign nationals.

If your address has changed, if you wish to be removed from our mailing list, or if your organization no longer employs the addressee, please notify AFWL/ARBI, Kirtland AFB, NM 87117-6008 to help us maintain a current mailing list.

This report has been reviewed and is approved for publication.

Leonard Hanko

LEONARD HANKO
Project Officer

FOR THE COMMANDER

Gerald A Hasen
GERALD A. HASEN
Lt Colonel, USAF
Chief, Advanced Chemical Laser Branch

HARRO ACKERMANN
Lt Colonel, USAF
Chief, Laser Science & Technology Office

DO NOT RETURN COPIES OF THIS REPORT UNLESS CONTRACTUAL OBLIGATIONS OR NOTICE ON A SPECIFIC DOCUMENT REQUIRES THAT IT BE RETURNED.

UNCLASSIFIED
SECURITY CLASSIFICATION OF THIS PAGE

AD-A201 225

REPORT DOCUMENTATION PAGE

1a. REPORT SECURITY CLASSIFICATION Unclassified	1b. RESTRICTIVE MARKINGS
2a. SECURITY CLASSIFICATION AUTHORITY	3. DISTRIBUTION / AVAILABILITY OF REPORT Approved for public release; distribution unlimited.
2b. DECLASSIFICATION / DOWNGRADING SCHEDULE	
4. PERFORMING ORGANIZATION REPORT NUMBER(S)	5. MONITORING ORGANIZATION REPORT NUMBER(S) AFWL-TR-87-112
6a. NAME OF PERFORMING ORGANIZATION University of Denver 6b. OFFICE SYMBOL (If applicable)	7a. NAME OF MONITORING ORGANIZATION Air Force Weapons Laboratory
6c. ADDRESS (City, State, and ZIP Code) University Park Denver, CO 80208-0179	7b. ADDRESS (City, State, and ZIP Code) Kirtland Air Force Base, NM 87117-6008
8a. NAME OF FUNDING / SPONSORING ORGANIZATION 8b. OFFICE SYMBOL (If applicable)	9. PROCUREMENT INSTRUMENT IDENTIFICATION NUMBER F29601-84-C-0094
8c. ADDRESS (City, State, and ZIP Code)	10. SOURCE OF FUNDING NUMBERS PROGRAM ELEMENT NO. 62601F; PROJECT NO. 3326; TASK NO. 1W; WORK UNIT ACCESSION NO. 15

11. TITLE (Include Security Classification)
CHEMICAL GENERATION OF NITROGEN METASTABLES

12. PERSONAL AUTHOR(S)
Coombe, R. D.

13a. TYPE OF REPORT	13b. TIME COVERED	14. DATE OF REPORT (Year, Month, Day)	15. PAGE COUNT
Final	FROM 1 Sep 84 TO 30 Apr 87	1988 September	114

16. SUPPLEMENTARY NOTATION

17. COSATI CODES			18. SUBJECT TERMS (Continue on reverse if necessary and identify by block number)
FIELD	GROUP	SUB-GROUP	Nitrogen, Metastables, Excited States, Interhalogens, Chemiluminescence, Kinetics, Lasers
18	05		
20	11		

19. ABSTRACT (Continue on reverse if necessary and identify by block number)

A number of chemical reactions were investigated as potential sources of $N_2(A^3\Sigma_u^+)$ metastables for use in proposed chemical laser systems. Candidate reactions were chosen on the basis of angular momentum constraints which should drive them to produce electronically excited N_2. Though exothermic, the $N(^4S) + NF(a^1\Delta)$ reaction is slower than expected, with a rate constant $< 5 \times 10^{-12} cm^3 s^{-1}$. The $N(^4S) + N_3(^2\Pi_g)$ reaction produces N_2 ($B^3\Pi_g$, $W^3\Delta_u$) in high yield as predicted by angular momentum correlations. The photon yield for N_2 B→A chemiluminescence in this system is about 20 percent. The rate constant of the $N(^4S) + N_3(^2\Pi_g)$ reaction is $1.4 \pm 0.2 \times 10^{-10} cm^3 s^{-1}$. N_3 radicals for these studies were generated by the $F + HN_3$ reaction, for which the rate constant is $1.6 \pm 0.4 \times 10^{-10} cm^3 s^{-1}$. Rate constants for deleterious N_3 loss processes are $1.8 \pm 0.4 \times 10^{-12}$ for the $F + N_3$ reaction, and $\leq 2.0 \times 10^{-12} cm^3 s^{-1}$ for the bimolecular $N_3 + N_3$ reaction. The rate of N_3 loss on Teflon walls of the reactor was measured to be 46 s^{-1}. $N_2(A)$ generated in the $N + N_3$ system

(over)

20. DISTRIBUTION / AVAILABILITY OF ABSTRACT	21. ABSTRACT SECURITY CLASSIFICATION
☐ UNCLASSIFIED/UNLIMITED ☐ SAME AS RPT. ☒ DTIC USERS	Unclassified
22a. NAME OF RESPONSIBLE INDIVIDUAL Mr. Leonard Hanko	22b. TELEPHONE (Include Area Code) (505) 846-4503 22c. OFFICE SYMBOL ARBI

DD FORM 1473, 84 MAR 83 APR edition may be used until exhausted. All other editions are obsolete.

SECURITY CLASSIFICATION OF THIS PAGE
UNCLASSIFIED

19. ABSTRACT (Continued)

(via radiation from $N_2(B)$) was used to collisionally pump IF to its excited $B^3\pi_{0+}$ state, producing IF B → X chemiluminescence. This system was operated in both continuous wave and pulsed modes, the latter via the generation of fluorine atoms by IRMPD of SF_6.

CONTENTS

I. INTRODUCTION

Molecular nitrogen is undoubtedly among the most thoroughly studied of all gas phase species. The ground state of the molecule, bound by 228 kcal mole^{-1}, is virtually inert, and recent interest has centered on a number of metastable excited electronic states which exhibit a rich chemical behavior. In particular, the $A^3\Sigma_u^+$ state, lying 143 kcal mole^{-1} above the ground state, has been studied extensively in low density discharge flow experiments (Ref.1) and in pulsed experiments based on the photolysis of azides. (Ref.2,3) These studies have shown that $N_2(A)$ metastables can efficiently transfer their energy to a number of atoms and molecules, often resulting in electronic excitation of the energy acceptors. In the majority of such systems, the energy transfer process would appear to be dominated by short range intermolecular forces, with Franck-Condon factors in both the N_2 and the energy acceptor being important. (Ref.4) Conservation of spin angular momentum may also affect the energy transfer rate and the population distribution among states of the energy acceptor. (Refs.1,5)

Based on this evidence, metastable N_2 $A(^3\Sigma_u^+)$ appears to hold promise as an energy carrier in potential short wavelength continuous wave chemical laser systems. The large amount of energy borne by individual $N_2(A)$ molecules can produce electronically excited energy acceptors which radiate in the visible or ultraviolet (UV) regions of the spectrum. The radiative lifetime of the $N_2(A)$ state is nearly 2 s (Ref.1) such that radiative losses would be negligible. Further, reactive quenching is hindered by the strong N-N bond in the excited molecule (85 kcal mole^{-1}). The Franck-Condon and angular momentum effects are also attractive features which can lead to state selectivity in the energy transfer process.

This picture is complicated considerably, however, by collision processes among the excited $N_2(A)$ molecules. These processes can lead to population of a number of other high lying excited electronic states. Figure 1 shows approximate potential energy curves (Ref.6) for the states thought to be important in this regard. At high densities of $N_2(A)$ metastables, a primary decay route will be near-resonant energy pooling producing the $C(^3\Pi_u)$, $C'(^3\Pi_u)$, $B(^3\Pi_g)$, and HIR states:

$$2N_2(^3\Sigma_u^+) \rightarrow N_2\,C(^3\Pi_u) + N_2\,X(^1\Sigma_g^+) \quad (1a)$$

$$\rightarrow N_2\,C'(^3\Pi_u) + N_2\,X(^1\Sigma_g^+) \quad (1b)$$

$$\rightarrow N_2\,B(^3\Pi_g, v) + N_2\,X(^1\Sigma_g^+) \quad (1c)$$

$$\rightarrow N_2(HIR) + N_2\,X(^1\Sigma_g^+) \quad (1d)$$

where HIR is the state responsible for the Herman infrared (IR) bands in N_2. The best known of these processes is 1a, for which the rate constant (Ref.1) is $\sim 2 \times 10^{-10}$ $cm^3 s^{-1}$. Production of the C state by 1a is followed by rapid $C^3\Pi_u \rightarrow B^3\Pi_g$ (second positive) emission at a rate 2.5×10^7 s^{-1} ($\tau = 40$ μs). The $B^3\Pi_g$ molecules thus formed can radiatively decay back to the $A^3\Sigma_u^+$ state with a collision-free lifetime of about 6 μs, or be collisionally quenched. Formation of the $C'^3\Pi_u$ state (process 1b) is a minor route with a rate constant about 6 percent of that for 1a. Production of the $B^3\Pi_g$ state by process 1c was first suggested in Reference 7, where a rate constant for this reaction was reported to be >4 times that for 1a, such that the overall energy pooling rate constant would be on the order of 10^{-9} cm^3 s^{-1}. Energy resonance would suggest that this process must populate high vibrational levels (on the order of v=10) of the $B^3\Pi_g$ state. Evidence to this effect was obtained in recent studies of the UV photolysis of ClN_3, a case where

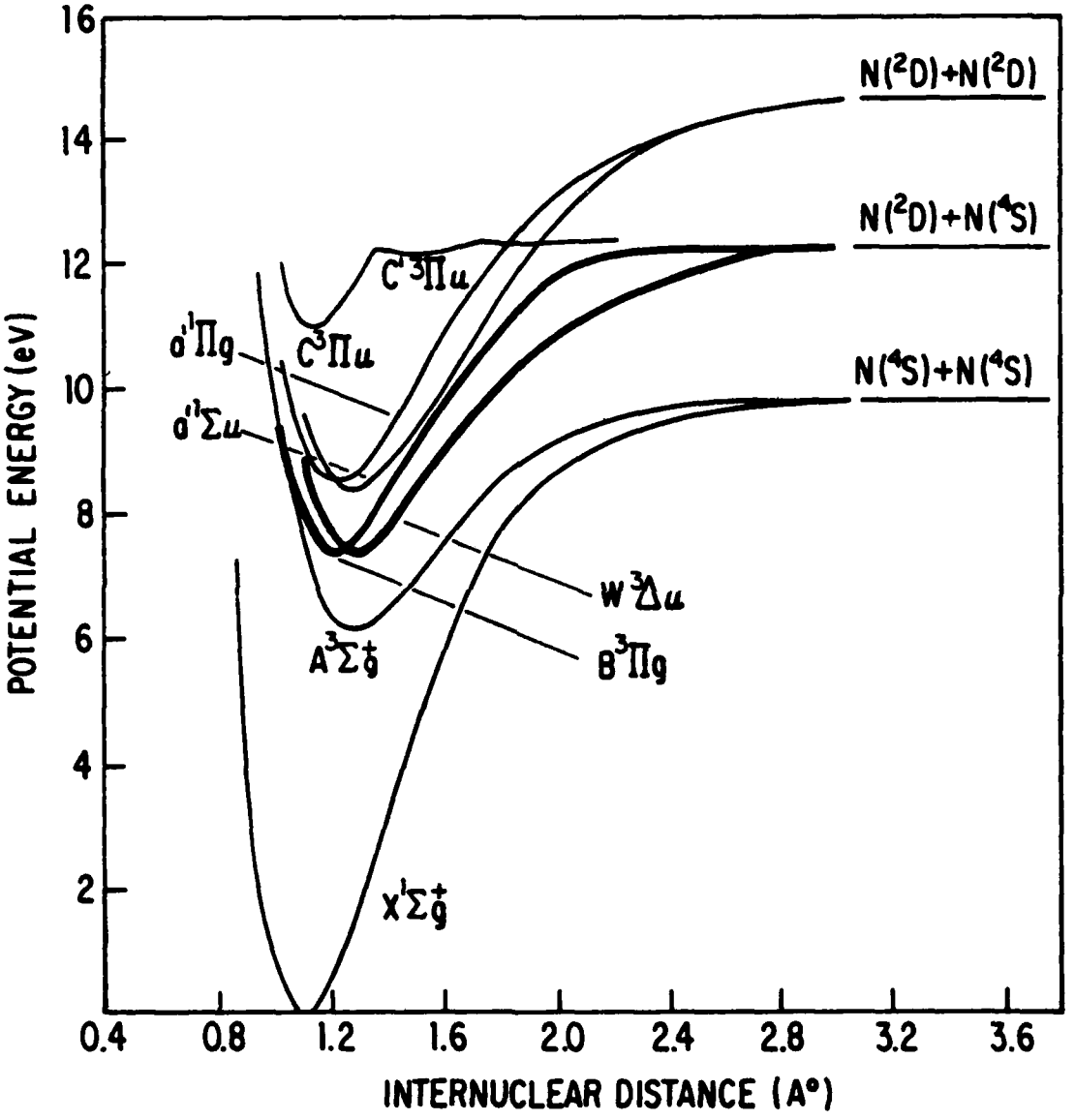

Figure 1. Potential energy curves of selected states of N_2.

energy pooling among $N_2(A)$ molecules produces intense N_2 C→B emission. In this case, lower levels of the B state do not appear to be generated by the pooling process. In Reference 8 it was found that higher vibrational levels of the B state (v' = 8-12) are in fact populated in some measure by pooling. Similarly, recent work shown in Reference 9 has indicated some production of the B state by the pooling process, but suggests that this route is much less significant than originally reported in Reference 7. In any case, it is clear that the overall rate constant for the pooling process must be in the range $2 \times 10^{-10} < k < 10^{-9}$ cm^3s^{-1}. This rate constant may have a significant negative temperature dependence, as suggested by data for process 1a. (Ref. 1)

The collision-free radiative lifetime of the $B^3\Pi_g$ state, about 6 μs, can be extended considerably by interaction with the nearby $W^3\Delta_u$ state (Ref. 10) This interaction occurs for even minute densities of diluent gases or ground state N_2, leading to the formation of a reservoir whose radiative lifetime varies between 20 and 90 μs.

From these considerations, it is apparent that direct chemical production of the N_2 A,B,C,C', or W states will lead rapidly to the formation of an energy pool consisting of some mixture of the $A^3\Sigma_u^+$, $B^3\Pi_g$, and $W^3\Delta_u$ metastable states. If, for example, an $N_2(A)$ density of $10^{15}cm^{-3}$ were produced instantaneously, the A-B-W pool would set up in about 10 μs, given the rate constants discussed. Such a pool would continuously lose energy via C→B radiation on each cycle and by collisional quenching of the A-B-W reservoir. The primary consideration in evaluating any method for the production of excited N_2 should therefore be how well it competes with energy loss from the $N_2(ABW)$ pool. Since the rate of energy loss is roughly one-half the energy pooling rate, the

kinetics of the formation process must be very fast. Also, since the lifetime of the energy pool will be quite short at the high densities required for a laser device, the energy acceptor will, in all likelihood, have to be present during the formation of the excited N_2 metastables. Hence, the chemistry of the formation process must be compatible with potential energy acceptors, as well as not adding further quenchers of $N_2(A)$.

This program has investigated two kinds of chemical systems as sources of $N_2(A)$ metastables scalable to the high densities required for a laser device. These systems are:

- The reaction of ground state nitrogen atoms with excited singlet NX(X = halogen).
- The reactions of ground state nitrogen atoms with molecular azides and azide radicals.

Both of these systems have previously been shown to generate triplet N_2 metastables. It is known, for example, that the reaction of ground state nitrogen atoms with nitrogen halide diatomic molecules produces $N_2(A)$ metastables. In the late 1960s, (Refs. 11 and 12) flames produced by the addition of molecular halogens to active nitrogen (i.e., discharged N_2 containing N atoms as the primary reactive agent) were studied. For the I_2 case (Ref. 11), $N_2(A)$ was directly observed by absorption on the $A(^3\Sigma_u^+) - B(^3\Pi_g)$ bands in the visible and near IR. Up to 10 percent absorption of the 0,0 and 1,0 bands was found for an 80 cm pathlength, corresponding to an $N_2(A)$ density on the order of 10^{12} to $10^{13} cm^{-3}$ (orders of magnitude greater than that produced by recombination of the nitrogen atoms). The mechanism proposed by the authors was as follows:

$$N + I \rightarrow NI + I \quad (2)$$

$$N + NI \rightarrow N_2^*(A,X) + I \quad (3)$$

Correlation arguments would suggest that reaction (3) would produce N_2 in states correlating to two $N(^4S)$ atoms, i.e., the $A^3\Sigma_u^+$ or $X^1\Sigma_g^+$ states. In fact, the yield of $N_2(A)$ was inferred to be rather small (perhaps a few percent), as expected from the availability of both product channels. From the iodine atom chemiluminescence found in the flame (Ref.12), it was inferred that the N_2 $W^3\Delta_u$ state (or a state of equal energy) was present. This result suggests the operation of the $N_2(A,B,W)$ energy pool, even at the low densities of this experiment. For the reaction of N atoms with NCl or NBr, emission from Cl or Br atoms was not observed, suggesting that N_2 states well above 8 eV (the energy of the B and W states) were not present.

To generate high yields of N_2 metastables, correlation arguments would suggest that $N(^4S)$ atoms must react with states of NX correlating to $N(^2D)$ atoms, such as the $a^1\Delta$ or $b^1\Sigma^+$ states. These reactions should produce molecular nitrogen in the B or W states. Evidence to this effect was found in Reference 13 and in studies of the reaction of $N(^4S)$ atoms with gas phase O_2F radicals. The $N + O_2F$ reaction liberates about 60 kcal $mole^{-1}$, sufficient to populate the $a^1\Delta$ and $b^1\Sigma^+$ states of NF. Although weak NF $b^1\Sigma^+ \rightarrow X^3\Sigma^-$ emission was found in the chemiluminescence from this system, the spectrum was dominated by intense N_2 first positive (B→ A) bands. This emission was more than 50 times more intense than the normal yellow afterglow produced by recombination of the N atoms, although the density of O_2F generated was small. The vibrational distribution in the $B^3\Pi_g$ state indicated the large majority of the population to be present in two zones, peaked below v' = 3 and v' = 7, corresponding to the energy limits for reactions of $N(^4S)$ atoms with $NF(a^1\Delta)$ and $NF(b^1\Sigma^+)$, respectively:

$$N(^4S) + NF(a^1\Delta) \rightarrow N_2 + F \qquad E = -183 \text{ kcal mole}^{-1} \ (N_2(B),\ v' = 3) \qquad (4)$$

$$N(^4S) + NF(b^1\Sigma^+) \rightarrow N_2 + F \qquad E = -204 \text{ kcal mole}^{-1} \ (N_2(B),\ v' = 7) \qquad (5)$$

The reaction of N atoms with ground state NF releases energy sufficient to produce only $N_2(X^1\Sigma_g^+)$ or $N_2(A^3\Sigma_u^+)$, in accord with the earlier work given in References 11 and 12.

Reactions of ground state nitrogen atoms with molecular azides were first reported in Reference 14. It was found that the reaction of $N(^4S)$ atoms with ClN_3 produced intense N_2 first positive emission, and the following mechanism was postulated to account for this result:

$$N(^4S) + ClN_3 \rightarrow NCl + N_3 \qquad (6)$$

$$N(^4S) + N_3(^2\Pi_g) \rightarrow N_2(B^3\Pi_g) + N_2(X^1\Sigma_g^+) \qquad (7)$$

Similar results were reported later in Ref. 15. A steady-state treatment was used to extract a rate constant for reaction 7, $k = 1.6 \pm 1.1 \times 10^{-11} cm^3 s^{-1}$. Although this reaction has an exothermicity of about 215 kcal $mole^{-1}$, the $B(^3\Pi_g)$ state is populated only up to v = 8 The angular momentum constraints on this reaction should be strong, in view of the weak spin-orbit coupling in both N and N_3. From spin conservation, the reaction of a quartet atom with a doublet N_3 molecule should produce one ground state (singlet) N_2 molecule and an excited N_2 in either triplet or quintet states. A number of such states exist at energies accessible to the reaction (Fig. 1). If only spin conservation were important, one would expect preferential population of the lowest energy triplet, $N_2(A^3\Sigma_u^+)$. Additional constraints are placed on the reaction by orbital angular momentum correlations. Considering the system in a simple way, we expect N_3 to behave chemically like an $N(^2D)$ atom weakly bound to ground

state $N_2(X^1\Sigma_g^+)$, such that the reaction with ground state N atoms should produce excited states of N_2 correlating to $N(^2D) + N(^4S)$, i.e., the $B^3\Pi_g$ or $W^3\Delta_u$ states (Fig. 1). These ideas can be expressed by consideration of possible orbital correlations in the manner originally described in Reference 16. Figure 2 shows a partial correlation diagram for the $N+N_3$ system, assuming that the intermediate N_4 configuration is of C_s symmetry (as are the molecular azides RN_3), and the spin-orbit coupling is small. As shown in the figure, the reactants $N(^4S) + N_3(^2\Pi_g)$ correlate adiabatically only to products $N_2(B^3\Pi_g) + N_2(X^1\Pi_g^+)$ or $N_2(W^3\Delta_u) + N_2(X^1\Pi_g^+)$ by a potential energy surface of species $^3A' + {}^3A''$. The ground state products $N_2(X) + N_2(X)$ correlate via a $^1A'$ surface to $N(^4S) + N_3(^4\Sigma^-)$. This excited state of N_3 is repulsive and dissociates to $N(^4S) + N_2(X)$. These same reagents $[N(^4S) + N_3(^4\Sigma^-)]$ correlate via a $^3A'$ surface to $N_2(A^3\Sigma_u^+) + N_2(X)$, and via a $^5A'$ surface to the proposed $^5\Sigma_g^+$ state of N_2 and $N_2(X)$. The surface of species $^3A''$ arising from $N(^4S) + N_3(^2\Sigma_u^+)$ is likely to correlate to $N_2(B'^3\Sigma_u^+) + N_2(X^1\Sigma_g^+)$. The $^2\Sigma_u^+$ state of N_3 (the upper state of the well-known transition (Ref.17) near 270 nm) and $N_2(B')$ are both thought to dissociate to $N(^2P)$. Several singlet and triplet surfaces of species $A' + A''$ arise from the reagents $N(^2D) + N_3(^2\Pi_g)$. These surfaces may lead to a number of excited N_2 products, including $a\,^3\Pi_g$, $a'^1\Sigma_u^-$, $w^1\Delta_u$, $b^1\Pi_u$, $h^3\Phi_u$, and $b'^1\Sigma_u^+$, all of which are thought to dissociate to $N(^2D) + N(^2D)$. Hence, it is apparent that the reaction of $N_3(^2\Pi_g)$ radicals with ground state N atoms should be constrained to produce only the $B^3\Pi_g$ or $W^3\Delta_u$ states of the excited N_2 product, whereas a much broader array of excited states may be produced by reaction with $N(^2D)$ atoms. In a sense, the constraints on the $N(^4S) + N_3(^2\Pi_g)$ reaction arise from the large amount of spin angular momentum and

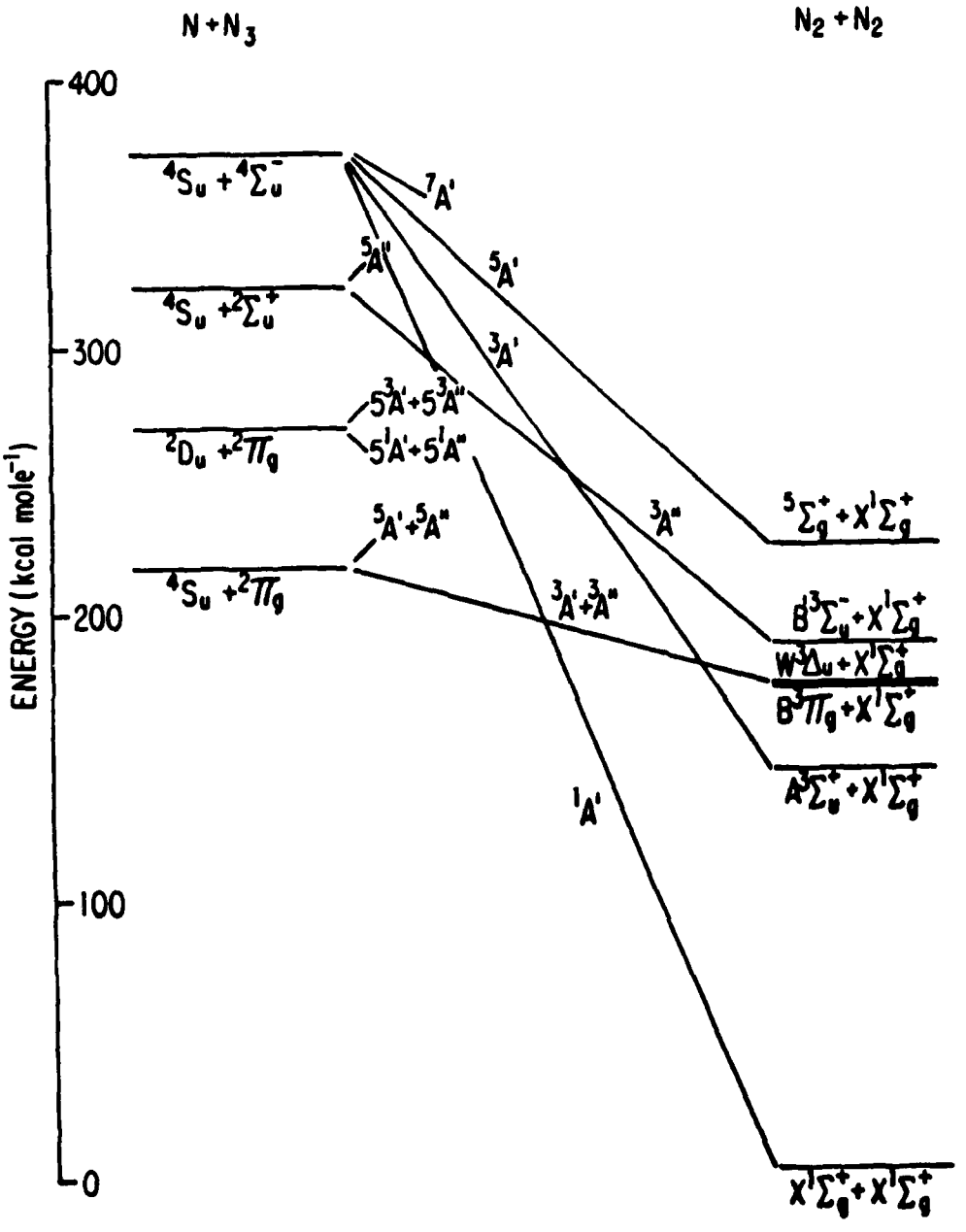

Figure 2. Correlation diagram for the N + N_3 reaction.

the small amount of orbital angular momentum in these reagents, coupled with the fact that one of the product fragments ($N_2(X^1\Sigma_g^+)$) has no orbital or spin angular momentum. Hence, the high spin, low orbital angular momentum of the reagents must be consolidated in one of the product N_2 molecules, a situation which strongly drives the reaction to produce specific excited states.

The specific objective of this program was the evaluation of the $N(^4S) + NF(a^1\Delta)$, $N(^4S) + XN_3$ (X=halogen), and $N(^4S) + N_3$ reactions as chemical sources of triplet N_2 metastables useful for potential laser systems. Rate constants of elementary processes and yields of excited states were determined as appropriate. From these measurements, an optimum system (the $N(^4S) + N_3$ reaction) was chosen, and its compatibility with the $N_2(A)$-IF energy transfer system (a potential IF laser) tested. These results are detailed in the following sections.

II. The $N(^4S) + NF(a^1\Delta)$ Reaction

It can be argued that the reaction of ground state nitrogen atoms with $NF(a^1\Delta)$ should be strongly constrained to produce states of N_2 correlating to $N(^2D) + N(^4S)$; i.e., the $B^3\Pi_g$ and $W^3\Delta_u$ states. The reaction has an exothermicity sufficient to produce $N_2(B)$ only in vibrational levels below v = 4. Hence, it is only slightly exothermic for the reaction channel it may be constrained to follow ($\Delta H \simeq -19$ kcal mole^{-1} to v = 0 of the B state) and may well have a substantial barrier resulting in a small rate constant. The present experiments were directed toward measurement of the rate constant of this elementary reaction and the distribution of product states.

The experiments were performed with two different discharge-flow systems which were typical of those used throughout this work. These systems are shown in Figures 3 and 4. Figure 3 shows a 2.54 cm. Pyrex flow reactor, with two sidearms equipped with 2450 MHz microwave discharges. The reactor has a concentric sliding inlet to provide time resolution. For this chemical system, $NF(a^1\Delta)$ molecules were produced by the reactions

$$F + HN_3 \rightarrow HF + N_3 \qquad (8)$$

$$F + N_3 \rightarrow NF(a^1\Delta) + N_2 \qquad (9)$$

Reaction 8 is very rapid ($k = 1.6 \pm 0.4 \times 10^{-10}$) and reaction 9 has moderate velocity with $k \simeq 2 \times 10^{-12} cm^3 s^{-1}$. Hence, $NF(a^1\Delta)$, produced in high yield (Ref.18) from reaction 9, can be generated by admission of a flow of HN_3 to a large excess flow of fluorine atoms. In the apparatus shown in Figure 3, F atoms were created by a discharge through either CF_4 or F_2, diluted heavily in Ar or He. The HN_3 was admitted to the gas stream

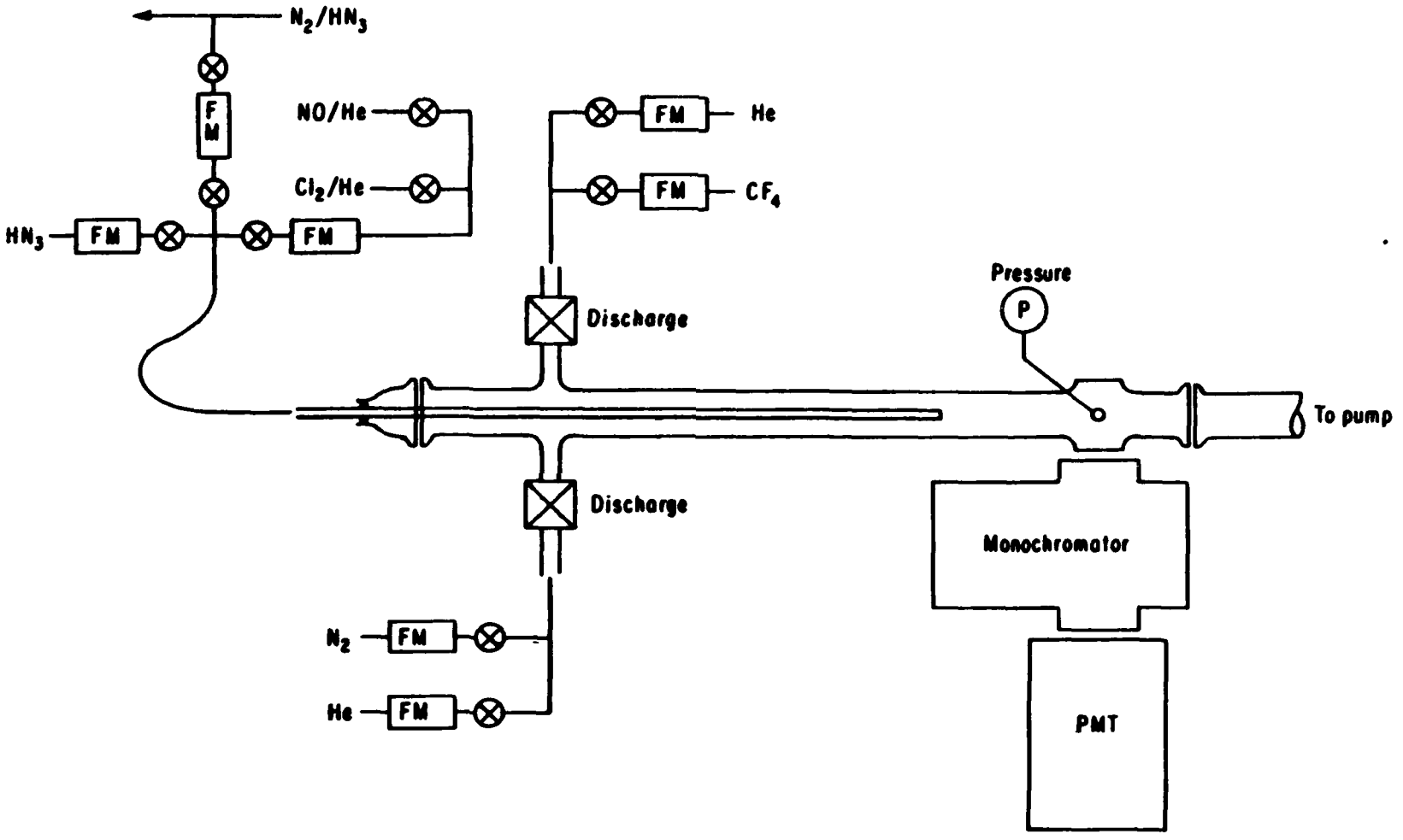

Figure 3. General discharge-flow apparatus with Pyrex flow tube.

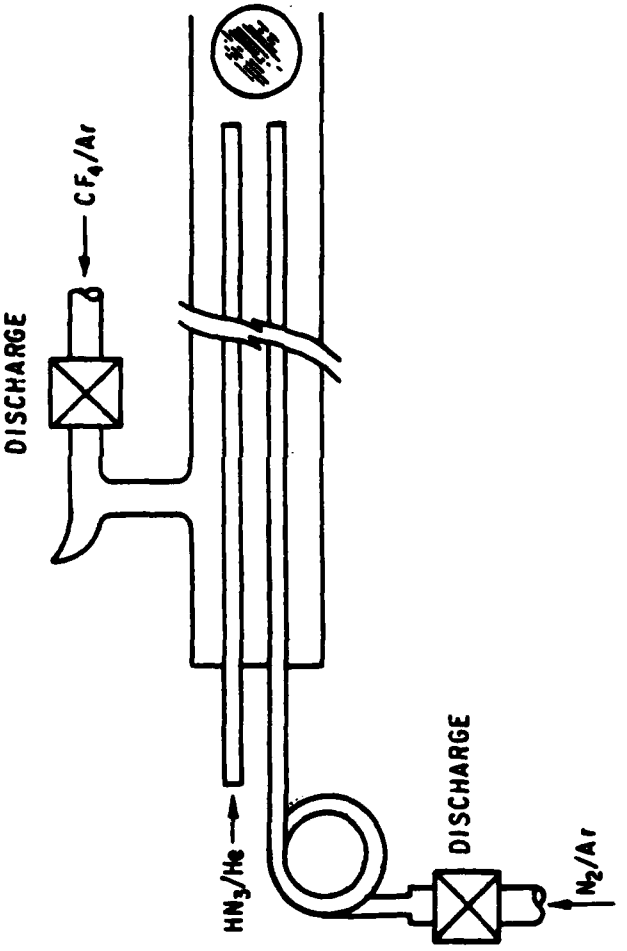

Figure 4. Teflon discharge-flow apparatus.

through the sliding injector. The azide was prepared by the standard reaction between stearic acid and NaN_3 at temperatures near 100°C, and stored in 3 ℓ Pyrex bulbs as 2 to 10 percent mixtures in helium. Nitrogen atoms were prepared by passage of N_2/Ar mixtures through the second discharge sidearm. The system was pumped by a 650 lpm mechanical pump, such that a linear velocity near 1800 cm s^{-1} was produced at a total pressure near 1.0 Torr. These conditions, typical of the experiments, are such that the plug flow assumption should hold. The flow rates of the reagent gases were measured with mass flowmeters (Tylan FM360). Flow rates of the fluorine and nitrogen atoms produced by the discharges were determined by chemiluminescent titrations with Cl_2 and NO, respectively. (Refs.19 and 20) Emissions from the flame of reactions 8 and 9 were dispersed by a 0.25 m Jarrell-Ash monochromator and detected by a cooled GaAs photomultiplier tube (RCA C31034).

The second flow reactor used was made entirely from Teflon and is shown in Figure 4. The flow reactor was a Teflon pipe with an internal diameter of 3.5 cm, with one sidearm equipped with a 2450 MHz microwave discharge. Two movable injectors made from 0.6 cm of Teflon tubing were used to admit reagents to the flow reactor at variable distances from a fixed observation port. One of these movable injectors was used to admit gases which had passed through a second microwave discharge. The linear velocity in this reactor at 1.0 Torr was near 930 cm s^{-1}. The gas handling and optical detection system used in this system were similar to that described previously.

The first experiments on the N + NF($a^1\Delta$) system were run with the Pyrex flow tube shown in Figure 3. Excited NF($a^1\Delta$) was produced by admission of HN_3 to excess fluorine atoms. Green NF $b^1\Sigma^+ \rightarrow X^3\Sigma^-$ emission

peaked near 529 nm was readily visible to the eye. It has been shown previously that this emission is produced from the rapid energy transfer process:

$$NF(a^1\Delta) + HF(v) \rightarrow NF(b^1\Sigma^+) + HF(v-2), \qquad (10)$$

where the vibrationally excited HF is produced in the initial $F + HN_3$ reaction. However, the NF $a^1\Delta \rightarrow X^3\Sigma^-$ emission was weak. A low resolution spectrum of this emission is shown in Figure 5. The time profile of the emission exhibited a rapid rise followed by a decay over only a few miliseconds. In fact, the decay of the emission corresponded to the rate of the limiting formation steps ($F + N_3$), and the unresolved rise corresponded to the rate of $NF(a^1\Delta)$ quenching. These results are contrary to those from previous experiments in which the $F + HN_3$ system was studied in a Teflon flow reactor, and suggest the possibility of wall removal of the $NF(a^1\Delta)$ or N_3 intermediate in the Pyrex tube. This possibility is particularly plausible in light of likely reaction between the F atom stream and the Pyrex wall. To test this possibility, the Teflon flow reactor was assembled.

Experiments with the Teflon system yielded results quite different from those obtained with the Pyrex reactor. The NF(a → X) intensity was considerably greater, and exhibited a long decay (> 15 ms) down the length of the reactor. The NF a → X and b → X features dominated the spectrum of the emission, as expected. These results suggest that the walls of the Pyrex tube were indeed a factor. Much greater flows of fluorine atoms could be used in the Teflon reactor, such that short (< 6 ms) $F + N_3$ reaction times could be achieved. To observe the $N + NF(a^1\Delta)$ reaction, the N atom inlet (one of the 6 mm Teflon injectors) was positioned 8 cm downstream of the HN_3 inlet (the other injector), such that the $NF(a^1\Delta)$ formation process was essentially over by the time the N atoms entered the

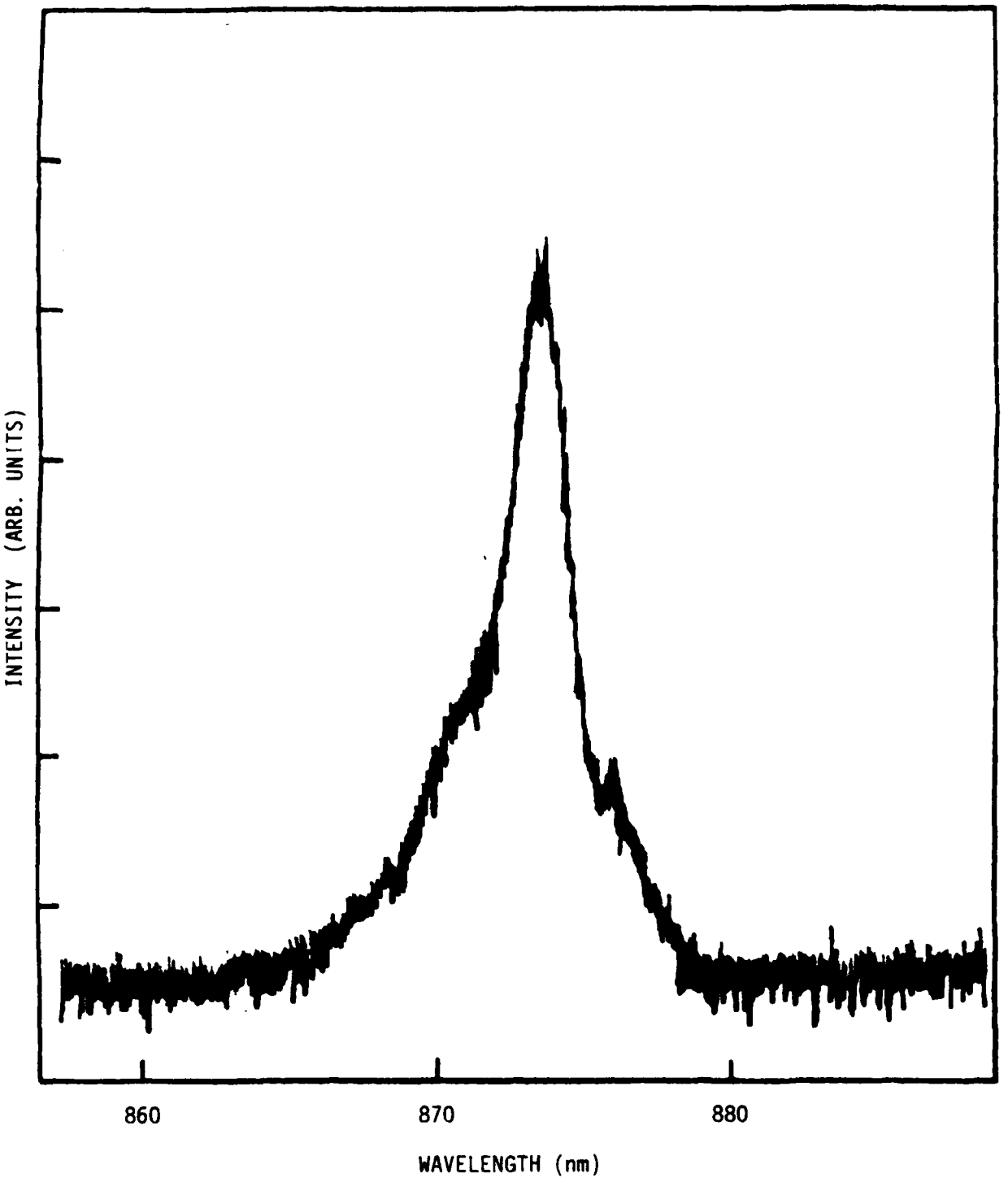

Figure 5. Low resolution spectrum of NF a --> X emission from the reaction of HN_3 with excess F atoms.

stream. Qualitatively, admission of N atoms at densities near $10^{13}cm^{-3}$ had little or no effect on the $NF(a^1\Delta)$ emission intensity or its time profile. No visible or UV emission from excited states of N_2 was produced. Figure 6 shows a portion of the data for the time decay of $NF(a^1\Delta)$ in the presence of various densities of N atoms. Clearly, there is little effect on the rate of $NF(a^1\Delta)$ removal. Figure 7 shows the results of a number of such experiments as a plot of the first order rate (s^{-1}) of the decay of the NF a → X intensity (measured at 874 nm) for various densities of added N atoms. In each case, the N atom density was determined by titration with NO, and the F atom density was held constant near 6 X $10^{13}cm^{-3}$. It is apparent that there is no real evidence of reaction (or quenching) within the uncertainty of the measurements. From the uncertainty in the slope of the plot (from a least squares analysis), the rate constant for the $N(^4S)$ + $NF(a^1\Delta)$ reaction can be no greater than 10^{-13} cm^3s^{-1}.

In view of the huge exothermicity of the N + $NF(a^1\Delta)$ reaction with respect to production of ground state products ($N_2(X^1\Sigma_g^+)$ + $F(^2P_J)$) these results would seem to indicate that the reaction is indeed strongly constrained to produce excited triplet states of N_2, in particular $N_2(B^3\Pi_g, W^3\Delta_u)$. The small rate constant may well result from the presence of a barrier in the reaction channel to these allowed products. As noted, this is not unusual, given that 90 percent of the energy released by the reaction is required for the generation of $N_2(B, v = 0)$. If the reaction dynamics are such that some of the energy release is channeled preferentially into N_2 rotation or vibration or relative translation, then such a barrier will be present. We note also that the reaction rate may show a substantial temperature dependence, increasing with increasing temperature.

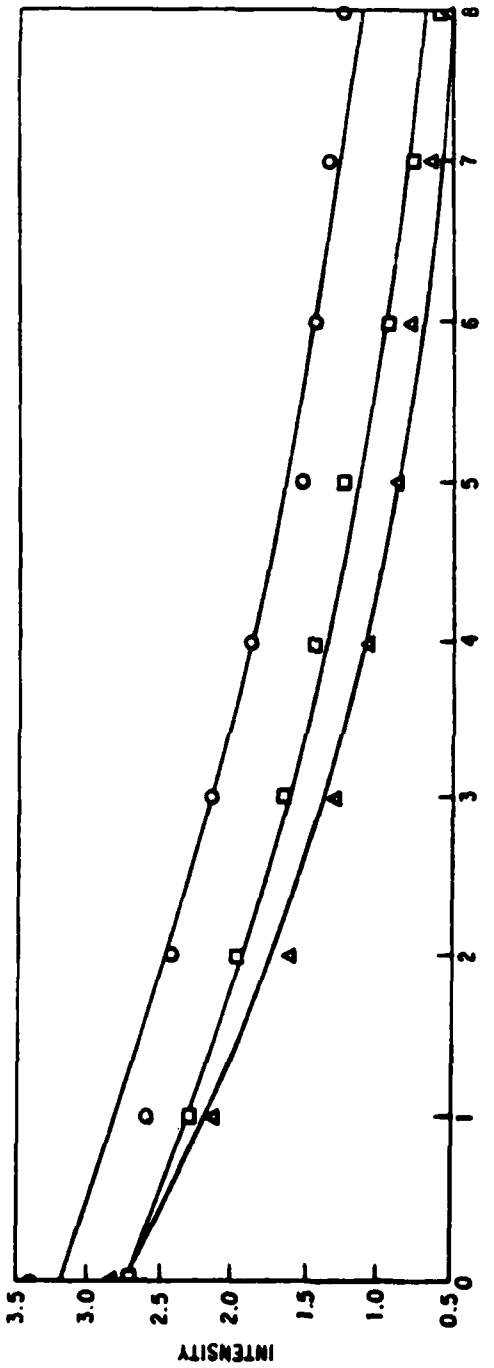

Figure 6. Time decay of $NF_2(a'\Delta)$ in the presence of N atoms. (o), $[N] = 0$; (□), $[N] = 1.36 \times 10^{13} cm^{-3}$; (Δ), $[N] = 1.93 \times 10^{13} cm^{-3}$. The 1 cm of distance corresponds to 1.07 ms.

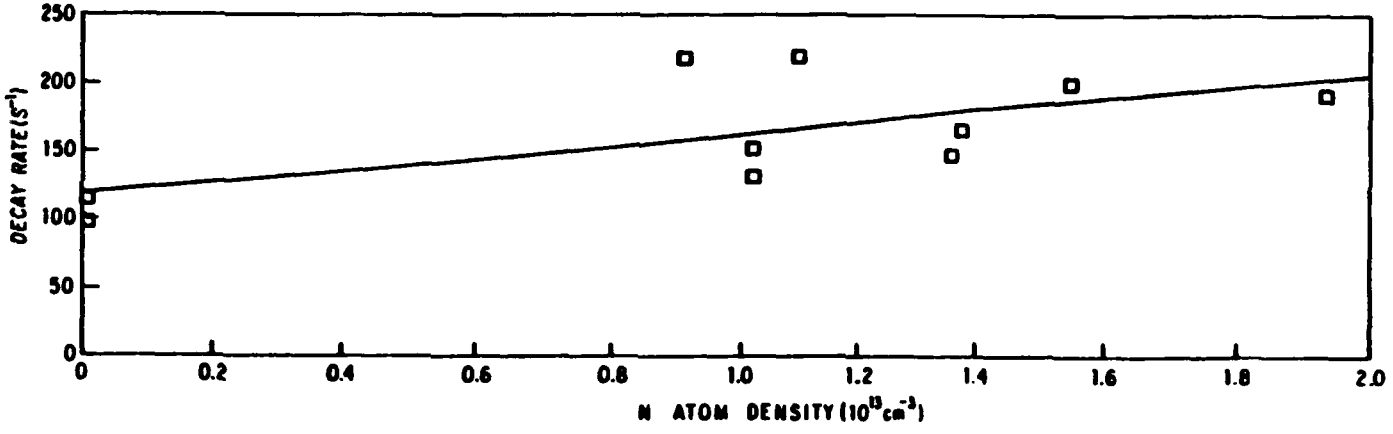

Figure 7. Rate of decay of $NF(a^1\Delta)$ intensity versus the density of added N atoms. Slope of the least squares line through the data suggests a rate constant $k = 5 \times 10^{-12} cm^3 s^{-1}$.

III. The $N(^4S_u) + N_3(^2\Pi_g)$ Reaction

The $N + N_3$ reaction is expected to be constrained to produce excited electronic states of N_2 by the operation of both spin and orbital angular momentum conservation rules. These expectations were tested in a series of discharge-flow experiments. The experiments were based on the production of N_3 radicals by $F + HN_3$ as in reaction 8. The method was similar to that described in Section II, except that the flow of fluorine atoms was reduced so as to allow N_3 radicals to react with added N atoms, rather than using a large excess flow of F atoms to ensure production of $NF(a^1\Delta)$ by reaction 9. In the initial experiments, F and N atoms were produced in separate discharges and allowed to mix upstream of the HN_3 inlet. Hence, N_3 is produced rapidly by reaction 8 and then removed by N atoms rather than by F atoms.

1. Spectroscopy of the $F/N/HN_3$ Flame

For these experiments, the initial densities of N and F atoms were both near $10^{13}cm^{-3}$, determined by titrations with NO and Cl_2, respectively. (Refs. 19 and 20) The HN_3 was admitted through the sliding injector at an initial density near $10^{12}cm^{-3}$. The diluent in the system (admitted through the nitrogen and fluorine discharges) was Argon, to produce a total pressure near 1.0 Torr. When the HN_3 was admitted to a flow of F atoms only, the familiar green NF $b \rightarrow X$ flame characteristic of reactions 8, 9, and 10 was observed. Admission of the N atom flow to this system produced an intense orange flame, extending for a few miliseconds beyond the mixing zone. The spectrum of this visible emission is shown in Figure 8. All of the features evident in the spectrum are attributable to $B^3\Pi_g \rightarrow A^3\Sigma_u^+$ transitions in N_2. Features corresponding to the $b \rightarrow X$ and $a \rightarrow X$ transitions

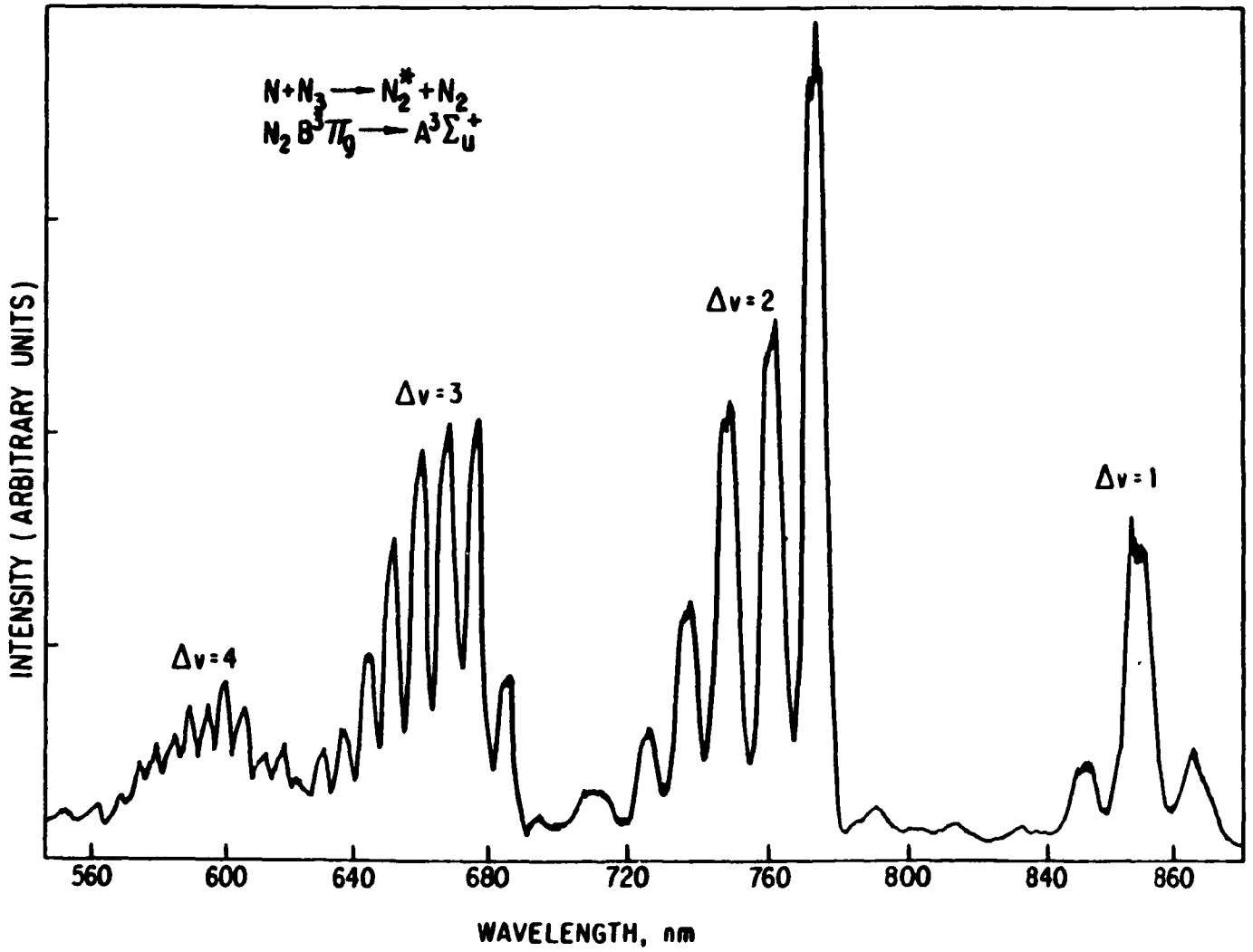

Figure 8. Uncorrected spectrum of N_2 first positive emission produced by the N + N_3 reaction.

in NF (529 and 874 nm, respectively) are absent, suggesting that reactions 9 and 10 do not occur in the presence of N atoms.

The steady-state vibrational distribution among the $N_2(B^3\Pi_g)$ molecules in the flame can be calculated from data such as that shown in Figure (8) and the known radiative lifetimes (Ref.21) for the bands of the B→A transition. The results of this treatment are shown in Figure (9). The data indicate a substantially relaxed vibrational distribution heavily favoring the lower levels. Some population of levels up to v = 12 (near the dissociation limit of the N_2 ground state) is observed, although a knee in the distribution near v = 8 suggests that these higher levels may not be directly populated by the reaction. Indeed, the thermodynamic limit for the N + N_3 reaction (ΔH = -215 kcal $mole^{-1}$) is such that only levels up to v = 8 may be populated directly. It seems likely that the levels above v = 8 arise from scrambling of the nascent population distribution in collisions with the N_2 and Ar present (densities 2 X 10^{15} and 2 X 10^{16} cm^{-3}, respectively). Such processes, involving collision-induced coupling with near-resonant levels of the $W^3\Delta_u$ state,[10] are known to be rapid. The strongly relaxed character of the distribution as a whole is a further indication of the occurrence of such processes. The relative populations of v = 0 and v = 1 were estimated by extrapolation of an exponential fit (T_{vib} = 14060K) to the data for levels v = 2 through v = 8 (Fig. 9).

A plot of the relative intensity of the B → A emission, monitored at the 6,3 band near 661 nm, versus the limiting flow of HN_3 is shown in Figure 10. The linear varriation of the intensity with HN_3 indicates that the $B^3\Pi_g$ population arises directly from the N + N_3 reaction, rather than from second order processes such as energy pooling among other excited

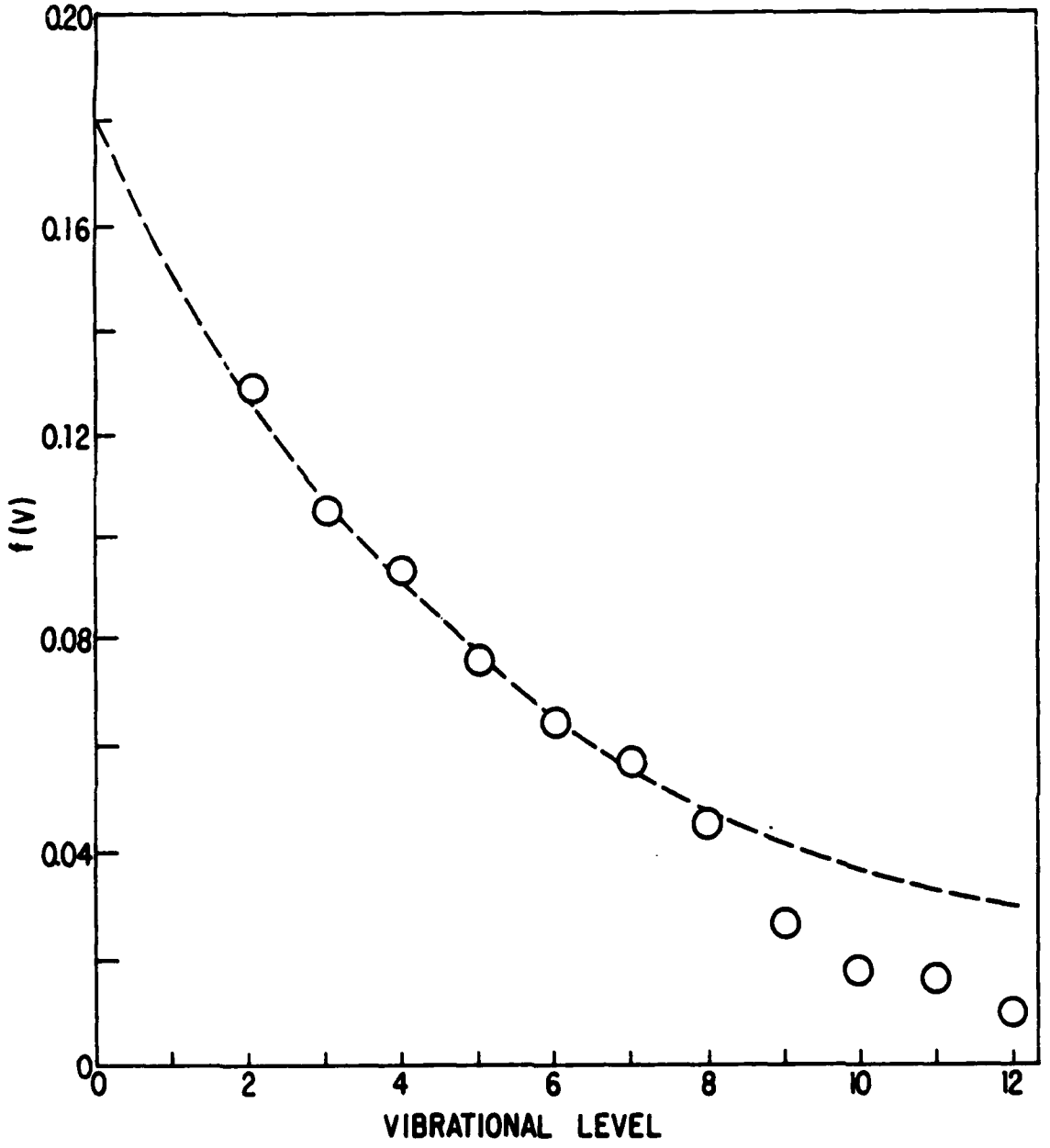

Figure 9. Steady-state vibrational distribution in $N_2(B)$ produced by the N + N_3 reaction, where f(v) is the fractional population of level v. The broken line is an equilibrium thermal distribution corresponding to T = 14,060 K.

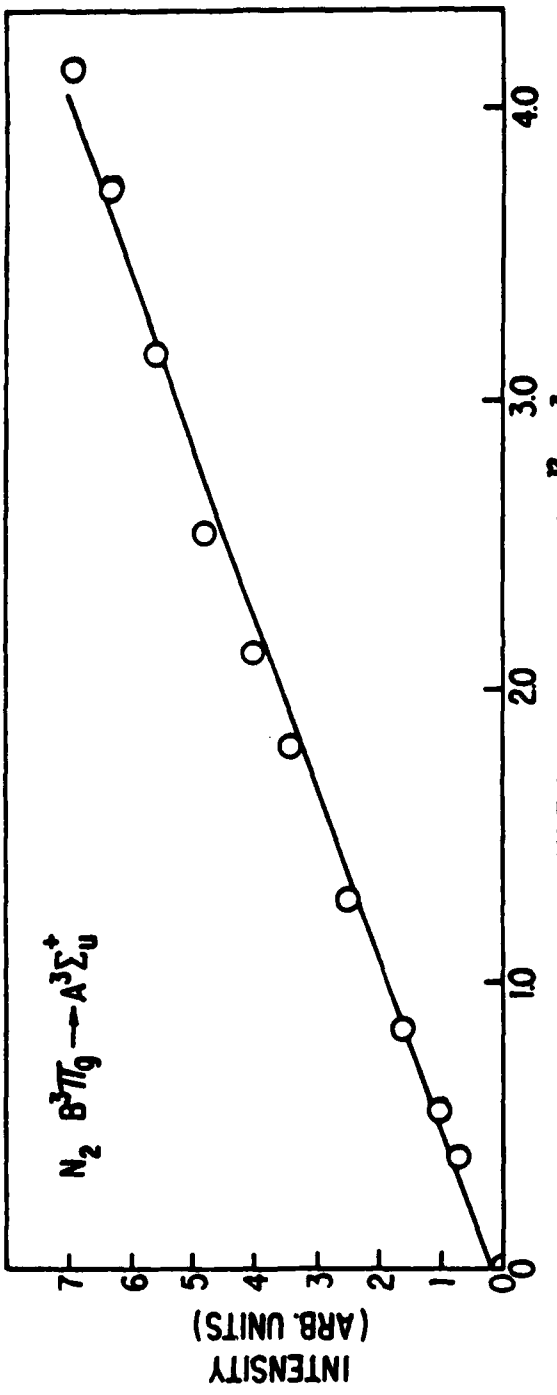

Figure 10. Intensity of the N_2 first positive emission, measured at the 6, 3 band, from $N + N_3$ versus the initial density of HN_3.

states of N_2. It has been suggested, (Ref.7) for example, that $N_2(B)$ is produced by energy pooling among $N_2(A)$ metastables.

A portion of the spectrum of the flame in the UV region is shown in Figure 11. Features corresponding to the $A^2\Sigma^+ \rightarrow X^2\Pi$ transition (γbands) in NO, the $C^3\Pi_u \rightarrow B^3\Pi_g$ (second positive) transition in N_2, and the $A^3\Pi \rightarrow X^3\Sigma^-$ transition in NH were readily evident. Much weaker features attributable to $A^3\Sigma_u^+ \rightarrow X^1\Sigma_g^+$ (Vegard-Kaplan) bands in N_2 were observed in the wings of some of the NO bands. The excited NO arises from an oxygen impurity in the flow through the microwave discharges. Separate experiments have shown that the $O + N_3$ reaction indeed produces intense NO γ-band emission. Gas purifiers (Oxyclear DPG-250) were installed in the Argon and N_2 source lines in an attempt to alleviate this problem, and in fact a reduction of roughly 75 percent was observed in the NO intensity. No reduction in features identified as Vegard-Kaplan bands was observed. The remainder of the NO intensity no doubt arises from an O_2 impurity in the F_2 or CF_4 sources of fluorine atoms. The NH emission arises from interaction of $N_2(A)$ metastables with the HN_3 reagent. The HN_3 is dissociated in this process, generating $NH(A^3\Pi)$. (Ref.22) In view of the energy of the $N_2(C^3\Pi_u)$ state, it cannot be produced directly by reactions of ground state reagents present in the flow. Figure 12 shows a plot of the N_2 C $\rightarrow$ B intensity (measured at the 1,2 band) versus the HN_3 flow. As indicated in the figure, the data are closely fit by a quadratic function. This result indicates that $N_2(C)$ is produced by a process which is second order in HN_3. Since $N_2(B)$ [and, hence, $N_2(A)$] vary linearly with HN_3, the origin of $N_2(C)$ is identified as the well-known energy pooling reaction among $N_2(A)$ metastables:

$$2\ N_2(A^3\Sigma_u^+) \rightarrow N_2(C^3\Pi_u) + N_2(X^1\Sigma_g^+). \qquad (11)$$

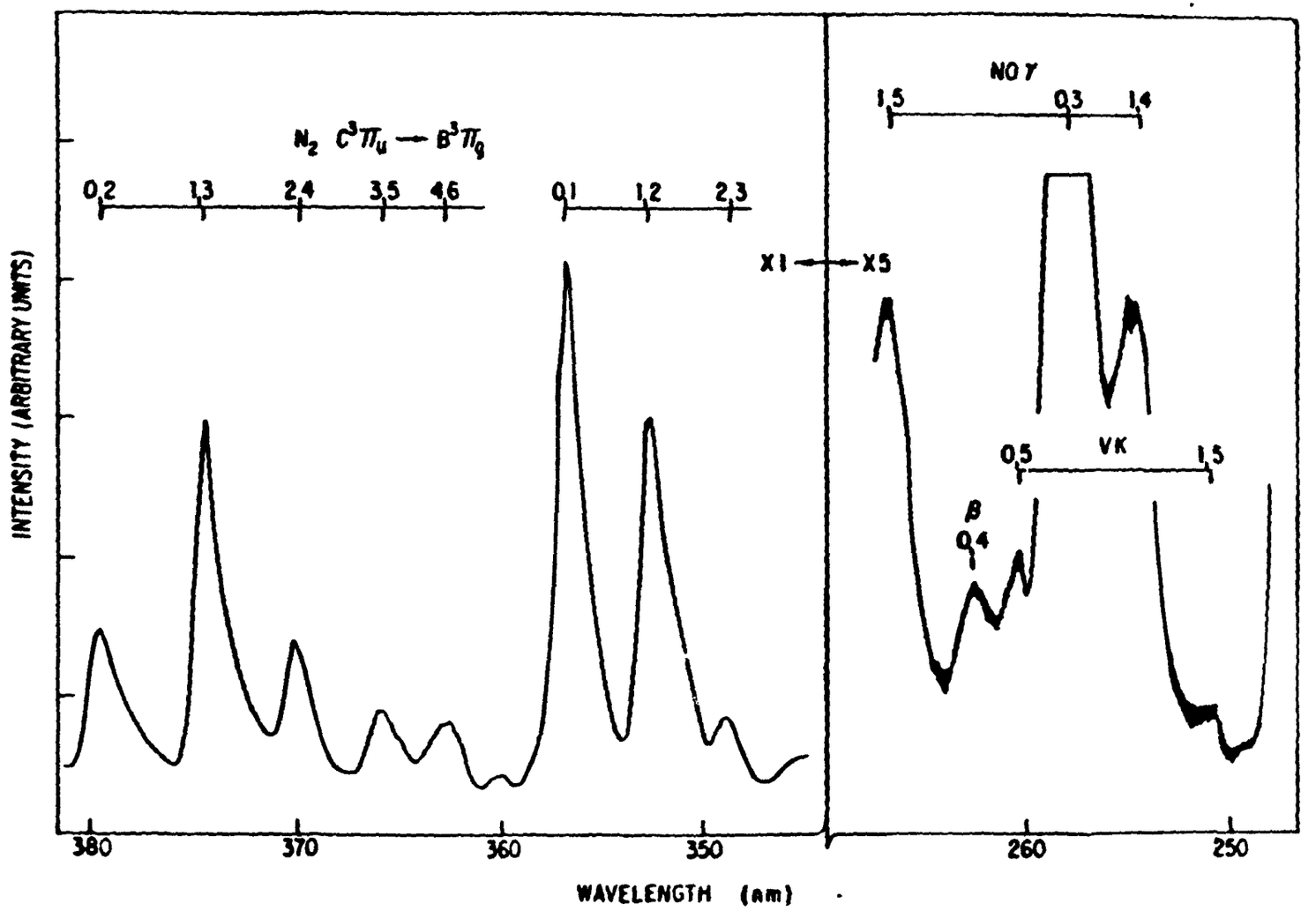

Figure 11. A portion of the spectrum of UV emissions produced by the N + N_3 reaction.

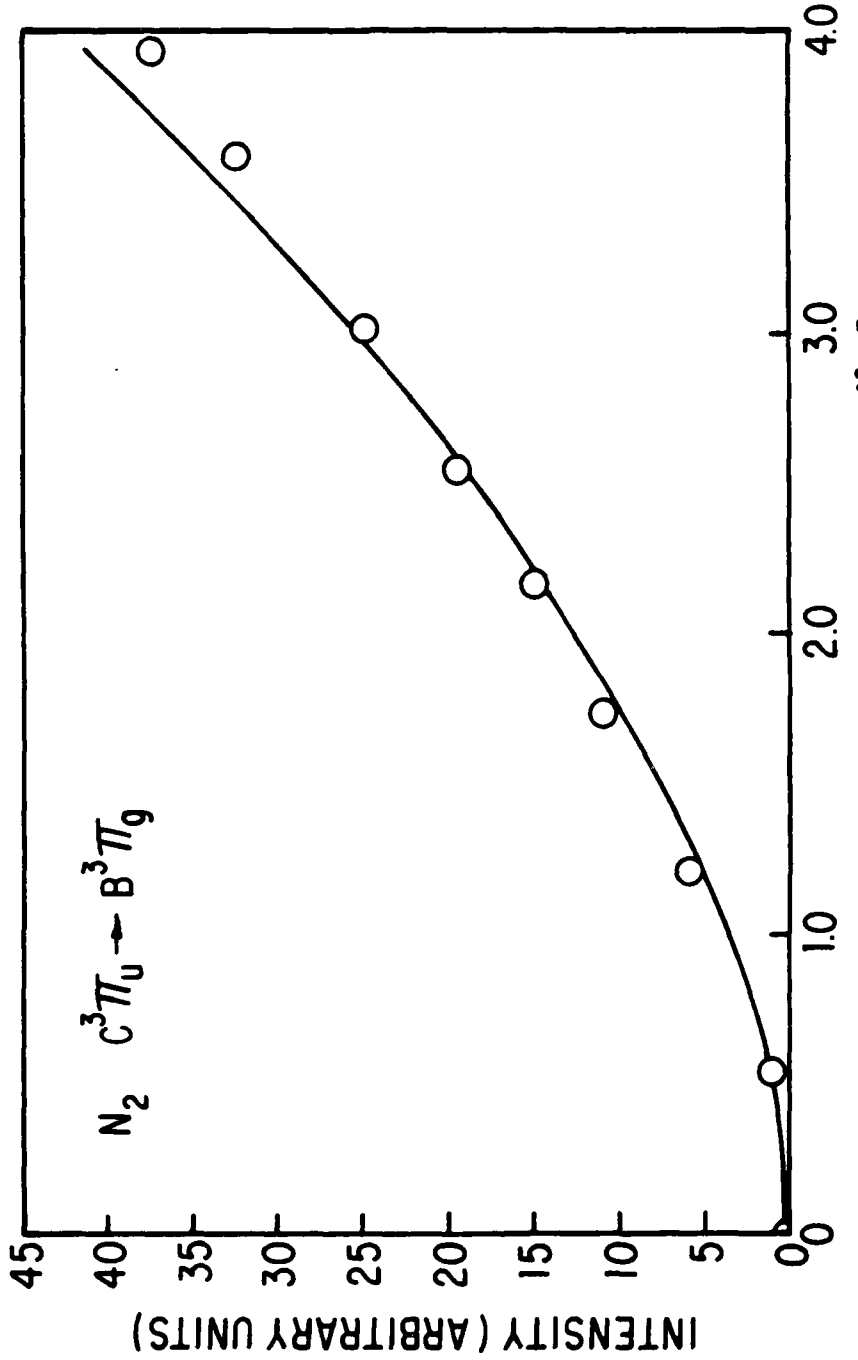

Figure 12. Intensity of the N_2 second positive emission, measured at the 1,2 band, versus the initial density of HN_3. The solid line represents a quadratic fit to the data.

The rate constant (Ref.1) for reaction 11 is near 2 X 10^{-10} $cm^3 s^{-1}$.

2. Time Behavior of the N_2 Emissions

The time profile of the N_2 first positive emission was measured by movement of the sliding injector (the HN_3 source) with respect to the fixed observation port. A typical profile, measured for the 6,3 band near 661 nm, is shown in Figure 13. The finite rise time of the emission was unaffected by changes in the flow rates of any of the reagents and, hence, corresponds to the mixing rate. The decay is well fit by an exponential function. Measurements of the time profile and total intensity of the N_2 B → A emission were made as the concentrations of F atoms and N atoms (both pseudo-first-order reagents) were systematically varied. Concentrations of these species were determined by chemiluminescent titrations with Cl_2 and NO, respectively.

The decay time of the first positive emission was found to vary inversely with the fluorine atom density. This behavior is identified as corresponding to changes in the rate of formation of N_3 by the F + HN_3 reaction. Figure 14 shows a plot of the decay rate of the N_2 B → A emission versus the initial density of F atoms. The line shown is a linear least-squares fit to the data. The slope of the line gives a rate constant k_2 = (1.6 ± 0.4) X 10^{-10} $cm^3 s^{-1}$ for the F + HN_3 reaction. The intercept near the origin indicates that, within the uncertainty of the data shown, this reaction is the only source of N_3 [and hence $N_2(B)$] in the system.

The time profile of the emission was also measured as a function of the N atom concentration. In this case, the complete time profile was fitted to an expression $I(t) = C(e^{-\lambda_1 t} - e^{-\lambda_2 t})$, where λ_1 and λ_2 are rates for the decay and rise of the emission. Within the uncertainty of

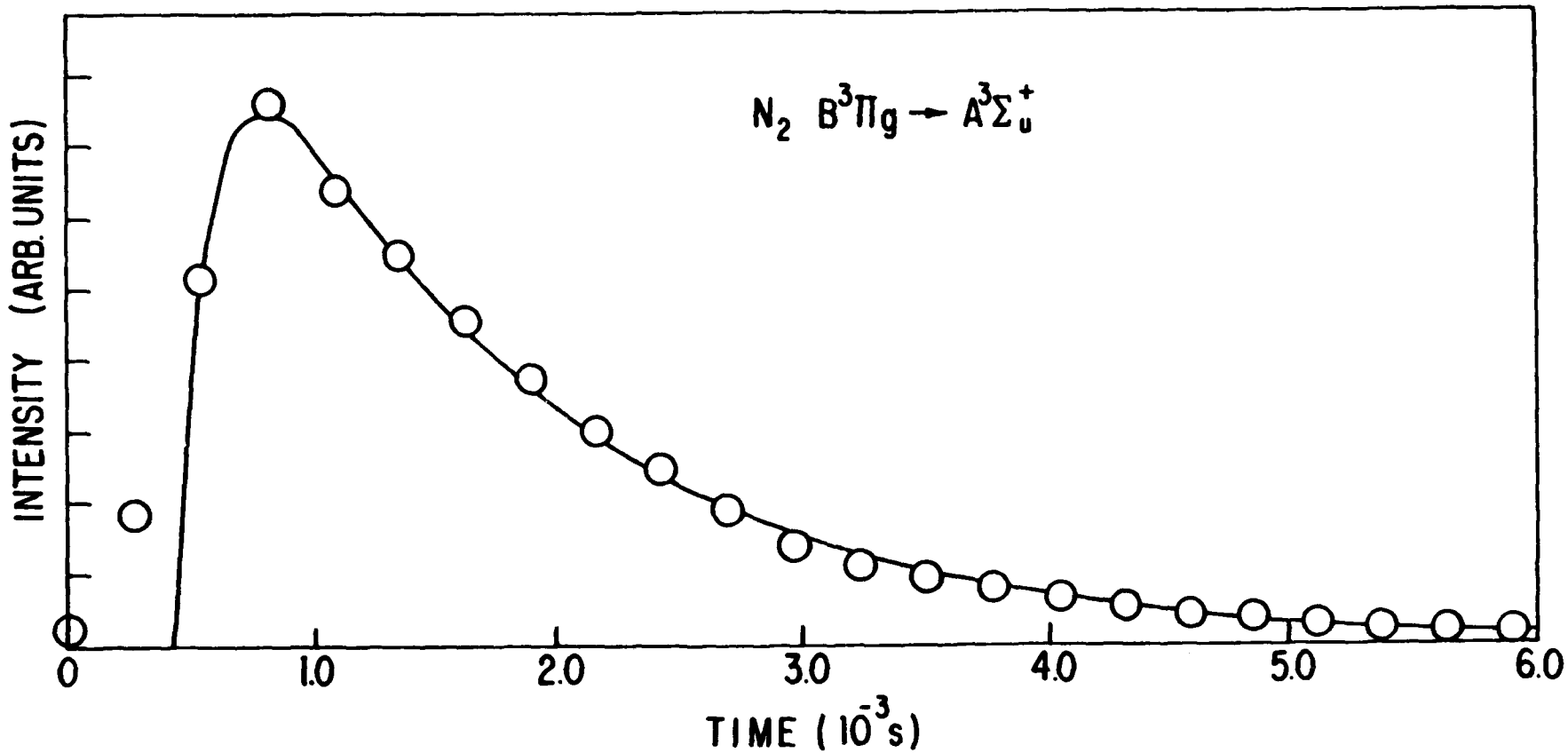

Figure 13. Time profile of the N_2 first positive emission from N + N_3 (6,3 band) for $[HN_3]_o$ = 6.7 X $10^{11}cm^{-3}$, [F] = 3.3 X $10^{12}cm^{-3}$, and [N] = 7.0 X $10^{13}cm^{-3}$.

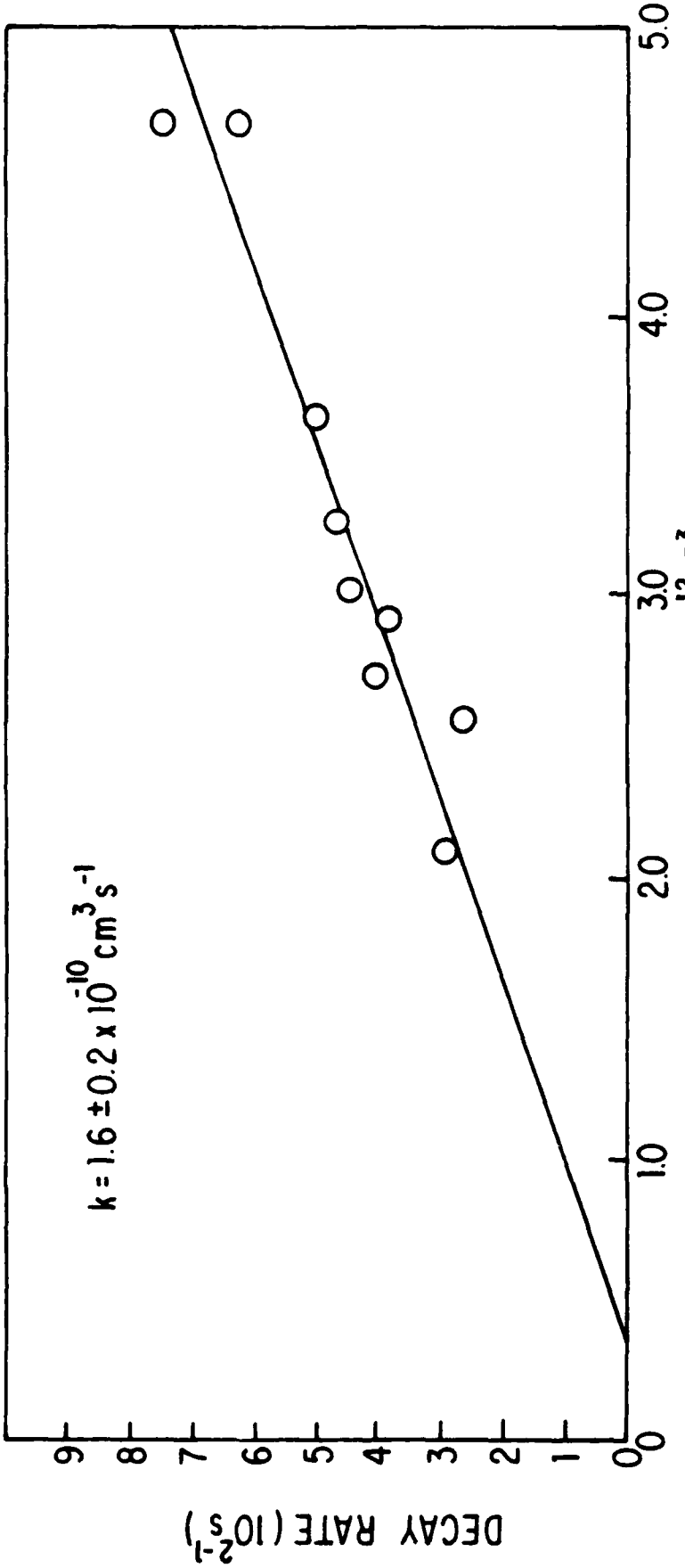

Figure 14. Rate of decay of the first positive emission versus the density of fluorine atoms. For these data, the initial HN_3 density was near $6.5 \times 10^{11} cm^{-3}$. The solid line is a least-squares fit to the data, whose slope yields a rate constant $k = 1.6 \pm 0.4 \times 10^{-10} cm^3 s^{-1}$.

the experiment, the values of λ_1 and λ_2 were found to be invariant with the N atom flow rate. The time-integrated intensity of the flame increased linearly with the measured N atom density (Fig. 15). These data suggest that N atoms compete with another process for removal of N_3 from the system. For high N atom densities ($> 4 \times 10^{13} cm^{-3}$), the intensity was invariant with increasing N atom flow, suggesting the dominance of the $N + N_3$ reaction in this region.

The time profile of the $N_2(A)$ density in the system was determined from the profile of the $C^3 \Pi_u \rightarrow B^3 \Pi_g$ emission. Since this emission is produced by reaction 11, its intensity varies as the square of the $N_2(A)$ density, such that the $N_2(A)$ time profile is given by the square root of the N_2 C → B time profile. The $N_2(A)$ profiles determined in this manner exhibited a finite rise time considerably slower than that found for the first positive emission (the mixing rate), followed by a decay which tracked the first positive decay. Hence, the decay is identified as the rate of formation of $N_2(A)$ [and $N_2(B)$] and the rise as a collisional decay rate. The measured rise times were found to be in good agreement with the measured N atom density and the rate constant reported (Ref.23) for $N_2(A)$ quenching by these atoms ($k = 5 \times 10^{-11} cm^3 s^{-1}$).

3. Yield of N_2 $B^3 \Pi_g \rightarrow A^3 \Sigma_u^+$ Photons

Measurements of the total yield of N_2 first positive photons were made by calibrating the light collection efficiency of the apparatus by comparison with chemiluminescence from the O + NO reaction. (Ref.24) For this purpose, the monochromator used in most experiments was replaced by a filter which transmitted wavelengths above 510 nm. The PMT cutoff was near 890 nm. To reduce the overall light intensity striking the photocathode of the PMT, a 500 μm slit was fixed over the reactor window, and the detector

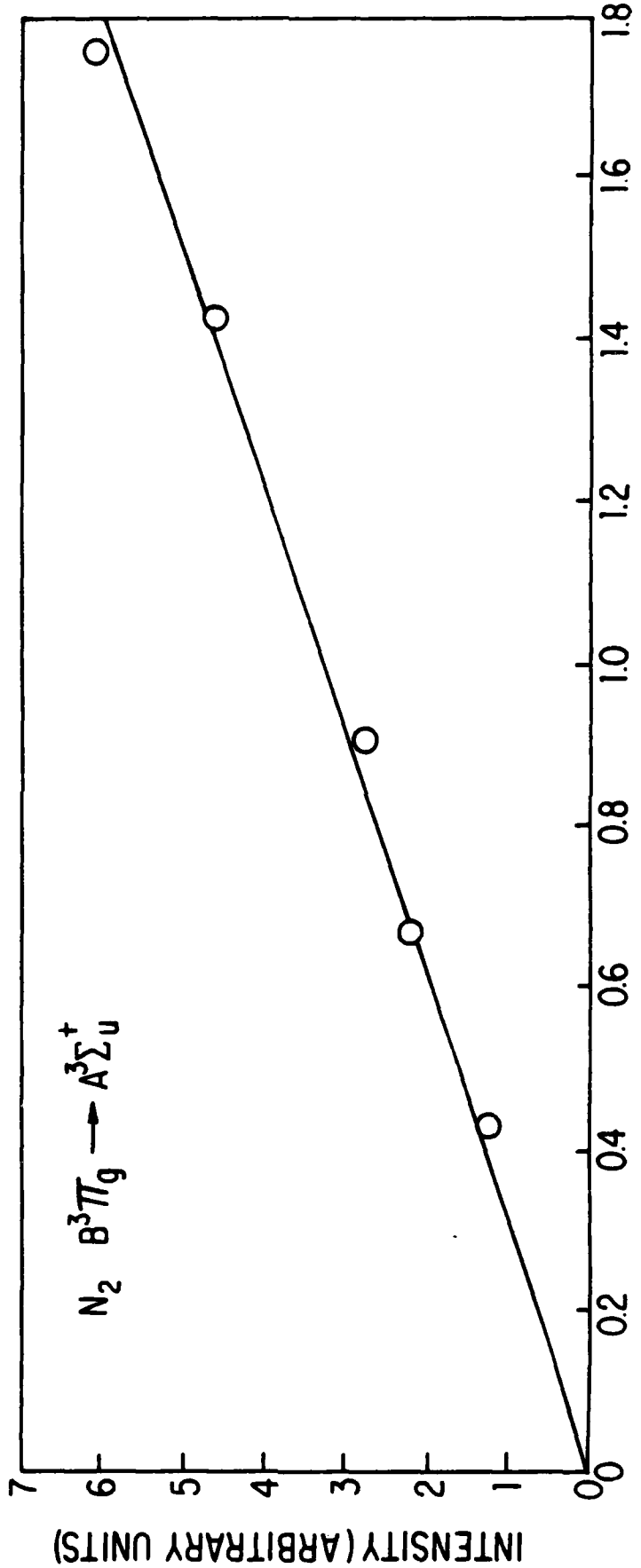

Figure 15. Intensity of the N_2 first positive emission from N + N_3 versus the density of N atoms. The solid line is a least squares fit to the data.

was moved a distance of 25 cm away from the slit. This geometry was used in measurements of intensities from both the NO_2 and N_2 systems. Known concentrations of O atoms and NO were produced in the reactor by the N + NO titration procedure. (Ref.20) Measurement of the NO_2 emission intensity produced by this reaction yields a calibration parameter α, given by

$$\alpha = \frac{\text{observed intensity}}{k[O][NO]} \qquad (12)$$

where γ is the fraction of the total NO_2 emission detected by the filter/PMT combination, determined from the NO_2 emission spectrum and the PMT response. The parameter k is the rate constant (Ref.24) for production of NO_2 photons by the O + NO reaction, taken to be $6.3 \times 10^{-17} cm^3 s^{-1}$. This two-body rate is appropriate (Ref.24) to the experiments, which were performed at total pressures near 0.9 Torr. The absolute rate of production of N_2 B → A photons from the $N/F/HN_3$ system is then determined from the first positive intensity as follows:

$$\text{photon flow} = \frac{\int I_{obsd} dV}{\gamma' \alpha} \qquad (13)$$

where the observed intensity is integrated over the flame volume, and γ' is the fraction of the B → A photons detected by the filter/PMT combination. The value of γ' was determined from the PMT response, the vibrational distribution shown in Figure 9 and published values (Ref.21) for the Franck-Condon factors of the transition. The N_2 B → A photon yield is defined as

$$\Phi \; B \rightarrow A = \frac{\text{photon flow}}{HN_3 \text{ flow}} \times 100\% \qquad (14)$$

where HN_3 is the limiting reagent in the system. A number of independent

measurements of Φ yielded very consistent values in the range 18 to 22 percent.

4. Yield of $N_2(A^3 \Sigma_u^+)$

The density of $N_2(A)$ present in the flame can be estimated by assuming that the N_2 C → B second positive radiation arises solely from $N_2(A)$ energy pooling, reaction 11. This assumption seems quite reasonable in light of the quadratic relation between the second positive intensity and the HN_3 flow rate. Under these circumstances, the steady-state density of $N_2(C)$ is given by

$$[C]_{ss} = \frac{k_{11}[A]_{ss}^2}{k_r^C} \tag{15}$$

where $[A]_{ss}$ is the steady-state density of $N_2(A)$ at a particular time (i.e., the point at which the second positive intensity is measured), and k_r^C is the known radiative rate (Ref.25) of the $C^3\Pi_u \rightarrow B^3\Pi_g$ transition, 2.5×10^7 s^{-1}. Since the density of an emitter is proportional to its emission intensity (in photon flux) divided by the radiative rate, the steady-state density of $N_2(A)$ is given by

$$[A]_{ss} = \frac{k_r^C[C]_{ss}}{k_{11}[A]_{ss}} = \frac{k_r^C(I_{C \rightarrow B}/k_r^C)}{k_{11}\,(I_{A \rightarrow X}/k_r^A)} = \frac{k_r^A I_{C \rightarrow B}}{k_{11} I_{A \rightarrow X}} \tag{16}$$

$$= 2.5 \times 10^9 \,(I_{C \quad B}/I_{A \rightarrow X})\ cm^{-3}$$

where published values (Ref.1) for k_r^A (the radiative rate of the $A^3 \Sigma_u^+ \rightarrow X^1 \Sigma_g^+$ transition) and k_{11} [the rate constant for energy pooling producing $N_2(C)$] have been inserted. The k_r^A value used, 0.5 s^{-1}, represents an average for the $^3\Sigma_u^+$ spin components. The intensities refer to the total frequency integrated intensities of the C → B and A → X

transitions, in photon flux. Data similar to that shown in Figure 11 indicate an intensity ratio of approximately 40 and, hence, an $N_2(A)$ density of about 1×10^{11} cm^{-3}, for a measurement near the peak of the $N_2(A)$ time profile. Calculations of the intensity ratio made use of published (Ref.6) Franck-Condon factors for the C → B and A → X transitions. Also, it was assumed that only v = 0 and v = 1 of the A state were populated, as seems reasonable (Ref.26) given the density of N_2 present.

The calculated $N_2(A)$ density refers to a particular point in the flame. To obtain an estimate of the total yield, the finite rates of production and removal of $N_2(A)$ must be taken into account. Given these data, it is reasonable to use the following model:

$$F + HN_3 \rightarrow HF + N_3 \qquad (8)$$

$$N + N_3 \rightarrow N_2(A) + N_2 \qquad (7)$$

$$N_2(A) + Q \rightarrow N_2(X) + Q \qquad (17)$$

where Q is any quencher of $N_2(A)$. The density of $N_2(A)$ at a time t is then given by

$$[A]_{max} = \frac{k_8[F][HN_3]_o}{k_8[HN_3]_o - k_{17}[Q]} \left(e^{-k_8[HN_3]_o t} - e^{-k17[Q]t}\right) \qquad (18)$$

Note that this treatment assumes process 7 to be much faster than process 8, as indeed the data would indicate, and further that the yield of $N_2(A)$ from the $N + N_3$ reaction is unity. This would be the case if, for example, the yield of $N_2(B)$ were unity and all of the $N_2(B)$ decayed radiatively to $N_2(A)$. Hence, this expression gives the maximum density of $N_2(A)$ at a time t. The values of $k_8[HN_3]_o$ and $k_{17}[Q]$ are determined by the measured rise and decay rates of the $N_2(A)$ time profile. For typical conditions, $[A]_{max}$ is found to be ~$6 \times 10^{11} cm^{-3}$ at the point of measurement

of the UV spectrum. Hence, the intrinsic yield of $N_2(A)$ would appear to be about 15 percent, in good agreement with the measured N_2 B→A photon yield. These data would suggest that all of the $N_2(A)$ present in the flame can be accounted for by first positive emission from the $N_2(B)$ state.

5. Kinetic Model for the $F/N/HN_3$ System

Based on the data presented for the $F/N/HN_3$ system, we propose the following mechanism to account for the behavior of the N_2 first positive emission:

$$F + HN_3 \rightarrow HF + N_3 \quad (8)$$

$$F + N_3 \rightarrow NF(a^1\Delta) + N_2 \quad (9)$$

$$N + N_3 \rightarrow N_2(B^3\Pi_g) + N_2(X^1\Sigma_g^+) \quad (7)$$

$$M + N_3 \rightarrow \text{products} \quad (19)$$

$$N_2(B^3\Pi_g) \rightarrow N_2(A^3\Sigma_u^+) + h\nu \quad (20)$$

$$N_2(B^3\Pi_g + M \rightarrow \text{products} \quad (21)$$

where M refers to unspecified molecules present in flow. Since the rate of removal of $N_2(B)$, $k_{20} + k_{21}[M]$, is rapid with respect to the rate of its formation, a steady-state expression can be used to describe the intensity of the first positive emission:

$$I_{B \rightarrow A} = \frac{k_7[N][N_3]}{k_{20} + k_{21}[M]} \quad (22)$$

For conditions under which the densities of N and M are much greater than those of HN_3 (and hence N_3), the intensity will track the time dependence of the N_3 density. From the proposed mechanism, the rate equation for N_3 is given by

$$d[N_3]/dt = k_8[F][HN_3] - (k_9[F] + k_7[N] + k_{19}[M])[N] \quad (23)$$

Since the value of k_9 has been reported (Ref.27) to be $2 \times 10^{-12} cm^3 s^{-1}$, process 9 is far too slow to be important for the fluorine atom densities used in these experiments. Also, since the density of HN_3 is much smaller than the density of fluorine atoms

$$[HN_3] = [HN_3]_o e^{-k_8[F]t} \tag{24}$$

The time dependence of the N_3 density is given by

$$[N_3] = \frac{k_8[F][HN_3]_o}{k_7[N]+k_{19}[M]-k_8[F]} (e^{k_8[F]t} - e^{-(k_7[N] + k_{19}[M]t)} \tag{25}$$

From the experiments, the term $e^{-k_8[F]t}$ corresponds to the decay of the B → A emission, and we find $k_8 = 1.6 \times 10^{-10} cm^3 s^{-1}$. Since the observed rise of the emission did not vary with [N], the term $k_7[N] + k_{19}[M]$ must exceed the finite mixing rate in the system. Further, $k_{19}[M]$ must be a significant contributor to the removal of N_3 at low N atom densities since, under these conditions, the intensity at a given time increased linearly with [N] or $[HN_3]_o$ for a fixed flow of F atoms. For N atom densities $>\sim 4 \times 10^{13} cm^{-3}$, reaction 7 would appear to dominate N_3 removal as indicated by the independence of the first positive intensity on [N] and the high photon yields found in this regime. In this case, the rise time sets a lower limit on the rate constant for reaction 7. This treatment yields a value $k_7 \geq 6 \times 10^{-11} cm^3 s^{-1}$. The rate constant reported in Reference 15 $(1.6 \pm 1.1) \times 10^{-11} cm^3 s^{-1}$, was obtained from a steady-state treatment of the $N/Cl/HN_3$ reaction. A mechanism was assumed in which N and Cl atoms compete for N_3 produced by $Cl + HN_3$, a relatively slow process with a rate constant (Ref.28) of $1 \times 10^{-12} cm^3 s^{-1}$. Since, in the present experiments, the $F + N_3$ reaction is completely negligible, the operation of a reaction such as process 19 is required to explain the increase in intensity with N

atoms for $[N] \leq 4 \times 10^{13} cm^{-3}$. In principle, reaction 19 should also be important in the $N/Cl/HN_3$ system, since in the experiments show the sum of the N and Cl atom densities was apparently on the order of $10^{13} cm^{-3}$. Inclusion of reaction 19 in the mechanism of the $N/Cl/HN_3$ system would result in calculation of a larger value of k_1 from the steady-state treatment. Hence, the data tend to support the higher value.

The exact nature of reaction 19 is unknown. Its operation has been suggested by a number of previous experiments with azide systems. In the reactions (Refs.2 and 18) of F atoms or mixed F and Cl atoms with HN_3, the admission of SF_6 or CO_2 to the reaction medium was observed to nearly double the intensities of emissions from excited singlet states of NF or NCl, respectively. One interpretation of this phenomenon is that these molecules serve to stabilize N_3 radicals produced by $F + HN_3$. This picture is supported by measurements (Ref.29) of the vibrational distribution in the HF product of this reaction, which is nearly statistical and heavily favor lower v levels. It seems likely, therefore, that a sizable proportion of the 55 kcal mol^{-1} released by $F + HN_3$ appears as internal excitation in N_3. Hence, loss of N_3 from the system may occur by unimolecular dissociation or by dissociation in collisions with species M (reaction 19). Since insufficient energy is available to produce the adiabatic dissociation products $N(^2D) + N_2(X^1\Sigma_g^+)$, collisions may be required to stimulate a jump to the quartet potential energy surface leading to $N(^4S) + N_2(X)$. Thermodynamically, dissociation to these ground-state fragments may require as little as 12 kcal mol^{-1}. The true barrier height, defined by the position of the doublet-quartet curve crossing, is likely to be considerably higher.

The measured N_2 B → A photon yields simply represent the flow of first positive photons relative to the HN_3 flow, for the particular conditions of the experiments. In all probability, the actual branching fraction for production of $N_2(B)$ by $N + N_3$ is much greater than the photon yield, since collisional quenching of $N_2(B)$ or removal of N_3 by other paths has not been taken into account. As noted, addition of large flows of CO_2 or SF_6 were found to nearly double the photon yields from halogen atom reactions with N_3, presumably by stabilization of the fragile azide radicals. No such additives were used in the present experiments, primarily because of the susceptibility of $N_2(B^3\Pi_g)$ to collisional quenching. This state is strongly coupled by collisions to the nearby $W^3\Delta_u$ state, such that the equilibrium-weighted lifetimes of coupled pairs of states can be considerably longer (by as much as an order of magnitude) than the lifetime of the $B^3\Pi_g$ state in the absence of collisions. (Ref.10) These extended lifetimes are such that collisional quenching can be a significant problem at the densities of the experiments. For example, admission of CO_2 to the system at a density of $2 \times 10^{14} cm^{-3}$ (about a factor of 30 smaller than the densities used in the halogen atom-N_3 experiments) was found to quench the visible first positive emission to one-half its initial value. It would seem, therefore, that optimum operation of the $N + N_3$ reaction may well involve a trade-off between stabilization of the N_3 radicals and quenching of excited N_2.

The high yield of $N_2(B)$ is as expected from the angular momentum constraints operative in the system. This result, coupled with an observation that the rate constant of the $N + N_3$ reaction is $> 6 \times 10^{-11} cm^3 s^{-1}$, suggests that this is a promising system for the production of large flows of $N_2(A)$ metastables as required by a laser

device. Further assessment of this potential requires investigation of the detailed kinetics of the N_3 radical in the reaction medium, and in particular measurement of the actual value of the rate constant for $N + N_3$.

IV. Rates of Reactions of the Azide Radical

A primary consideration in evaluating a chemical source of triplet N_2 metastables is how well its rate competes with energy loss from the $N_2(A^3\Sigma_u^+, B^3\Pi_g, W^3\Delta_u)$ pool. As the rate of energy loss will be roughly one-half the rate of the $2N_2(A) \rightarrow N_2(C) + N_2(X)$ pooling process ($k = 2 \times 10^{-10} cm^3 s^{-1}$), either the rate constant of the formation process must be large, or a large excess of the reagents (relative to $N_2(A)$) must be present. In the case of the $N + N_3$ reaction, the pseudo-first order reagent is N atoms, which can also act as a quencher of $N_2(A)$. Hence, the rate constant of the $N + N_3$ reaction must be substantially greater than that of $N_2(A)$ quenching by N atoms (Ref.23) ($k = 3 \times 10^{-11} cm^3 s^{-1}$) in order for this to be a viable system.

Another reaction of particular importance in all azide-based systems is the self-removal of N_3 radicals, $N_3 + N_3 \rightarrow$ products. Two mechanisms have been proposed for this process, a direct bi-molecular reaction yielding second order kinetics

$$N_3 + N_3 \rightarrow 3N_2 \ , \qquad (26)$$

and a two-step process in which free N atoms act as an intermediate:

$$N_3 + M \rightarrow N + N_2 + M \qquad (27)$$

$$N + N_3 \rightarrow 2N_2$$

As shown, reaction 27 efficiently produces $N_2(B^3\Pi_g)$ and, hence, $N_2(A^3\Sigma_u^+)$ by B → A radiation. The two-step process would have kinetics which are pseudo-first order in M. A number of authors have discussed the nature of the self-removal reaction and its rate. Evidence was found for both the first and second order processes (Ref.30), and determined a bimolecular rate constant on the order of $5 \times 10^{-12} cm^3 s^{-1}$. A similar rate

constant was reported in Reference 31. Reference 32 reports the generation of N_3 radicals from thermal decomposition of NaN_3, and shows evidence that the self-removal reaction produces N_2 first positive ($B^3\Pi_g \rightarrow A^3\Sigma_u^+$ emission. From a mass spectrometric study of the decomposition of ClN_3, Reference 33 reported the rate constant of reaction 26 to be $8 \pm 3 \times 10^{-11} cm^3 s^{-1}$. Finally, N_3 radicals have been produced from the rapid reaction of HN_3 with fluorine atoms (Ref.34). N_2 first positive emission was observed from the self-removal process, but pseudo-first and second order mechanisms could not be distinguished. The N_2 emission intensity was found to increase at a faster than linear rate with increasing N_3 concentration, which was monitored directly by absorption methods.

Observations of processes which remove N_3 radicals produced by the $F + HN_3$ reaction are described in this Section. Rate constants are reported for the reaction of N_3 with F atoms, N atoms, and the products of the $F + HN_3$ reaction (thought to be primarily HF and N_3) as well as the rate of N_3 removal at Teflon and Pyrex walls. Apart from this kinetic information, the data obtained offer insight regarding the mechanism of the azide self-removal process.

1. Rate Constant Measurements

The majority of these experiments were performed with the Teflon discharge-flow reactor shown in Figure 4. A few experiments were performed with the Pyrex (or halocarbon wax-coated Pyrex) reactor.

Admission of HN_3 to a large excess flow of fluorine atoms produced the bright green flame corresponding to the $b^1\Sigma^+ \rightarrow X^3\Sigma^-$ transition in NF, as discussed previously. As the flow rate of the fluorine atoms (produced by a discharge through CF_4 diluted in Ar) was reduced to the point where the

densities of F atoms and HN_3 were nearly equivalent (~ 3 X $10^{12}cm^{-3}$), a distinct color change was observed, the flame becoming a dull red color. The visible spectrum of the flame under these conditions was recorded and is shown in Figure 16. All features evident in the spectrum are attributed to the first positive ($B^3\Pi_g \rightarrow A^3\Sigma_u^+$) transition in N_2. It is evident from the spectrum (and from the visual color of the flame) that the steady-state vibrational population distribution in $N_2(B^3\Pi_g)$ heavily favors the lower vibrational levels. As shown in the figure, population of levels up to v = 7 is observed.

The time dependence of the N_2 first positive emission was determined by movement of the HN_3 injector with respect to the fixed position of the observation port. For experiments in which HN_3 was admitted to large excess flows of fluorine atoms ([F] > $10^{13}cm^{-3}$), the time profile of the emission exhibited a short rise (corresponding to the finite mixing time in the system) followed by a slow decay over several milliseconds. Since the initial reaction between fluorine atoms and HN_3 has a rate constant 1.6 ± 0.3 X $10^{-10}cm^3s^{-1}$, the products of this reaction are generated in < 1 ms for these densities of excess F atoms. Evidence from both chemiluminescence (Refs.18 and 27) and photoelectron spectroscopic studies (Ref.35) of the F + HN_3 system indicates that these products are largely HF and N_3. Consequently, we identify the decay of the N_2 first positive emission as corresponding to the rates of processes which remove N_3 from the system.

To investigate the rate of removal of N_3 by excess fluorine atoms, the time profile of the N_2 first positive emission was measured for a fixed initial HN_3 density near 1 X $10^{13}cm^{-3}$ and various F atom densities up to 3 X $10^{13}cm^{-3}$. In each case, the observed decay of the emission was

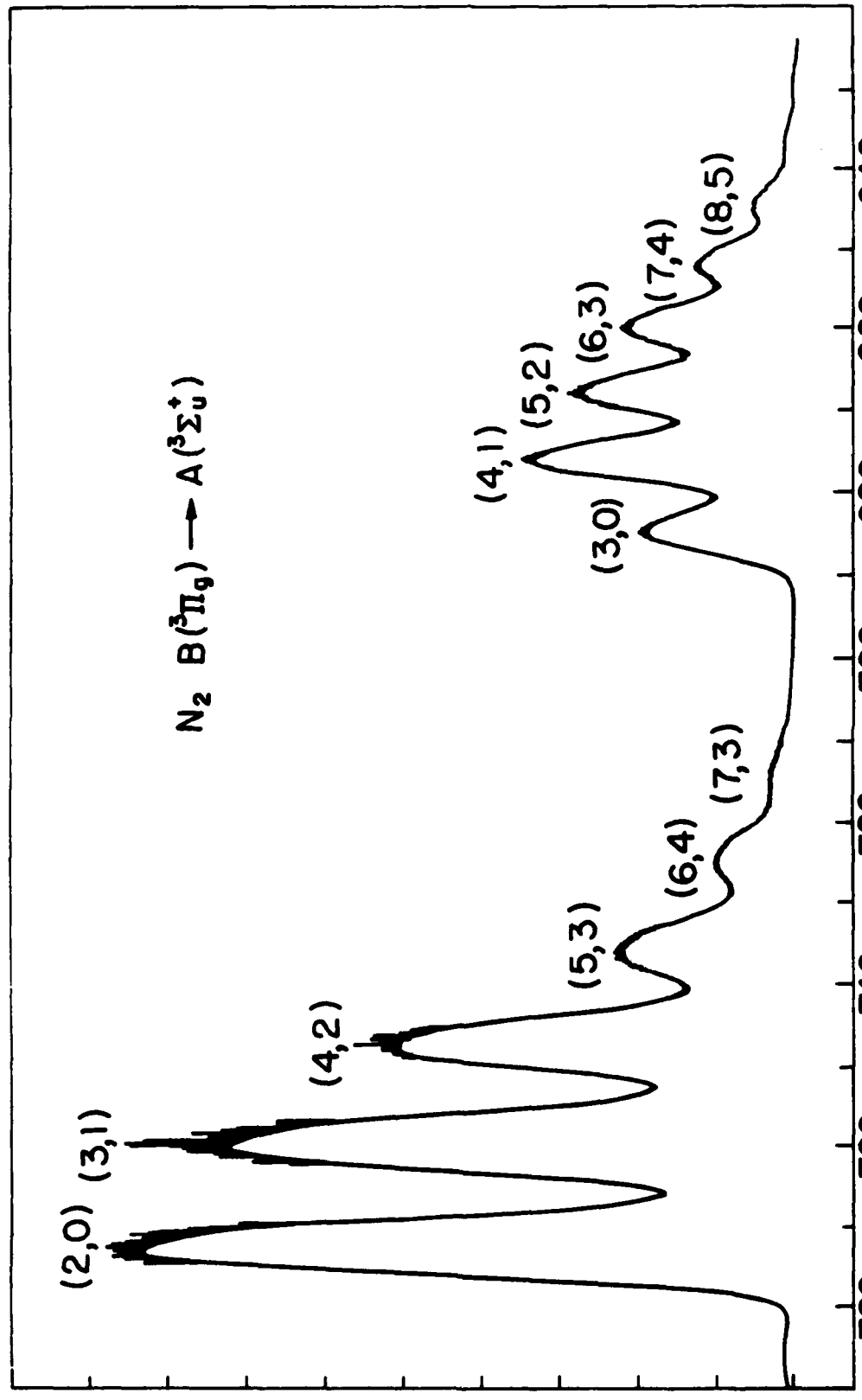

Figure 16. A portion of the spectrum of visible emission produced by the F + HN_3 reaction for $[F]_o = [HN_3]_o = 3 \times 10^{12}$ cm^{-3}.

well fit by an exponential function, although the reagent densities would suggest the kinetics of the system to be intermediate between first and second order (assuming F + HN_3 to produce a high yield of N_3). Attempts at fitting the data to second order kinetics gave poor results. Figure 17 shows a plot of the exponential decay rate of the N_2 emission versus the F atom density from a number of experiments. The slope of the linear least squares line through the data indicates the rate constant for the removal of N_3 by the excess F atoms. To evaluate this rate constant, however, we must know whether the production of excited N_2 is first or second order in N_3. Since the data suggest that production of one $N_2(B)$ requires two N_3 molecules, we calculate a rate constant $k = 1.8 \pm 0.4 \times 10^{-12} cm^3 s^{-1}$ for the F + N_3 reaction. This value is in excellent agreement with the approximate result reported several years ago (Ref.27). The uncertainty noted in the present result is larger than that corresponding to the scatter in Figure 17, in order to account for possible error associated with treatment of the N_3 decay as a pseudo-first order process.

The $[F]_{excess} = 0$ intercept in Figure 17 corresponds to the rate of N_3 removal by the products of the F + HN_3 reaction (HF and N_3) and by the Teflon surfaces in the flow reactor. To determine the rates of these processes, a series of experiments were performed in which the decay of the N_2 first positive emission was measured for various initial equivalent densities of fluorine atoms and HN_3 in the range 2×10^{12} to $2 \times 10^{13} cm^{-3}$. Here again, the measured decays were well fit by an exponential function. Figure 18 shows a plot of the decay rate versus the initial density of HN_3 and fluorine atoms. From the slope of the plot, the rate constant for N_3 removal by the products of the F + HN_3 reaction is $2.0 \pm 0.4 \times 10^{-12} cm^3 s^{-1}$. The intercept in Figure 18, $[F]_o = [HN_3]_o = 0$, gives the rate constant for

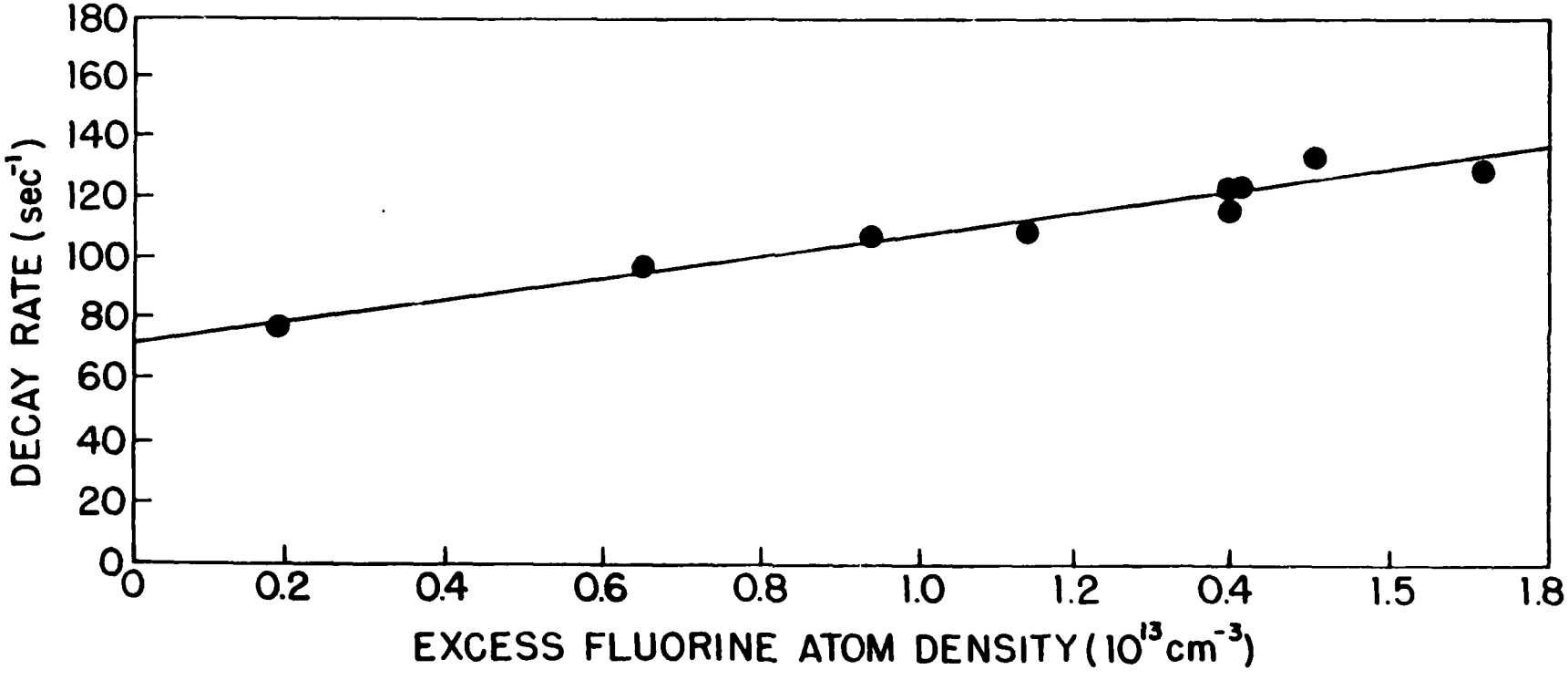

Figure 17. Rate of exponential decay of the N_2 first positive emission versus the excess density of fluorine atoms ($[F]_o$-$[HN_3]_o$). The slope of the least squares fit indicates a rate constant $k = 1.8 \pm 0.4 \times 10^{-12} cm^{-3} s^{-1}$ for the F + N_3 reaction.

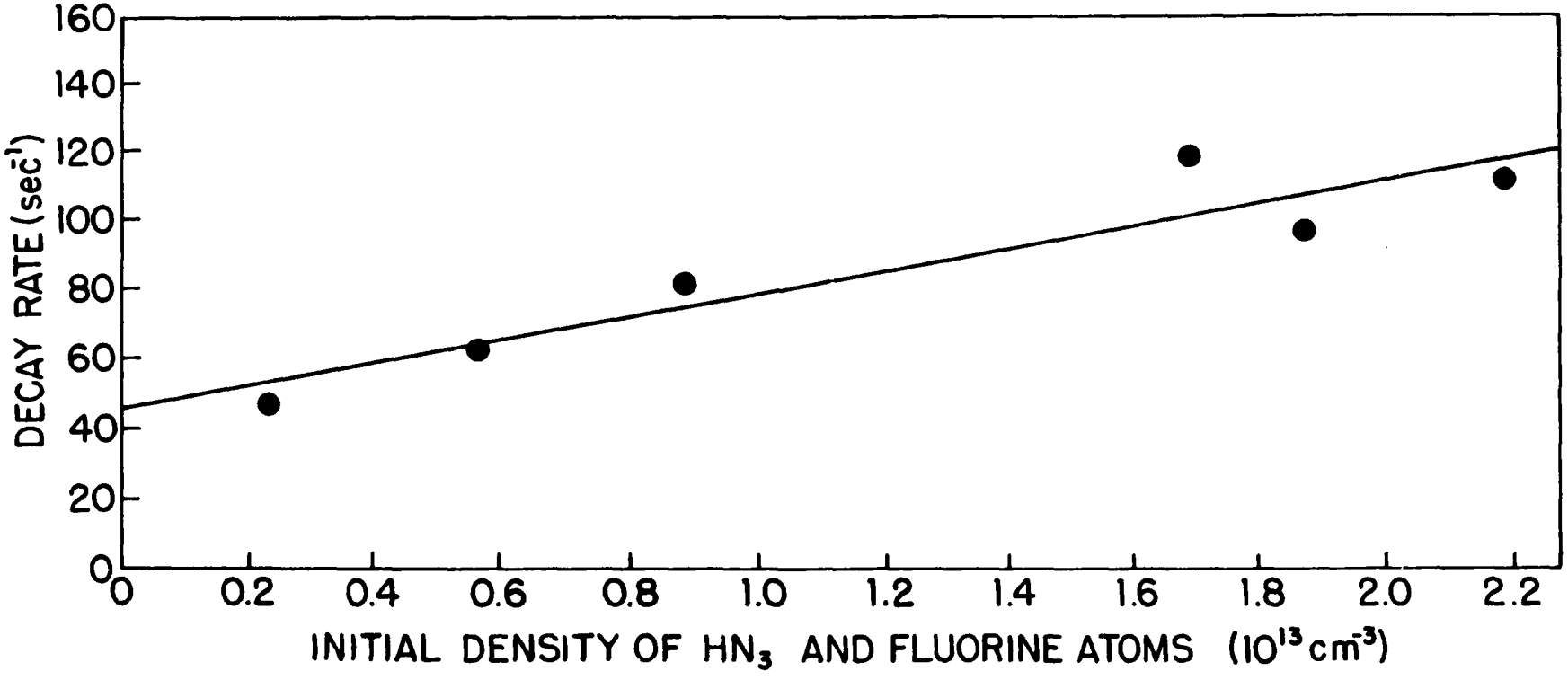

Figure 18. Rate of exponential decay of the N_2 first positive emission versus the initial equivalent densities of HN_3 and F atoms.

removal of N_3 by the Teflon surfaces, $46 \pm 0.4\ s^{-1}$. This value corresponds to a surface quenching efficiency $\gamma = 4X10^{-3}$ for our system. A series of analogous experiments were performed in order to measure N_3 removal rates for Pyrex and halocarbon wax-coated surfaces. These experiments were performed with Pyrex or wax-coated Pyrex flow reactors similar to the Teflon system. In these experiments, however, the intensity of the N_2 first positive emission was too low to be accurately measured, indicating the possibility of a large N_3 surface removal rate. To further investigate this issue, experiments were performed using the Teflon flow reactor with Pyrex rods of varying sizes inserted to give various relative surface areas of Teflon and Pyrex. It was observed that for a Teflon : Pyrex surface area ratio of 2.2 : 1 the peak intensity of the N_2 first positive emission was reduced by a factor of 2, but the time decay rate of the emission (corresponding to the removal of N_3) was unchanged.

Further information regarding the origin of the N_2 first positive emission in the F + HN_3 system was obtained from observation of the emission time profile in experiments where the initial density of HN_3 was very low ($< 5 \times 10^{12}$). In such cases, a distinct risetime was observed, as shown in Figure 19. This rise is substantially slower (by at least a factor of 3) than the rate of production of N_3 calculated from the reagent densities and the known rate constant of the F + HN_3 reaction. N_2 B → A time profiles were measured for a number of initial HN_3 densities in the range 2×10^{12} to $9 \times 10^{12} cm^{-3}$, for a fixed initial F atom density of $1 \times 10^{13} cm^{-3}$. The time profiles were fitted to a sum of rising and falling exponential functions to obtain a measure of the rate corresponding to the rise of the emission. Although these data showed considerable scatter, a real trend was evident in which the risetime shortened with increasing

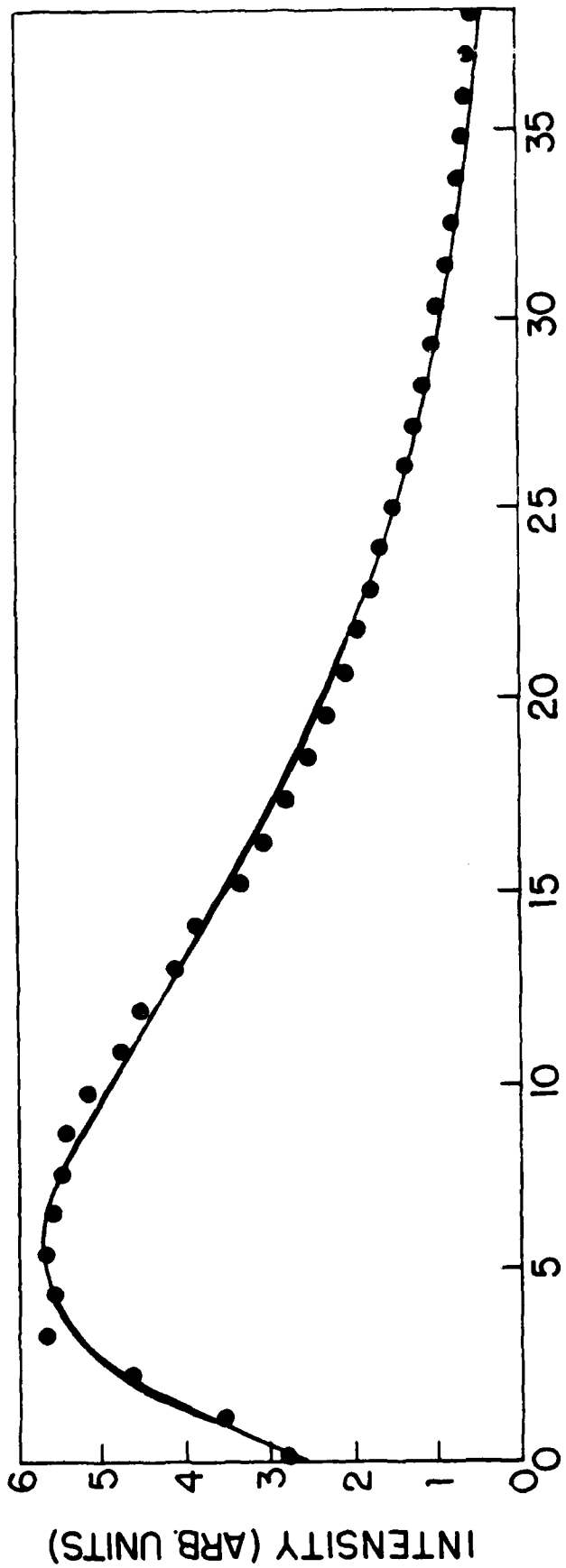

Figure 19. Time profile of the N_2 first positive emission for $[F]_o = 1 \times 10^{13} cm^{-3}$ and $[HN_3]_o = 2 \times 10^{12} cm^{-3}$.

HN_3 density. These observations of the risetime were interpreted to indicate the production of a species which reacts with N_3 to produce $N_2(B)$. In view of previous results, N atoms are the most likely candidate for the reactive species.

The rapid production of N_3 radicals by the F + HN_3 reaction in an environment where their decay is slow affords an opportunity to measure rate constants of reactions of N_3 with added species. An example is the measurement of the F + N_3 rate constant. A rate constant of particular importance in analyzing the present data is that of the N + N_3 reaction. In the initial work on this system, only a lower limit rate constant for this process, $k \geq 6 \times 10^{-11} cm^{-3} s^{-1}$ was measured. Hence, we performed a number of new experiments to obtain an explicit value for this parameter. For this purpose, N atoms were produced by microwave discharge through N_2/Ar mixtures upstream of the second movable injector. The N atom concentrations in the flow reactor were determined by titration with NO. In the experiments, HN_3 and N atoms were admitted to the F atom stream at the same point relative to the fixed observation port, and the decay of the N_2 first positive emission was measured by movement of the two injectors in unison. The F atom density was maintained at $1 \times 10^{13} cm^{-3}$ and the HN_3 density at $6 \times 10^{11} cm^{-3}$, such that N_3 radicals were produced in less than 1 ms at a density substantially less than that of the added N atoms (i.e., the system was pseudo-first order in N atoms). The N_2 first positive emission observed from addition of N atoms to the F + HN_3 system was more intense by about three orders of magnitude than that produced by F + HN_3 alone, as described previously. In this case, the emission is produced by the pseudo-first order reaction of N_3 with excess N atoms and the observed time decay of the emission reflects the rate of the N + N_3 reaction. A

number of experiments were performed in which the exponential decay rate was measured for various densities of N atoms, and the results are shown in Figure 20. From the slope of the linear plot, a rate constant $k = 1.4 \pm 0.2 \times 10^{-10} cm^3 s^{-1}$ is determined for the $N + N_3$ reaction. This value is consistent with the upper limit determined previously.

2. Kinetic Model for Competitive N_3 Reactions

The data suggest that the direct second order recombination of N_3 radicals is not in fact a rapid process. If it is accepted that the products of the $F + HN_3$ reaction are predominantly HF and N_3, then the rate constant for $N_3 + N_3 \rightarrow$ products can be no greater than $2 \times 10^{-12} cm^3 s^{-1}$. Further, the time decay of the N_2 B → A emission observed in the various experiments had an exponential form in every case, indicating that first order or pseudo-first order processes are most important in the removal of N_3 from the system. It is also clear from the data that $F + HN_3$ produces only a small fractional yield of N atoms, if any are produced at all. From the rate constant determined for the $N + N_3$ reaction ($1.4 \times 10^{-10} cm^3 s^{-1}$) and the observed rate constant for loss of N_3 from the system ($10^{-12} cm^3 s^{-1}$) the yield of N atoms must be much less than 1 percent. As noted above, the N_2 first positive intensity increases by more than two orders of magnitude when N atoms are admitted to the flow reactor from a microwave discharge source. In fact, the $N + N_3$ reaction is an extremely sensitive detector for the presence of N atoms.

On the other hand, the data suggest that the N_2 B → A emission observed from $F + HN_3$ is not produced by direct N_3 recombination, but rather by reaction of N_3 with another species, probably N atoms. The slower rise of the N_2 emission intensity observed at lower reagent flows may well correspond to the initial build-up of a small N atom density in the system.

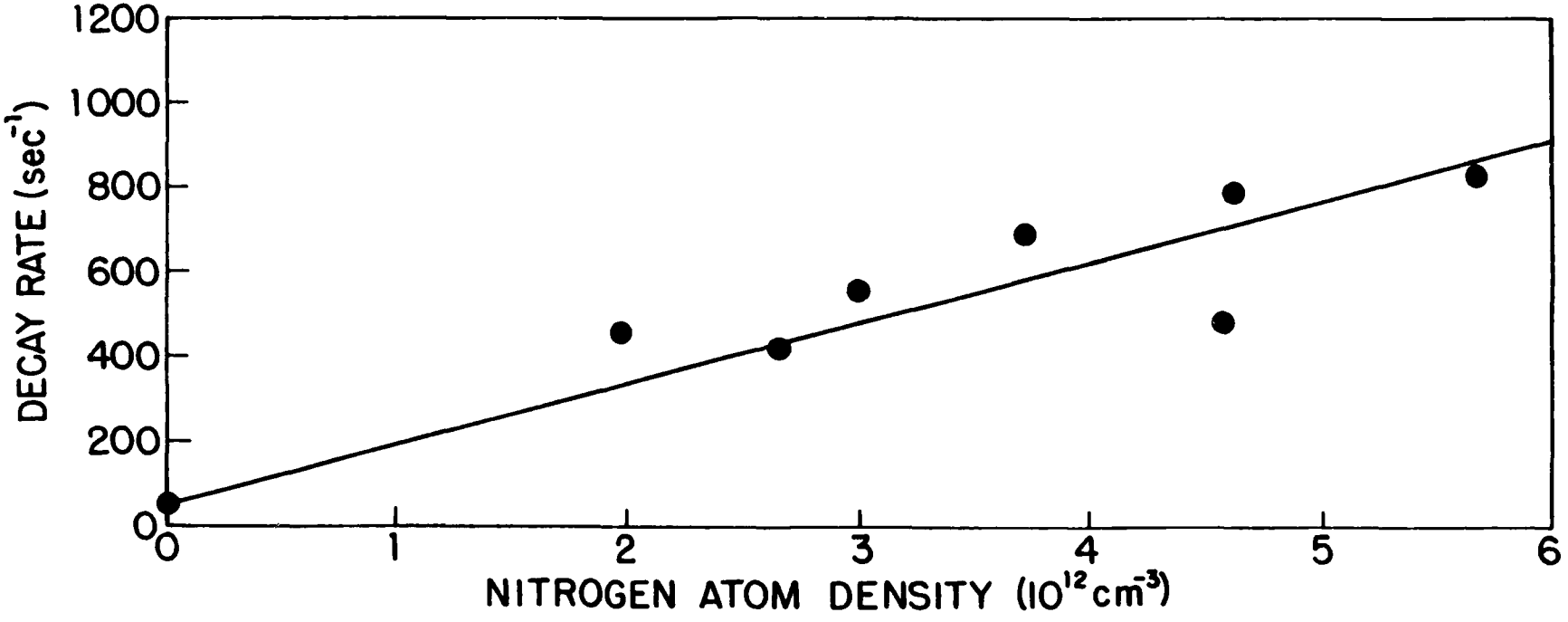

Figure 20. Rate of exponential decay of the N_2 first positive emission versus the density of added nitrogen atoms. The $[F]_o = 1 \times 10^{13}cm^{-3}$, $[HN_3]_o = 6 \times 10^{11}cm^{-3}$. The slope of the least squares fit yields a rate constant $k = 1.4 \pm 0.2 \times 10^{-10}cm^3s^{-1}$ for the $N + N_3$ reaction.

Since this rise is slower than the rate of the F + HN_3 reaction for those conditions, the atoms are not produced directly but must arise from subsequent N_3 dissociation. For example, N_3 may be dissociated by collisions with the surfaces of the flow reaction or by collisions with vibrationally excited HF produced as a coproduct of the F + HN_3 reaction. In view of the speed of the N + N_3 reaction, which would rapidly remove N atoms under the conditions of our experiment, the atoms must be continuously produced over the time duration of the observed N_2 first positive emission. This fact argues against dissociation by excited HF (for which collisional and radiative relaxation is rapid) (Ref.36) and supports a surface dissociation mechanism for the source of the N atoms in the system. In any event, the steady state N atom density produced in the system must be small indeed so as to make only a small contribution to the removal of N_3 from the system. For example, the measured surface removal rate of 46 s^{-1} may reflect a mechanism in which N_3 is dissociated in a small fraction of its collisions with the walls. The N atoms produced react with other N_3 radicals to efficiently generate $N_2(B)$ and subsequently $N_2(A)$ metastables. The $N_2(A)$ metastables can dissociate collisionally other N_3 radicals, regenerating the N atoms. Hence, the observed surface removal rate may reflect the operation of such a chain rather than the efficiency of individual wall collisions.

If it is assumed that the N_2 first positive emission is produced by the N + N_3 reaction, its intensity can be described by the following steady-state expression:

$$I \propto [N_2(B)] = \frac{k_7[N][N_3]}{k_r} \qquad (28)$$

where k_7 is the N + N_3 rate constant (1.4 X $10^{-10}cm^3s^{-1}$) and k_r is the N_2 B → A radiative rate (1.6 X 10^5s^{-1}). Hence the intensity varies as the product of the N and N_3 densities. Since the fluorine atom densities used in these experiments are such that the time constant of the F + HN_3 reaction is short (mixing limited), the N_3 density can be described as an exponential decay:

$$[N_3] = [N_3]_o e^{-(k_w + k_q[Q])t} \qquad (29)$$

where $[N_3]_o$ is the initial N_3 density produced by F + HN_3 (approximately equal to the initial HN_3 density), k_w is the measured wall removal rate (46 s^{-1}) and $k_q[Q]$ refers to the rate of pseudo-first order removal by other species Q (e.g., excess fluorine atoms, HF, or added N atoms). We propose the following model to describe the time dependence of the nitrogen atom density:

$$N_3 \xrightarrow{k_w} N + N_2 \qquad (30)$$

$$N \xrightarrow{k_7[N_3]} N_2 + N_2 \qquad (7)$$

$$N \xrightarrow{k^N_w} 1/2N_2 \qquad (31)$$

In reaction 7, N atoms are removed at a pseudo-first order rate $k_3[N_3]$. Although the N_3 density decays in time as in Equation 29, this decay (on the order of 100 S^{-1}) is slow relative to the time constant of Reaction 7 (on the order of 1000 s^{-1} for a typical HN_3 flow rate). Reaction 31 describes first order removal of N atoms by the reactor walls at a rate k^N_w. Although this process is in principle much slower than Reaction (7), it may affect the N_2 first positive intensity when the N_3 density is low. From Reactions 29, 30, 7, and 31, the time dependence of the N atom density is given by a sum of rising and falling exponential terms:

$$[N] = C_1 e^{-(kw+k_q[Q])t} - C_2 e^{-(k_7[N_3]+k^N_w)t} \quad (32)$$

where C_1 and C_2 are constants. Note that the exponential in $[k_7[N_3] + k^N_w]$ reflects the apparent rise of the N atom density. The intensity of the N_2 B → A emission is proportional to $[N][N_3]$:

$$I \propto C'_1 e^{-2(k_w+k_q[Q])t} - C'_2 e^{-(k_7[N_3]+k^N_w+k_w+k_q[Q])t} \quad (33)$$

For small $k_q[Q]$, as in the case of excess fluorine atoms, the rise of the emission is dominated by $k_7[N_3]$, the rate of the N + N_3 reaction. The rise shortens with increasing $[N_3]$ (i.e., $[HN_3]_o$), as observed. The decay is given by twice the rate of removal of N_3 from the system (in agreement with the fact that two N_3 radicals are still required to produce one N_2(B) molecule; one to generate an N atom and one to react with that N atom). This factor of 2 was taken into account in the rate constants reported.

In the experiments with the Pyrex inserts in the Teflon reactor, the decay of the N_2 emission was found to be unchanged relative to the decay without the inserts (suggesting that k_w and $k_q[Q]$ are unchanged), but the overall intensity was reduced. From this model, we interpret this observation to reflect an enhanced removal of N atoms by the Pyrex surface (i.e., a larger k^N_w). In reality, the surface was not clean Pyrex but Pyrex exposed to a substantial flow of fluorine atoms and HF. This model also offers an explanation for the widely varying values of the apparent N_3 + N_3 rate constant reported in References 30,31,32,33. When the experimental circumstances are such that only a small proportion of the azide radicals dissociate (as in the present case), the N_3 + N_3 reaction has a minimal effect on the overall rate of N_3 removal and this rate is determined to be slow. For conditions which favor greater fractional dissociation of N_3, the chain driven by N + N_3 may result in a large

apparent N_3 removal rate. Indeed, production of N_3 under conditions where a large fraction (50%) dissociates may well offer a rapid and efficient source of $N_2(B)$ and $N_2(A)$ metastables for use as storage agents in potential laser systems.

V. Reactions of N Atoms With Molecular Azides

Some years ago, the production of $N_2(B^3\Pi_g)$ by the interaction of ClN_3 with excess nitrogen atoms was noted in Reference 14. On the basis of these data, the operation of the two step mechanism reactions 6 and 7 (in which N_3 radicals act as an intermediate) was postulated. To further illucidate the operation of the N atom/molecular azide systems, the reactions of N atoms with HN_3, ClN_3, and BrN_3 have been studied. In these systems, excited N_2 may be produced by processes analogous to Equasions 6 and 7, if the initial interaction produces N_3 radicals. Since $N + N_3$ is rapid and efficiently generates $N_2(B)$, it is likely that these systems will in fact be limited by their ability to generate N_3. The $BrN_3 + N$ reaction is of particular interest since, because of the metastability of this fragile azide, direct production of excited N_2 is also possible:

$$N + BrN_3 \rightarrow Br + N_2 + N_2 \quad \Delta H = -223 \text{ kcal/mole} \qquad (34)$$

The effort on these systems was comprised of measurements of the rates of removal of N atoms by HN_3, ClN_3, and BrN_3, investigation of the $N + BrN_3$ chemiluminescent system, and measurement of rate constants for $N_2(A)$ quenching by HN_3, ClN_3, and BrN_3. This work was supported in part by grants from AFOSR (Grant No. AFOSR-0031-84) and NSF (Grant No. CHE-820533).

1. $N(^4S_u)$ Removal by Molecular Azides

Rate constants for the reactions of nitrogen atoms with various azide species were determined by using a discharge-flow apparatus in conjunction with an apparatus for detection of relative densities of $N(^4S_{3/2})$ atoms by vacuum-UV resonance fluorescence on the ^4S-^4P transition at 120 nm. Nitrogen atoms, at densities on the order of $10^{11} cm^{-3}$, were produced by passage of N_2/He mixtures through a 2450 MHz microwave discharge. Reagent

species (BrN_3, ClN_3, or HN_3) were admitted to the flow through a sliding injector. The pressure in the flow reactor was measured with an oil manometer. Typical conditions were such that a linear flow velocity of 1050 cm s^{-1} was obtained for a pressure near 750 m Torr. The resonance fluorescence cell was fabricated from an aluminum block which served to configure the flowing gas stream, N atom lamp, and detection system in mutually perpendicular directions. The lamp consisted of a microwave discharge through a flowing N_2/He mixture. The detection system consisted of a 0.2 m monochromator (Acton Research VM-502) coupled with a CsI solar blind photomultiplier tube. The response of the PMT was monitored with a discriminator and scaler for photon counting. A curve of growth for the resonance fluorescence system was determined by measurement of signal intensities for N atom densities determined by chemiluminescent titration with NO. The curve of growth (intensity versus density) was found to be linear only for atom densities below 10^{12} cm^{-3}.

The flow rates of reagent and diluent gases were measured with Tylan FM-360 mass flowmeters. The HN_3 was prepared by the NaN_3-stearic acid reaction. Gaseous ClN_3 and BrN_3 were generated as described in detail previously (Refs. 2 and 3) by passage of the molecular halogen over H_2O-moistened NaN_3 suspended on glass wool at 273 K. Concentrations of ClN_3 and BrN_3 were determined by on-line continuous measurement of IR and UV absorptions.

In the experiments, large excess flows of the azides (corresponding to densities greater than 3 X $10^{13}cm^{-3}$) were admitted to the N/Ar flow via a sliding injector, upstream of the position at which N atoms were detected by resonance fluorescence. The time decay of the N atom signal was measured for various flows of the azides. For the greatest azide flows,

the N atom density was found to decay a maximum of 20 percent over the entire length of the flow reactor, corresponding to a decay rate no greater than 5 s^{-1}. From this observation and the azide densities (determined by spectroscopic means), the rate constants for reactions of $N(^4S_u)$ atoms with BrN_3, ClN_3, and HN_3 would appear to be no greater than 1.5 X $10^{-13} cm^3 s^{-1}$.

During the course of the N + BrN_3 experiments, emission spectra recorded in the 150 nm range were found to exhibit a number of distinct features attributable to excited electronic states of bromine atoms. This spectrum is shown in Figure 21. The transitions in question are the well-known 4^2P_J - 5^2P_J resonance lines of these atoms. The same emission features were found when a flow of Br_2 (also at a steady-state density near $10^{13} cm^{-3}$) was added to the N atom stream. Results similar to these were reported some years ago in References 11 and 12 from experiments in which molecular halogens were added to active nitrogen flows. The rate constants for the initial reactions between N atoms and the halogen molecules were reported to be quite small (Ref. 37); for example, the rate constant for N + Br_2 was found to be 3.4 X 10^{-15} $cm^3 s^{-1}$. To observe the rates of these processes in the flow reactor, a series of brief experiments was performed with much higher flows of N atoms, such that the steady-state density was near that used in the chemiluminescence experiments described in paragraph 2 below. Admission of a comparable flow of Br_2 to the stream (such that the initial densities of both N and Br_2 were near 1 X $10^{13} cm^{-3}$) resulted in rapid quenching of the visible nitrogen afterglow. The half time of the decay of the emission was near 5 ms, suggesting a second order rate constant on the order of $10^{-11} cm^3 s^{-1}$. The emission from electronically excited bromine atoms exhibited a rise over the same time frame, followed by a slow decay.

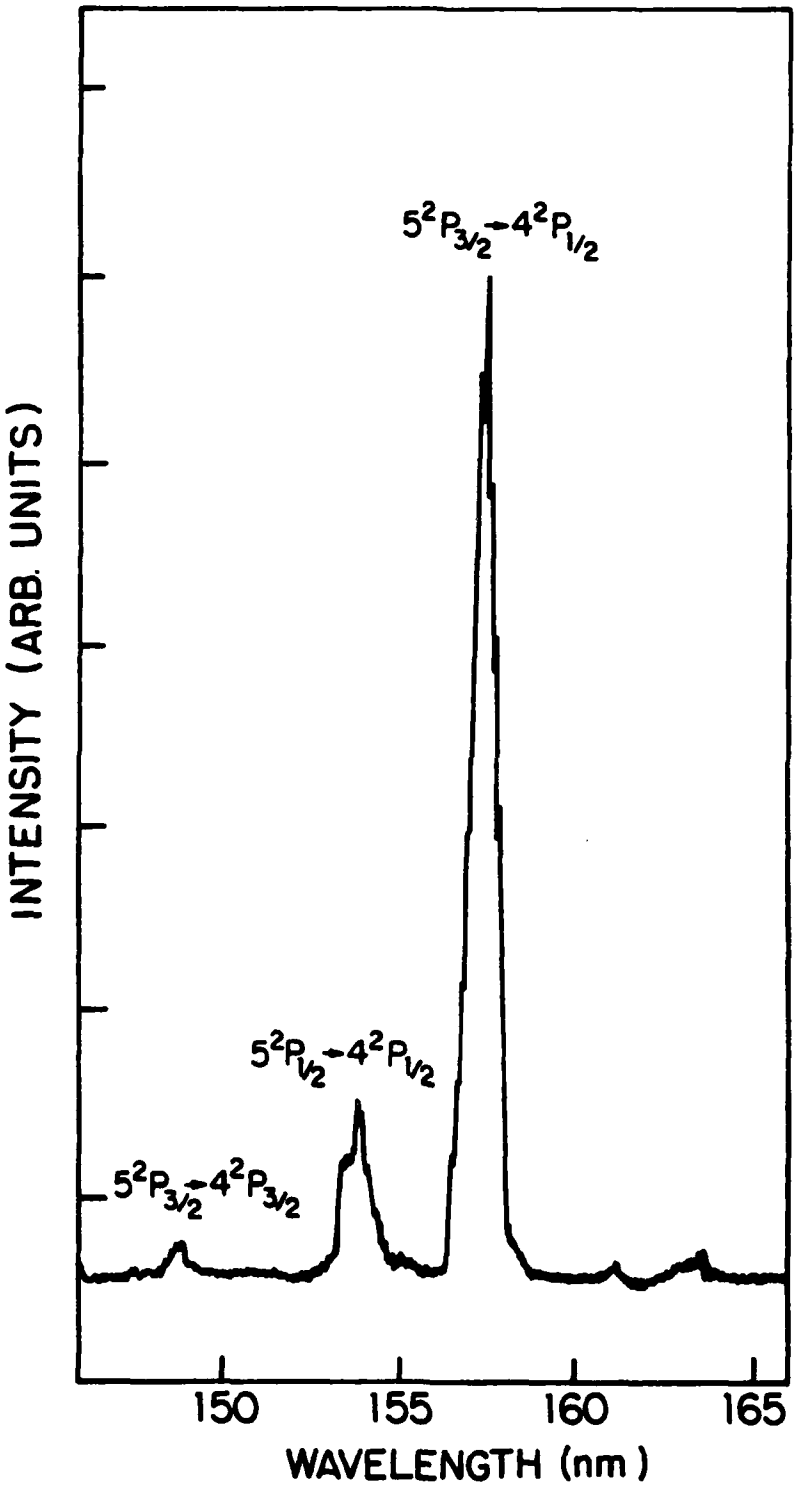

Figure 21. Spectrum of vacuum-UV emission produced by addition of excess BrN_3 to N atoms. The resonance lines of atomic bromine are labeled.

From these observations, it seems that the chemistry in the N + BrN_3 system may well occur at a much faster rate than is implied by the apparent loss of N atoms from the system. It is possible that the N + BrN_3 reaction regenerates the N atom reagent with the coproducts NBr and N_2. Excited bromine atoms might then be formed by a mechanism such as that suggested by Phillips,

$$N + NBr \rightarrow N_2^* + Br \quad (35)$$

$$N_2^* + Br \rightarrow N_2 + Br^* \quad (36)$$

where N_2^* and Br* are electronically excited species.

2. Chemiluminescence from Active Nitrogen + BrN_3

Chemiluminescence from the interaction of BrN_3 with a stream of active nitrogen was investigated with a Pyrex discharge flow reactor similar to that described previously and shown in Figure 3. Nitrogen atoms were produced by passage of N_2 heavily diluted in Ar through the discharge. The density of N atoms produced in this manner was determined by using the standard NO titration (Ref. 20). Admission of small flows of BrN_3 through the sliding injector to large excess flows of N atoms ([N] > $10^{13}cm^{-3}$) produced a bright orange flame extending for several miliseconds down the length of the flow reactor. Figure 22 shows a portion of the spectrum of this flame recorded with the 0.25 m monochromator and GaAs PMT. The spectrum indicates that the emission corresponds to the N_2 first positive ($B^3\Pi_g \rightarrow A^3\Sigma_u^+$) system, with a number of excited vibrational levels of the $N_2(B)$ state having significant population. From spectra such as that shown in Figure 22 and published values for the radiative lifetimes (Ref. 21) of the relevant vibrational levels, the steady-state vibrational distribution in the $N_2(B)$ state was calculated. The distribution heavily favors the lower vibrational levels, and is fit reasonably well by an equilibrium

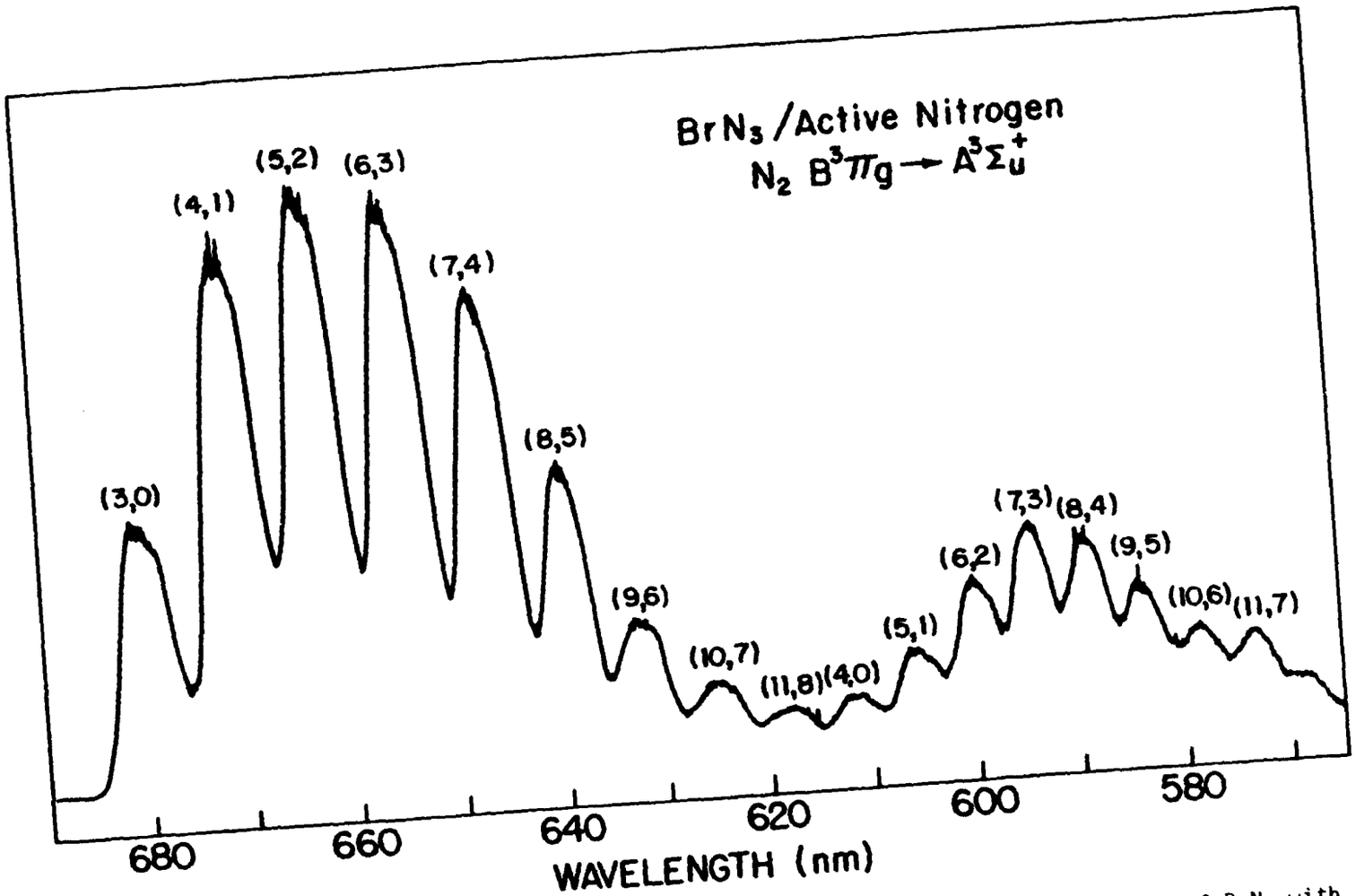

Figure 22. A portion of the spectrum of visible emission produced by the interaction of BrN_3 with active nitrogen.

thermal distribution corresponding to $T_{vib} \simeq 10,000$ K. This distribution (and, consequently, the visual appearance of the flame) is quite similar to that observed in previous experiments with the N + N_3 chemiluminescent reaction.

The time dependence of the N_2 first positive intensity was determined by movement of the BrN_3 injector with respect to the fixed position of the observation port. Figure 23 shows a typical time profile determined in this manner. The profiles exhibited a rise over a few milliseconds followed by a long decay, and were fitted well by a sum of rising and falling exponential terms as follows:

$$I(t) = Ce^{-\lambda_d t} - Ce^{-\lambda_r t} \qquad (37)$$

where λ_r and λ_d represent the rise and decay rates, respectively, and C is a constant. A number of experiments were performed to determine the behavior of the N_2 (B → A) time profile as the flow rates of BrN_3 and N atoms were varied. For a constant (excess) flow of N atoms, it was found that the decay (λ_d) was invariant with the BrN_3 flow rate but the rise rate (λ_r) decreased slightly with increasing BrN_3 flow. The time integrated intensity of the flame (determined from the fit to Eq. 37) was found to increase linearily with increasing BrN_3 flow. For a constant BrN_3 flow, the values of λ_r and λ_d were found to be independent of the flow rate of excess N atoms. The integrated intensity increased in a nearly linear fashion with the N atom density, however, as shown in Figure 24. As noted, similar behavior was observed from the N_2 first positive emission produced by the F + N + HN_3 chemiluminescent system, suggesting competition between the N atoms and another (unidentified) species for free N_3 radicals.

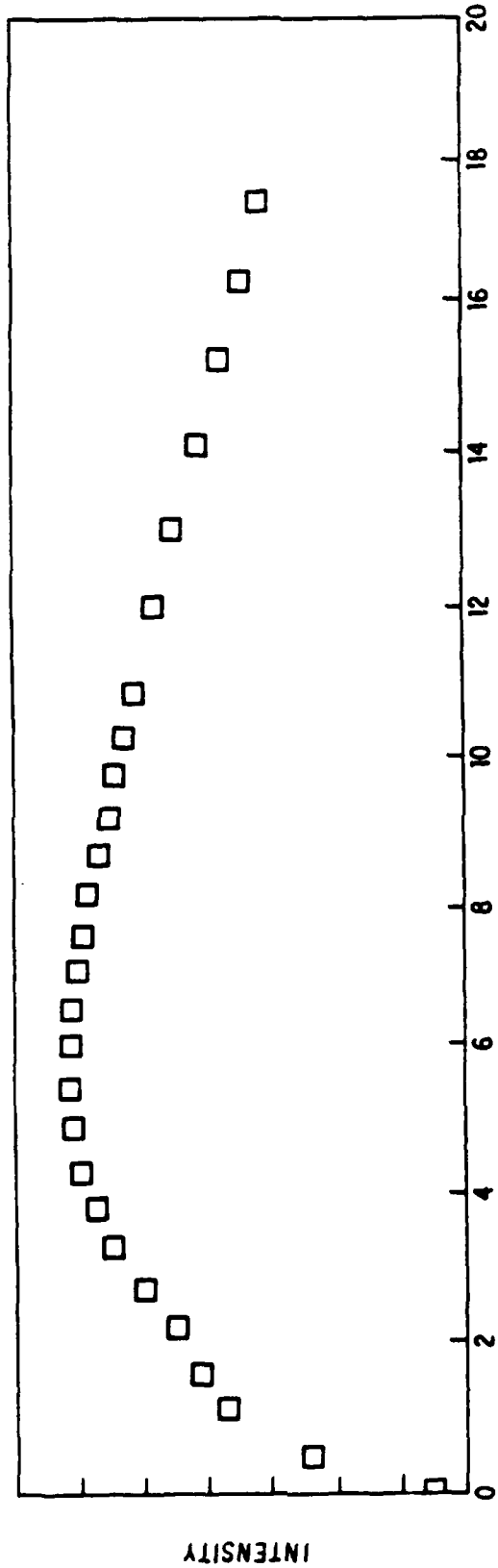

Figure 23. Typical time profile of the N_2 first positive emission produced by addition of BrN_3 to active nitrogen.

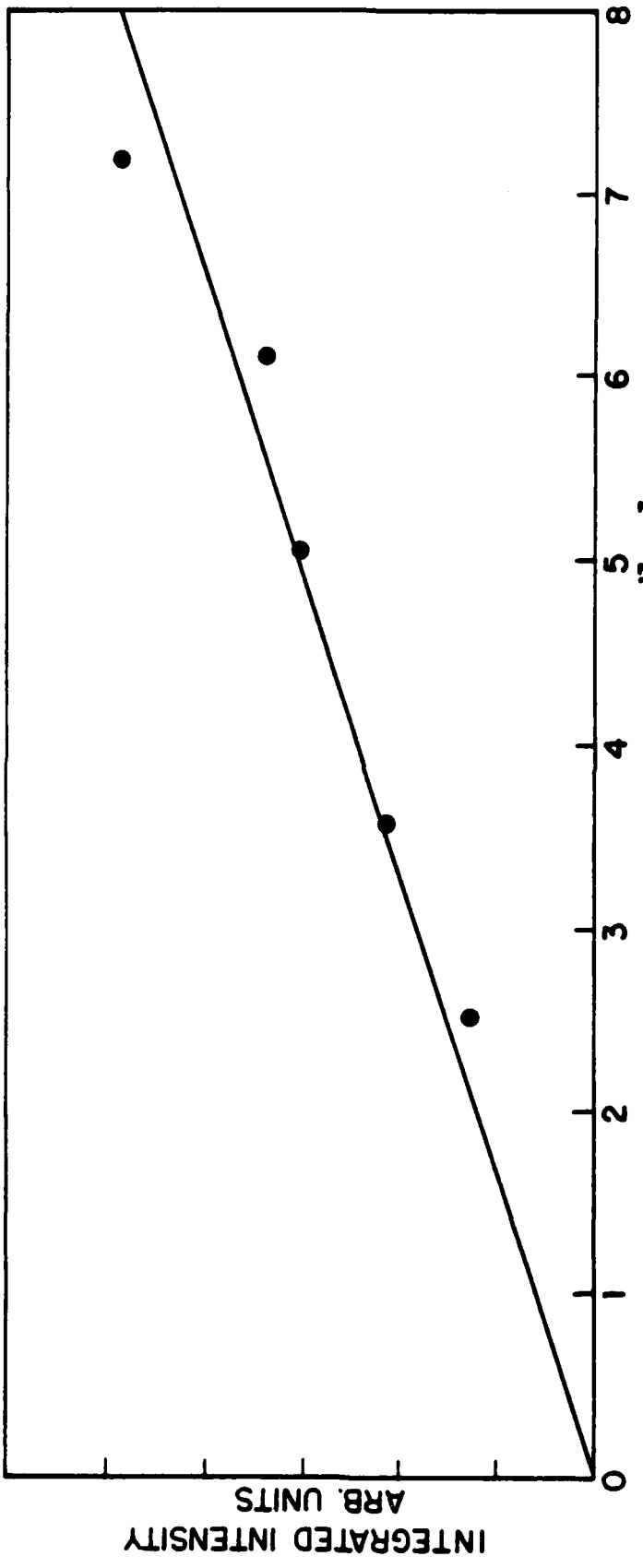

Figure 24. Variation of the time-integrated intensity of N_2 first positive emission from BrN_3/active nitrogen with the density of N atoms.

The yield of N_2 B → A photons produced by the N/BrN_3 system was determined by calibrating the light collection efficiency of the detection system with the O + NO chemiluminescent reaction (Ref. 24). The procedure used in the calibration was identical to that described previously. A number of independent measurements of the photon yield were made, resulting in a value $\Phi \simeq 30\%$ with respect to the limiting flow of BrN_3. As with all such measurements, the uncertainty in this result is a minimum of 50 percent of the stated yield. Nonetheless, the data clearly indicate that the photon yield is, in fact, quite large and is on the order of that previously determined for the N + N_3 reaction (≈20%).

A number of inferences concerning the origin of the chemiluminescence can be drawn from these observations. First, the time profile of the first positive emission, Figure 23, precludes the possibility of the direct reaction 34 being the pumping step. If $N_2(B)$ were produced directly, its time dependence would exhibit a mixing limited rise (corresponding to the N_2 B → A emission rate) followed by a decay characteristic of the rate of reaction 34. A rise over several miliseconds was found, and the decay was invariant with the densities of both N atoms and BrN_3.

In view of the rapid radiative decay of $N_2(B)$, the intensity of the chemiluminescence should be proportional to the rate of production of this excited species. From the spectrum of the first positive emission (i.e., the vibrational distribution in $N_2(B)$) and the photon yield relative to the BrN_3 flow rate, it seems quite probable that the pumping reaction is the N + N_3 process described in detail in Sections III and IV. Hence,

$$\text{Intensity} \propto k_7[N][N_3] \qquad (38)$$

and since k_7 and [N] are constant, the intensity will track the time dependence of the N_3 density. This time dependence will be essentially the

rate of formation of N_3, since azide radicals are removed at a constant rapid rate by the large excess of N atoms present. If the N_3 radicals are produced by reaction of BrN_3 with some species R, then the observed rise of the N_2 first positive emission must be characteristic of the rate of formation or decay of R. The decay of the emission would correspond to a combination of the decay or formation of R and the loss of BrN_3 from the system. Since the emission decays at a rate on the order of 30 s^{-1}, the density of R must be on the order of $10^{12} cm^{-3}$ (close to the densities of BrN_3 or Br_2) for a rate constant on the order of $10^{-11} cm^3 s^{-1}$. Bromine atoms are an obvious choice for the species R, since BrN_3 and Br_2 are present in comparable densities and the rate constant (Ref. 38) for Br + BrN_3 is $3.0 \times 10^{-11} cm^3 s^{-1}$. Just how the bromine atoms are produced is an intriguing question. As noted, Reference 37 reports the rate constant for N + Br_2 to be $3.4 \times 10^{-15} cm^3 s^{-1}$, far too slow to account for the formation of bromine atoms in the experiments. Nonetheless, the observation of emission from excited bromine atoms from both N + BrN_3 and N + Br_2 as described is clear evidence of the formation of these atoms. Further quenching of the first positive emission by large Br_2 flows suggests a rate constant near $10^{-11} cm^3 s^{-1}$ for these processes in our apparatus. Rapid nitrogen atom-molecular halogen reactions have also been reported from molecular beam experiments. Reference 39 finds relatively large cross sections for these processes, although the experiments were performed at high relative translational energies. Another possibility is that bromine atoms are produced by dissociation of BrN_3 or Br_2 in collisions with vibrationally excited N_2 present in the flow. Vibrationally excited N_2 is produced in the microwave discharge and by N atom recombination downstream. As noted, this species would have to be

present at a density on the order of $10^{12} cm^{-3}$ and dissociate Br_2 or BrN_3 with a rate constant near $10^{-11} cm^3 s^{-1}$ in order to account for the experimental observations.

In any case, the primary conclusion to be drawn from these data is that the efficient production of N_2 first positive emission in the BrN_3+ active nitrogen system is based on the $N + N_3$ reaction, just as in the $F/N/HN_3$ system discussed previously. The N_3 radical appears to be a primary source of excited N_2 in azide systems, and optimizing these systems for laser applications may well center on optimizing the chemical environment for production of these radicals.

3. $N_2(A^3 \Sigma_u^+)$ Quenching by Molecular Azides

Rate-constants for quenching of $N_2(A^3 \Sigma_u^+)$ metastables by collisions with various species were determined by using a discharge-flow apparatus in which the N_2 metastables were produced by energy transfer from $Ar(^3P_{0,2})$ metastables, which were generated by passage of argon through a low-current dc discharge. The discharge zone was located in a sidearm of the flow reactor, which was a 2.54 cm id Pyrex tube pumped by a 500 $\ell\, m^{-1}$ mechanical pump. Relative densities of the N_2 metastables at a fixed observation port downstream of the discharge zone were determined by using the NO tracer method. (Ref. 1) Small quantities of NO were added to the gas stream at the position of the observation port, such that the intensity of the resultant NO γ band emission (produced by energy transfer from $N_2(A)$) varied linearly with the $N_2(A)$ density. The NO emission was detected by a solar blind photomultiplier tube which viewed the emission through a bandpass filter with transmission centered at 240 nm. Quenching species were added to the flow through a movable sliding injector.

The Reynolds number for conditions typical of our experiments was approximately 39, suggesting that the time required for development of a parabolic $N_2(A)$ flow profile (an effect related to loss of $N_2(A)$ at the reactor walls) (Ref. 40) was comparable to the time regime over which the decay measurements were made. Hence, multiplication of the measured rate constants by a factor of 1.6 (as for a fully-developed parabolic flow) was inappropriate in the present case. Instead, a factor of 1.3 was used to account for the deviation from plug flow. Application of this factor to the intermediate case has been discussed in Reference 41. The apparatus was tested by measurement of rate constants for $N_2(A)$ quenching by O_2 and N_2O. The values obtained ($^{k}O_2$ = 2.9 ± 0.7 X $10^{-12}cm^3s^{-1}$ and $^{k}N_2O$ = 7.2 ±1.8 X $10^{-12}cm^3s^{-1}$) are in good agreement with values previously reported in (References 1 and 42).

Gaseous ClN_3 and HN_3 were produced and analyzed by using methods described previously (Ref. 2). These azides were admitted to the flow of $N_2(A)$ metastables upstream of the observation port through the sliding injector. The time decay of the $N_2(A)$ density was measured by varying the position of the azide injector for fixed azide flow rates. The measured decays were found to be exponential, the rates varying linearly with the azide flow. Figures 25 and 26 show plots of the $N_2(A)$ decay rate versus the densities of ClN_3 and HN_3, respectively. The slopes yield rate constants $^{k}ClN_3$ = 6.2 ±0.4 X $10^{-11}cm^3s^{-1}$ and $^{k}HN_3$ = 7.3± 2 X $10^{-11}cm^3s^{-1}$, respectively, where the uncertainties represent 1 σ.

The similar magnitudes of $^{k}ClN_3$ and $^{k}HN_3$ suggests that a common mechanism is operative. For HN_3, this mechanism is well-known. The $N_2(A)$ excites HN_3 to a repulsive triplet state (by a spin-allowed energy transfer process) which dissociates to excited $NH(A^3\Pi)$ and ground state N_2

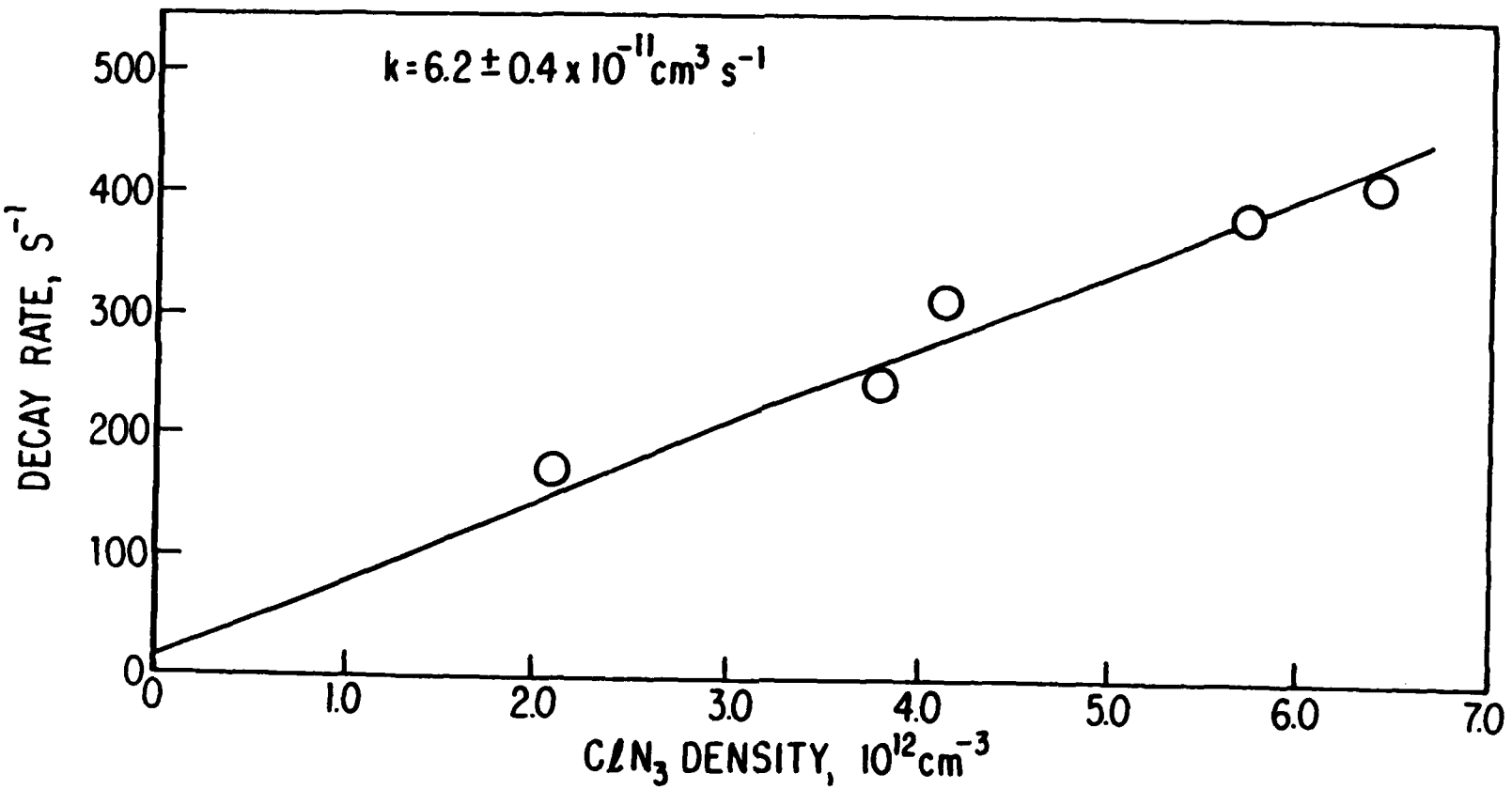

Figure 25. Rate of exponential decay of the density of $N_2(A)$ versus the density of ClN_3. The rate constant shown is obtained from the slope of the least squares fit.

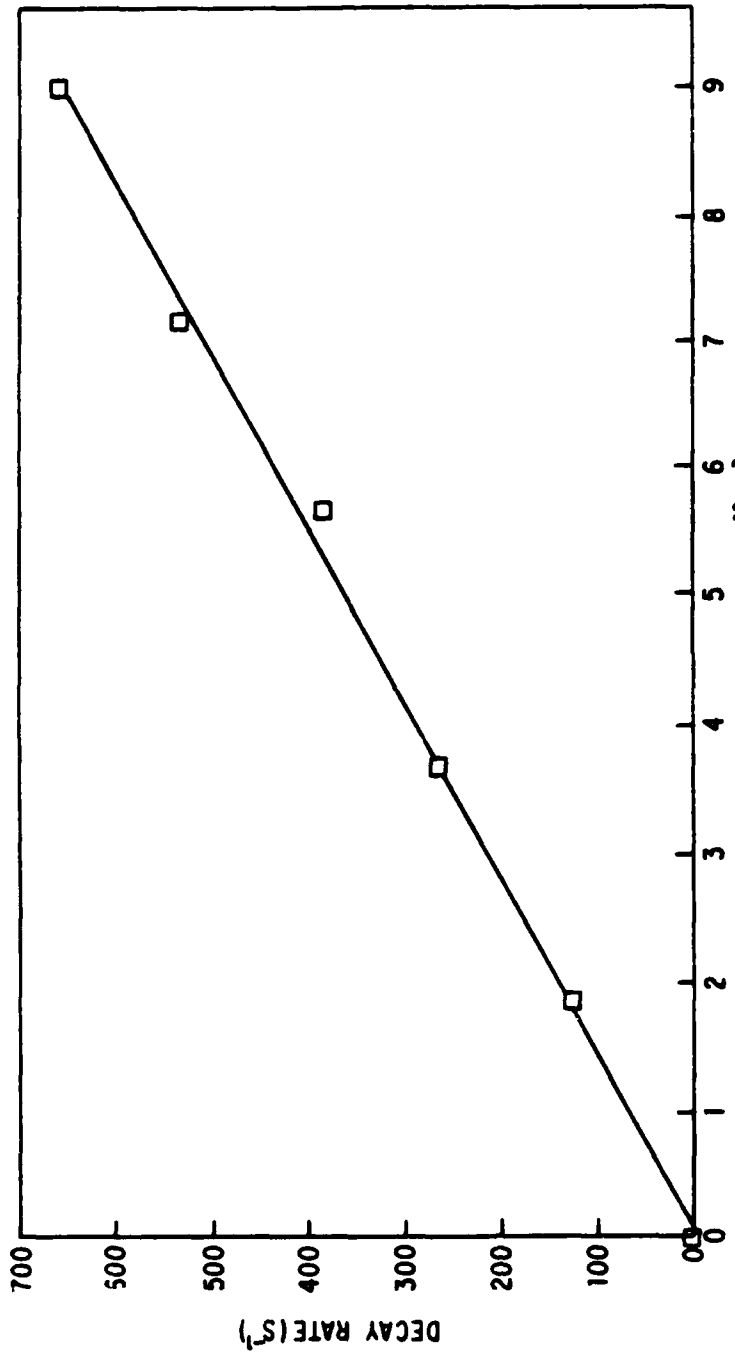

Figure 26. Rate of exponential decay of the density of $N_2(A)$ versus the density of HN_3. The slope of the least squares fit yields a rate constant $k = 7.3 \pm 0.2 \times 10^{-11}$ $cm^3 s^{-1}$.

(Ref. 22). Intense NH $A^3\Pi \rightarrow X^3\Sigma^-$ emission is observed as a result of this process. In contrast, a thorough spectral search of the UV-visible region revealed no observable emission produced as a result of the $N_2(A)$-ClN_3 interaction. Hence, it seems likely that excited triplet states of NCl produced as a result of this interaction may well be repulsive, such that the dissociation fragments are Cl + N + N_2. This contention is supported by recent ab initio calculations of the potential energy curves of excited electronic states of NCl (Ref. 43).

As with ClN_3 and HN_3, admission of BrN_3 to a flowing stream of $N_2(A^3\Sigma_u^+)$ metastables, the latter at a density of the order of $10^9 cm^{-3}$, produced no visible emission detectable by eye. The time decay of the $N_2(A)$ in the presence of large excess flows of BrN_3 was measured by using the NO tracer method (Ref. 1). Two components were readily evident in the decay (Fig. 27). An initial rapid decay is followed by a slowly decaying component of considerable intensity. This behavior is similar to that observed for the time decay of $N_2(A)$ produced by the photodissociation of ClN_3 (Ref. 44). In that case, the initial decay was assigned to $N_2(A)$ quenching by the parent azide and the slow component was thought to correspond to regeneration of the excited N_2 by a chain process. By analogy, it is expected that the initial decay evident in Figure 27 corresponds to $N_2(A)$ quenching by BrN_3. Determination of a rate constant for this process from the observed decay is complicated by the presence of a substantial Br_2 impurity in the BrN_3 reagent stream. This impurity arises from the finite efficiency of the BrN_3 generator and from decomposition of the azide during transport. Hence, a series of separate experiments were performed to measure the rate constant for $N_2(A)$ quenching by Br_2. This rate constant was determined by measurement of the decay of

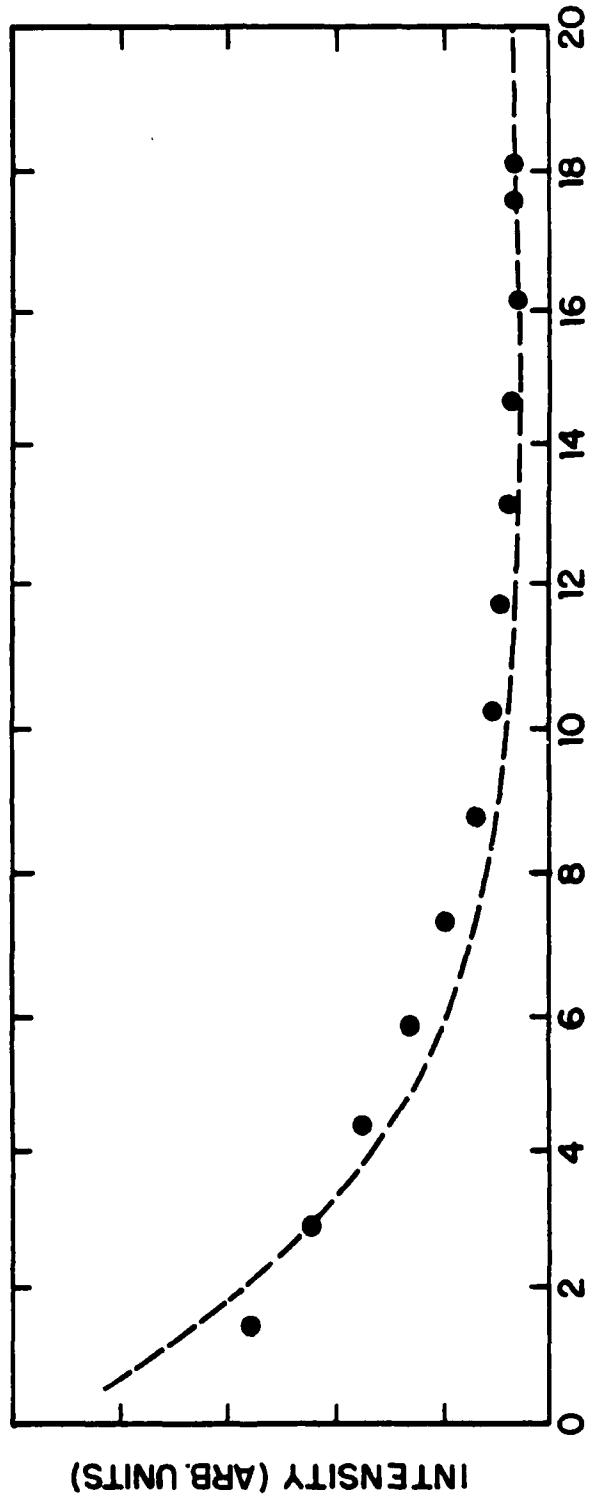

Figure 27. Time decay of $N_2(A)$ in the presence of an excess flow of BrN_3.

the initial $N_2(A)$ density in the presence of various added flows of a Br_2/He mixture. In these experiments, the $N_2(A)$ decay was exponential in every case (i.e., no long tail was observed as in Fig. 27). A plot of the decay rate versus the Br_2 density yielded a rate constant $k = 1.0 \pm 0.2 \times 10^{-10} cm^3 s^{-1}$, in reasonable agreement with a value recently reported in Reference 45, $k = 1.2 \pm 0.2 \times 10^{-10} cm^3 s^{-1}$.

For experiments in which the rapid component of the $N_2(A)$ decay in the presence of BrN_3/Br_2 was observed, the data were correlated to a rate expression

$$\lambda = \text{decay rate} = k'[BrN_3] + k[Br_2] \qquad (39)$$

where λ represents the rate of the initial rapid decay as in Figure 27. The BrN_3 density was determined by on-line measurement of the UV and IR absorption spectra of the generator effluent. The Br_2 density was determined from the difference between Br_2 flow entering the generator and the BrN_3 flow. If it is assumed that quenching by the azide is negligible (i.e., k' is small as reported previously from BrN_3 photolysis experiments), then Eq. 39 reduces to $\lambda = k[Br_2]$. A plot of λ versus $[Br_2]$ exhibits a strong linear correlation (as expected), but its slope yields a value $k = 1.5 \times 10^{-10} cm^3 s^{-1}$, considerably larger than the value determined from direct measurements. Hence, a significant portion of the rapid decay is attributable to $N_2(A)$ quenching by BrN_3. The apparent value of k', the rate constant for this process, was determined from a plot of $(\lambda - k'[Br_2])$ versus $[BrN_3]$ as shown in Figure 28. For this treatment, the value of k was taken to be $1.0 \times 10^{-10} cm^3 s^{-1}$. Although the data exhibit considerable scatter (reflecting the deconvolution procedure), a linear correlation is apparent. The slope of a least-squares line drawn through

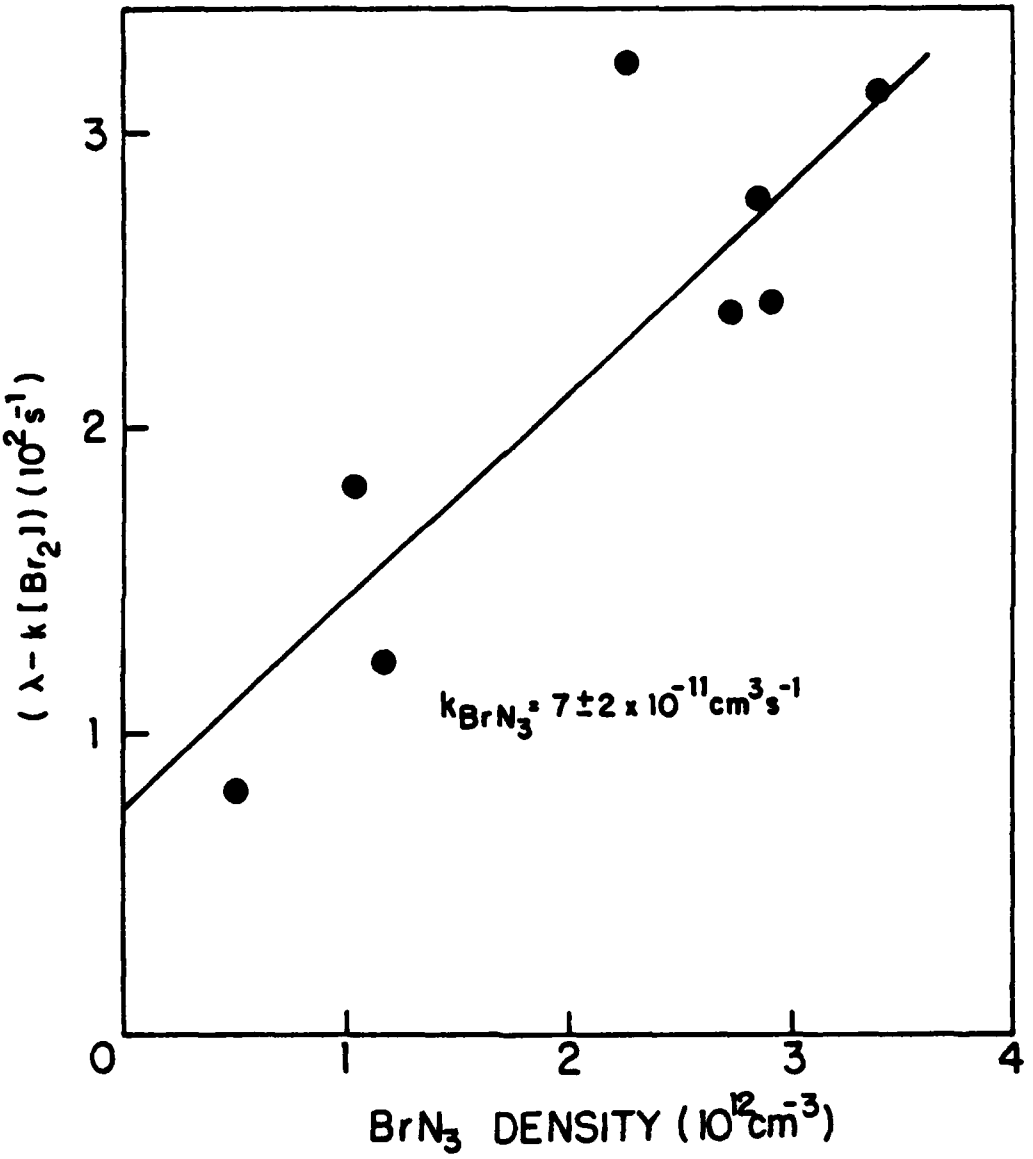

Figure 28. A plot of λ -k[Br_2] versus the density of BrN_3, where λ is the measured $N_2(A)$ decay rate and k is the rate constant for $N_2(A)$ quenching by Br_2, 1.0 X $10^{-10} cm^3 s^{-1}$.

the data yields a value $k' = 7 \pm 2 \times 10^{-11} cm^3 s^{-1}$, very similar to rate constants noted for $N_2(A)$ quenching by collisions with ClN_3 and HN_3.

This information has been used to reinterpret data obtained from the first experiments on the photodissociation of BrN_3, performed some years ago (Ref. 3). In brief, photolysis of BrN_3 at 222 nm produced N_2 $B \rightarrow X$ emission which decayed over about 200 μs, indicating collisional formation of $N_2(B)$. At the time, it was postulated that $N_2(B)$ arose from an upconversion in which $N_2(A)$ collided with the metastable BrN_3, dissociating it to $N_2(B) + NBr(X)$. From the variation of the time decay with the BrN_3 density, a rate constant $k = 1.2 \times 10^{-12} cm^3 s^{-1}$ was assigned to this process. The present data show that $N_2(A)$ is quenched by BrN_3 with a rate constant $k' = 7 \pm 2 \times 10^{-11} cm^3 s^{-1}$, indicating the previous interpretation of the photolysis results to be incorrect. The previous experiments did show the production of $N_2(A)$ as an initial photoproduct. From the present data, this $N_2(A)$ density will be quenched by the parent BrN_3 (at a density near $5 \times 10^{15} cm^{-3}$) in about 3 μs, generating Br and N atoms. The Br atoms would be removed by BrN_3 in about 6 μs, producing N_3. Hence, it seems that the long decay of the N_2 $B \rightarrow A$ emission in this system must represent its rate of production by the subsequent $N + N_3$ reaction. From the original data for the decay rate versus the BrN_3 density, the initial yield of $N_2(A)$ can be calculated, assuming that one $N_2(A)$ metastable produces one N atom to react with whatever N_3 is present. This treatment indicates an $N_2(A)$ yield of 21 percent from photolysis of BrN_3 at 222 nm. This value is in excellent agreement with that reported in Reference 46 for 193 nm photolysis of FN_3, a species whose stability (heat of formation) is roughly equivalent to that of BrN_3 (Ref. 47).

VI. Chemical Generation of Excited IF($B^3\Pi_o^+$)

In the Introduction, it was noted that an acceptable chemical scheme for producing useful densities of $N_2(A)$ metastables must be sufficiently rapid to compete with energy loss from the collisional $N_2(ABW)$ pool. A correlary to this hypothesis is that the chemical pumping scheme must be compatible with the desired energy transfer process between the $N_2(A)$ metastables and the laser candidate species (NO, IF, or other interhalogens, SO, etc.). Since this process must also compete with energy loss from the $N_2(ABW)$ pool, it is likely that the laser candidate must be present in the reactant mixture in which $N_2(A)$ is generated.

These data would seem to indicate that the $N(^4S_u) + N_3(^2\Pi_g)$ reaction is an acceptable chemical source of triplet $N_2(A)$ metastables. Hence, a number of experiments were performed which addressed the coupling of this scheme to actual laser candidate molecules, in particular IF. This molecule is a species which has spectroscopic characteristics appropriate for supporting lasing in the visible, as has been shown by the demonstration of both pulsed and CW optically pumped lasers operating on the $B^3\Pi_o^+ \rightarrow X^1\Sigma^+$ transition of this molecule (Refs. 48 and 49). Reference 50 shows that IF is efficiently pumped to its B state by collisions with $N_2(A)$.

$$IF(X^1\Sigma^+) + N_2(A^3\Sigma_u^+) \rightarrow IF(B^3\Pi_o^+) + N_2(X^1\Sigma_g^+) \qquad (40)$$

The rate constant of this process is reported to be $2 \times 10^{-10} cm^3 s^{-1}$, and the yield of IF(B) is near 50 percent. In principle, reaction 40 can be readily coupled to the $N + N_3$ system since both N_3 radicals and IF are typically produced by reactions of fluorine atoms. As noted, azide

radicals are rapidly produced by the F + HN_3 reaction, and IF can be produced, for example, by F + CF_3I:

$$F + CF_3I \rightarrow IF + CF_3 \qquad (41)$$

Reaction 41 has a rate constant (Ref. 51) $k_{41} = 1.6 \times 10^{-10} cm^3 s^{-1}$. Hence, excited IF should be produced by mixing F atoms, N atoms, HN_3, and CF_3I in a continuous flow. Alternatively, this process might be operated in a pulsed mode by pulsed production of F atoms in a premixed stream of N atoms, HN_3, and CF_3I. In this section, experiments are described in which this chemical mechanism was operated in both continuous and pulsed modes. The results indicate the potential utility of this system as a chemical laser.

1. Continuous Generation of Excited IF.

The chemical system desired is described by the simultaneous operation of the following four reactions:

$$F + HN_3 \rightarrow HF + N_3 \qquad (8)$$

$$N + N_3 \rightarrow N_2(B) + N_2 \qquad (7)$$

$$N_2(B) \rightarrow N_2(A) + h\nu \qquad (20)$$

$$N_2(A) + IF(X) \rightarrow IF(B) + N_2(X) \qquad (40)$$

To generate this medium, HN_3 and CF_3I must be admitted to a flow containing both nitrogen and fluorine atoms. The Teflon discharge-flow apparatus described previously and shown in Figure 4 was used for this purpose. The F atoms were produced by passage of either CF_4/Ar or F_2/Ar mixtures through a microwave discharge. Nitrogen atoms were generated by a microwave discharge through N_2. The N_2 discharge was on the upstream end of one of the movable inlets, such that N atoms entered the flow well downstream of the F atoms. The F and N atom densities were determined by standard

chemiluminescent titrations (Refs. 19 and 20) and were both typically on the order of $10^{13}cm^{-3}$. Under these conditions, the familiar yellow-orange N_2 afterglow was readily visible downstream of the N atom orifice. Admission of HN_3 to this flow (at an initial density on the order of $10^{13}cm^{-3}$), about 2 cm downstream of the N atom orifice, produced a bright orange N_2 first positive ($B^3\Pi_g \rightarrow A^3\Sigma_u^+$) flame about two orders of magnitude more intense than the nitrogen afterglow. This result has been observed in previous experiments and is indicative of the operation of reactions 8, 7, and 20. To generate excited IF, a metered flow of CF_3I was premixed with the HN_3 flow such that both species entered the F/N/Ar stream through the same inlet. The initial density of CF_3I was on the order of $10^{13}cm^{-3}$. The addition of CF_3I dramatically changed the visual appearance of the flame, from bright orange to a more diffuse yellow-green. The spectrum of the yellow-green flame is shown in Figure 29, and is readily identified as bands of the IF $B \rightarrow X$ transition. Although some N_2 first positive emission (particularly the $\Delta v = 2$ sequence) was still evident at longer wavelengths, the intensity of individual IF bands was much greater than that of the N_2 features. By comparison of the total intensity of the IF emission (integrated from the recorded spectrum) to the total intensity of the nitrogen first positive emission produced with no CF_3I flow, it was determined that the total IF $B \rightarrow X$ intensity was $\approx$25% of the original N_2 intensity. The N_2 intensity was corrected for the portion emitted in the IR beyond the cut-off of the detection system (~50% of the total). In view of the possibility of efficient loss of $N_2(A)$ by collisions with other species and the reactor walls, this substantial fraction testifies to the efficiency of the $N_2(A)$-IF energy transfer process in this system.

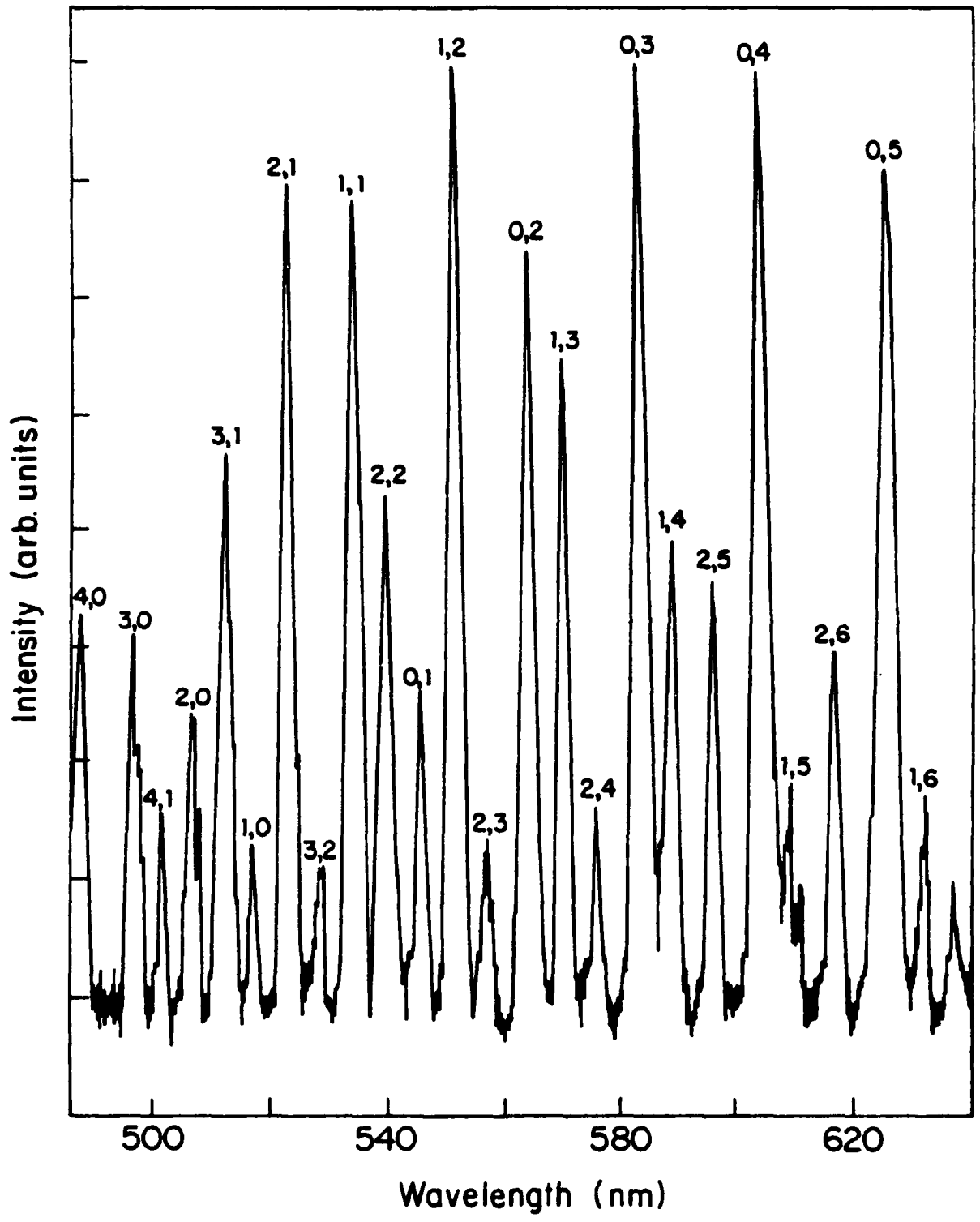

Figure 29. A portion of the spectrum of visible emission produced when CF_3I is added to the $F/N/HN_3$ reaction medium. IF B-->X bands are labeled.

Some IF emission was observed with no flow of HN_3, i.e., when CF_3I was added to a stream of F and N atoms such that only reaction 41 might occur. In this case, the N_2 metastables which pump the IF are produced by N atom recombination. The overall intensity of this emission was more than an order of magnitude smaller than that produced with a flow of HN_3, in agreement with previous estimates of the relative density of $N_2(A)$ produced by a discharge versus that produced by reactions 7 and 20 under conditions similar to those of the present experiments.

2. Pulsed Generation of Excited IF

The azide-IF reaction mechanism can be initiated by the introduction of fluorine atoms into a system containing HN_3, CF_3I, and N atoms. Since the latter three species can be premixed without appreciable reaction, the mechanism can be operated in a pulse by inclusion of an inert species from which F atoms can be generated by some pulsed means such as photolysis. Both CF_3I and HN_3 are strong absorbers in the UV such that UV photolysis of a fluorinated species would likely lead to complex chemistry. To avoid such complexity, IR multiphoton dissociation of SF_6 was used to produce fluorine atoms in the present experiments. The SF_6 is an effectively inert species which does not react with CF_3I, HN_3, or N atoms, and further, it is an inefficient quencher of IF(B) (Ref. 50). Neither HN_3 nor CF_3I have appreciable absorptions at 10.6 μm, the frequency used to dissociate SF_6 (Refs. 52 and 53).

The reactor used for pulsed experiments was made from 2.54 cm id Pyrex tubing and was 50 cm in length. It has one sidearm which was equipped with both a microwave discharge and a movable reagent inlet. The ends of this reactor were sealed with KCl windows to permit photolysis of the flowing gas stream. The linear velocity in this system was ~2000 cm s^{-1} for

pressures near 2.0 Torr. The pressures in both reactors were measured with capacitance manometers. As in continuous discharge-flow experiments, emissions from flames produced in the pulsed experiments were dispersed with a 0.25 m monochromator and detected by a cooled GaAs photomultiplier tube. Spectra of pulsed emissions were recorded with a gated integration system which has been described in Reference 54. Time profiles of the emissions were digitized and averaged by using a Nicolet 1270 data acquisition system. Both the Nicolet 1270 and the gated integrator (an SRS 235 system) were interfaced to an IBM PC microcomputer, which was used for data storage and handling.

The CO_2 laser used to produce the 10.6 μm pulse in the present experiments was a Lumonics 103 which routinely delivered ~8 J in an area of ~10 cm^2. The laser beam was focused into the center of the flow reactor with a BaF_2 lens which had a nominal focal length of 30 cm. Photolysis of a flowing mixture including SF_6, HN_3, and N atoms at densities 5 X 10^{14}, 1 X 10^{14}, and 7 X 10^{13} cm^{-3}, respectively, at a total pressure of 1.8 Torr produced a bright orange flame readily visible to the eye. The flame was produced along the entire pathlength of the laser beam in the reactor, although the fluence was < 3 J cm^{-2} over must of the path. The spectrum of this pulsed emission is shown in Figure 30, and is readily identified as bands of the N_2 first positive transition. The intensity distribution among the bands is quite similar to that observed from the continuous N + N_3 flame, as expected. A much less intense pulse of N_2 first positive emission was produced by pulsed photolysis of mixtures including SF_6 and N atoms only, i.e., when no HN_3 was present. This phenomenon appears to be similar to that observed in discharge-flow experiments, where addition of F

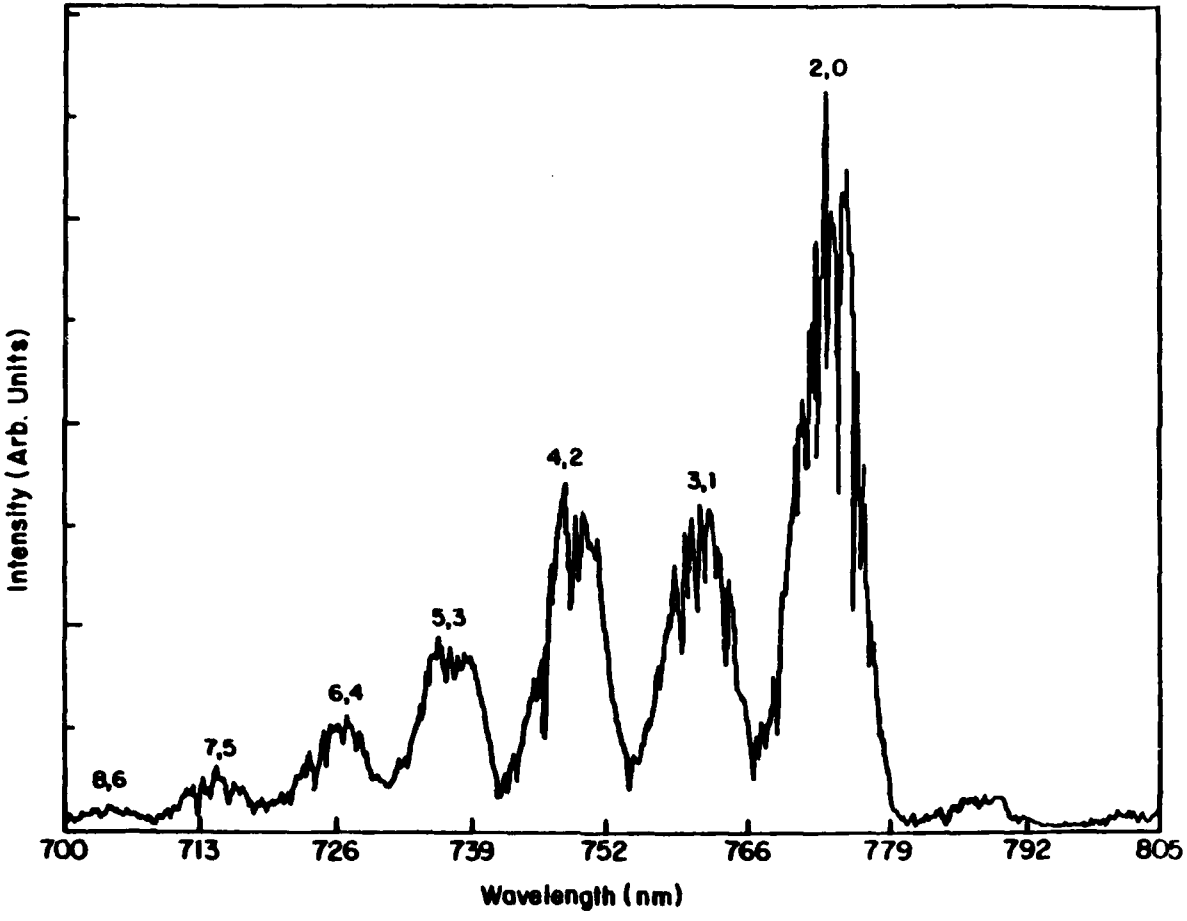

Figure 30. A portion of the spectrum of N_2 first positive emission produced by pulsed IR photolysis of $N/HN_3/SF_6/Ar$.

atoms to a stream of active nitrogen was found to substantially enhance the visible emission from the nitrogen afterglow.

The time profile of the pulsed N_2 emission exhibited a rise to a peak over a fraction of a ms followed by a slower decay over several milliseconds. A typical time profile is shown in Figure 31a. In principle, the rise and decay of the emission should reflect the rates of the $N + N_3$ and $F + HN_3$ reactions, or vice versa. In practice, physical processes such as longitudinal flow of the gas stream and radial diffusion of the emitting species can significantly contribute to the observed time profile under the conditions of our experiments. For example, Figure 31b shows an N_2 B→A time profile from an experiment where a much greater flow of SF_6 was used, resulting in a substantial increase in the total pressure. It was clear from such data that both the rise and decay times of the emission were proportionately shortened, suggesting that radial diffusion was slowed at the higher pressures. In this case, faster rates result from greater local densities of reagents. The rise and decay times in Figure 31 indicate that the densities of reagents (N and F atoms) in the reaction zone are $> 10^{13} cm^{-3}$, as expected from the flows of parent gases.

Addition of CF_3I to the $SF_6/N/HN_3$ stream produced a marked change in the pulsed emission. The orange N_2 flame was replaced by a yellow-green emission, which extended for 10 to 15 cm on either side of the focus of the laser beam. The spectrum of this emission is shown in Figure 32. The major features are readily identified as IF B→X bands, as indicated in the figure. Some N_2 first positive emission was apparent at longer wavelengths. When compared to the spectrum of continuous emission shown in Figure 29, it would appear that the pulsed IF emission is vibrationally colder, with most of the intensity in bands from $v' = 0$ or $v' = 1$. This

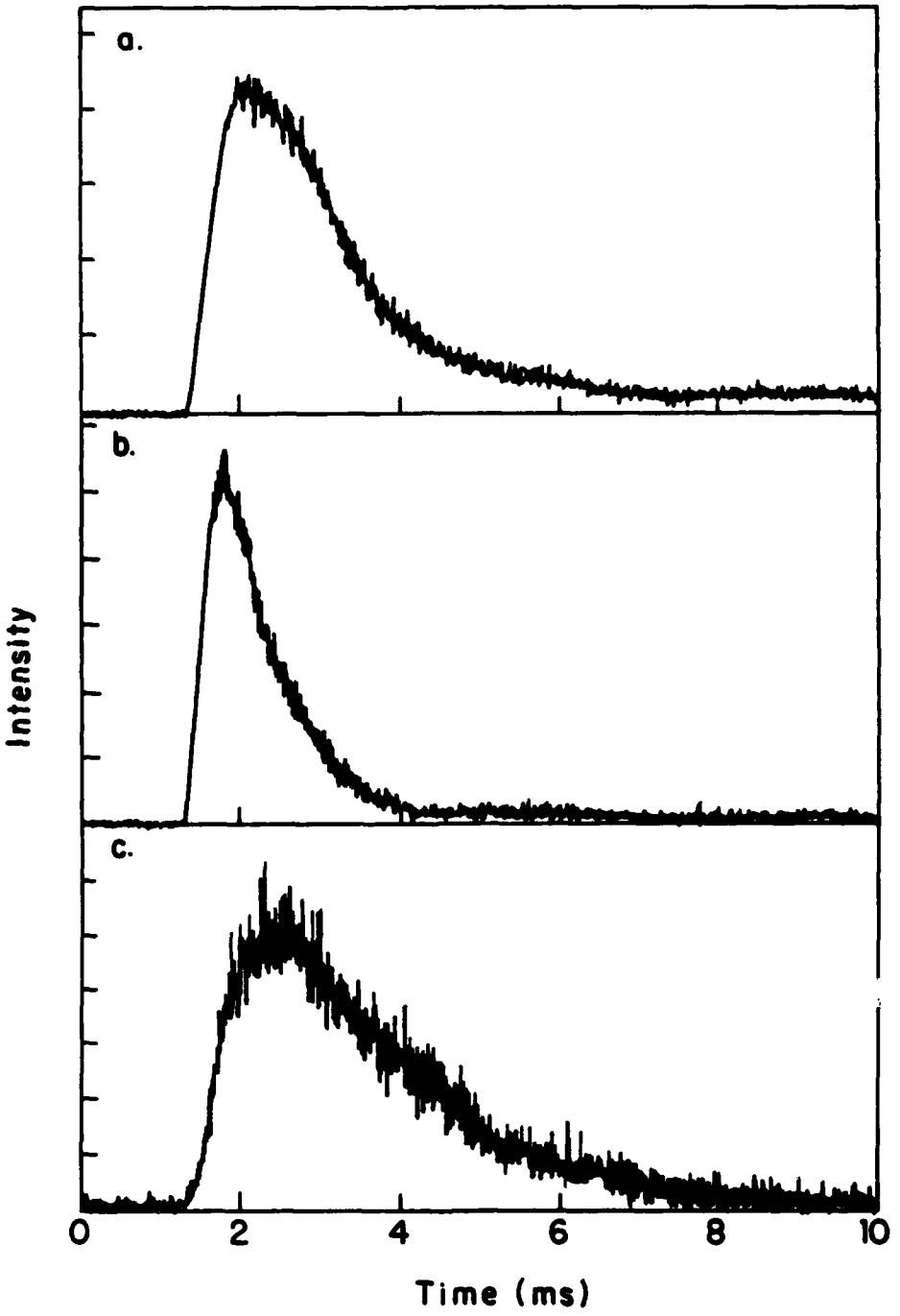

Figure 31. a. Time profile of pulsed N_2 B-->A emission from $N/HN_3/SF_6/Ar$ = 1/1.4/7.1/829 at 1.8 Torr. b. Time profile of pulsed N_2 B-->A emission from $N/HN_3/SF_6/Ar$ = 1/1.4/300/800 at 2.5 Torr. c. Time profile of pulsed IF B-->X emission from $N/CF_3I/HN_3/SF_6/Ar$ = 1/1.4/1.4/7.1/830 at 1.8 Torr.

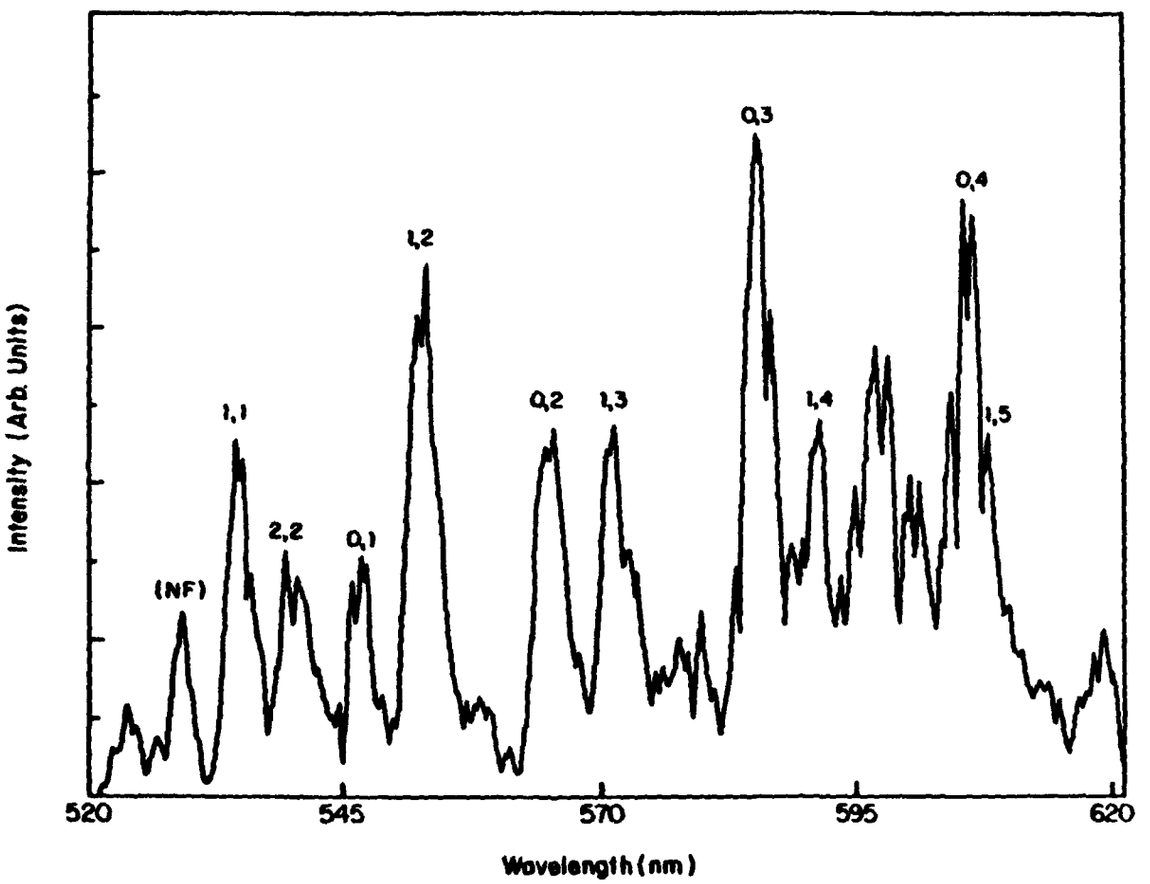

Figure 32. A portion of the spectrum of visible emission produced from pulsed IR photolysis of $N/CF_3I/HN_3/SF_6/Ar$. If B-->X bands are labeled.

result suggests the influence of collisional relaxation in the pulsed system, which was operated at a higher pressure (a considerable fraction of which was SF_6). The time profile of the IF emission is shown in Figure 31c. As expected, it follows the general pattern of the N_2 emission (Fig. 31a) but has a somewhat slower rise, since the production of IF is limited not by the N + N_3 rate, but by the rate of $N_2(A)$-IF energy transfer.

3. Attempted $N_2(A)$-IF Gain Measurement

These results serve to demonstrate the ready coupling of the azide mechanism for production of N_2 metastables to the IF B → X system. Observations of the optically pumped IF laser have estimated that a chemically pumped laser could be demonstrated if the pumping reaction could produce a density of IF(B) (in all vibrational levels) on the order of $10^{13} cm^{-3}$ (Ref. 49). The present data suggest that these levels might well be achieved by either CW or pulsed operation of the azide-IF mechanism. Figure 33 shows a calculation of the time evolution of IF(B) produced by reactions 8, 7, 40, and 41, including radiative decay of the excited IF at a rate $1.6 \times 10^5 s^{-1}$. The initial densities used in the calculation were F atoms ($3 \times 10^{15} cm^{-3}$), N atoms ($1 \times 10^{15} cm^{-3}$, CF_3I ($2 \times 10^{15} cm^{-3}$) and HN_3 ($2 \times 10^{14} cm^{-3}$). The intrinsic yield of excited N_2 ($N_2(A)$ and $N_2(B)$ were not distinguished) was taken to be 33 percent relative to HN_3. As shown in the figure, these conditions result in a maximum IF(B) density of $1.5 \times 10^{13} cm^{-3}$. In principle, larger IF(B) densities would result from larger initial HN_3 densities. Hence, it would seem that appropriate densities of excited IF might be produced from rather modest reagent flows. This result stems largely from the great speed of reactions 1 to 4, and the

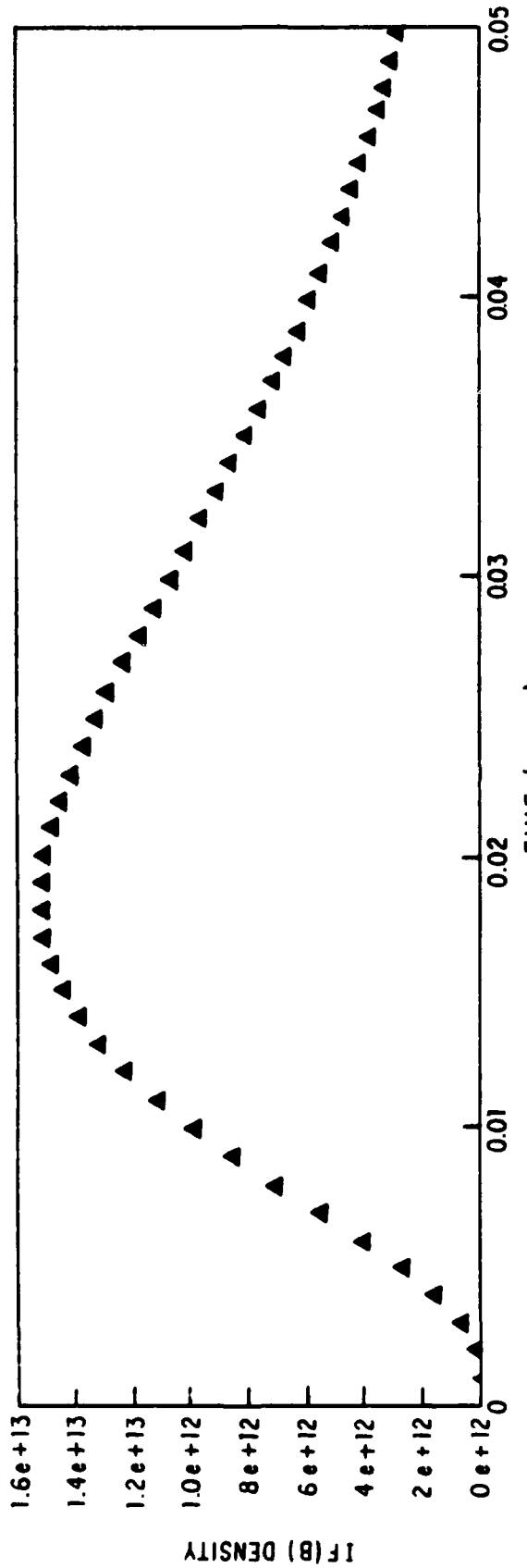

Figure 33. Calculated time evolution of the density of IF(B) produced in a reactive mixture of F atoms, N atoms, HN_3, and CF_3I.

high efficiency of reactions 3 and 4. For these same reasons, it is expected that second order processes such as quenching by reaction products or loss of N_2 metastables by energy pooling will have a minimal effect.

The gain experiment designed was one in which the pulsed IRMPD method for F atom production was used to produce N_2 metastables inside the cavity of an optically pumped IF laser. The IF laser was envisioned to be much like the pulsed device demonstrated previously (Ref.48). It was to be pumped by a Phase-R flashlamp-pumped dye laser and operated on collisionally populated lower v' levels of the $B_3\Pi_0^+$ state. Stimulated emission from these levels should occur after a delay of some microseconds from the dye laser pulse, the threshold time can be used as a sensitive measure of gain in the system.

The apparatus assembled for the gain experiment is shown in Figure 34. Our intention was to operate the IF laser in the same flow reactor used to generate the chemically pumped $N_2(A)$-IF system. This method has the advantage of lending insight as to how the individual elements of the chemical system (e.g., discharged N_2) may affect the IF population inversion. The IF was produced by reaction of CF_3I with fluorine atoms generated in a microwave discharge. Nitrogen atoms were produced in a second discharge through N_2/Ar as shown. The SF_6 and HN_3 entered the system through an injector positioned between the effluents of the two discharge sections, or, alternatively, through a rake injector which extended over the full length of the reactor. The chemical pulse of IF(B) was produced by off-axis pumping of the medium with 10.6 μm radiation from the Lumonics 103 pulsed CO_2 laser. A combination of reflective optics (gold coated) was

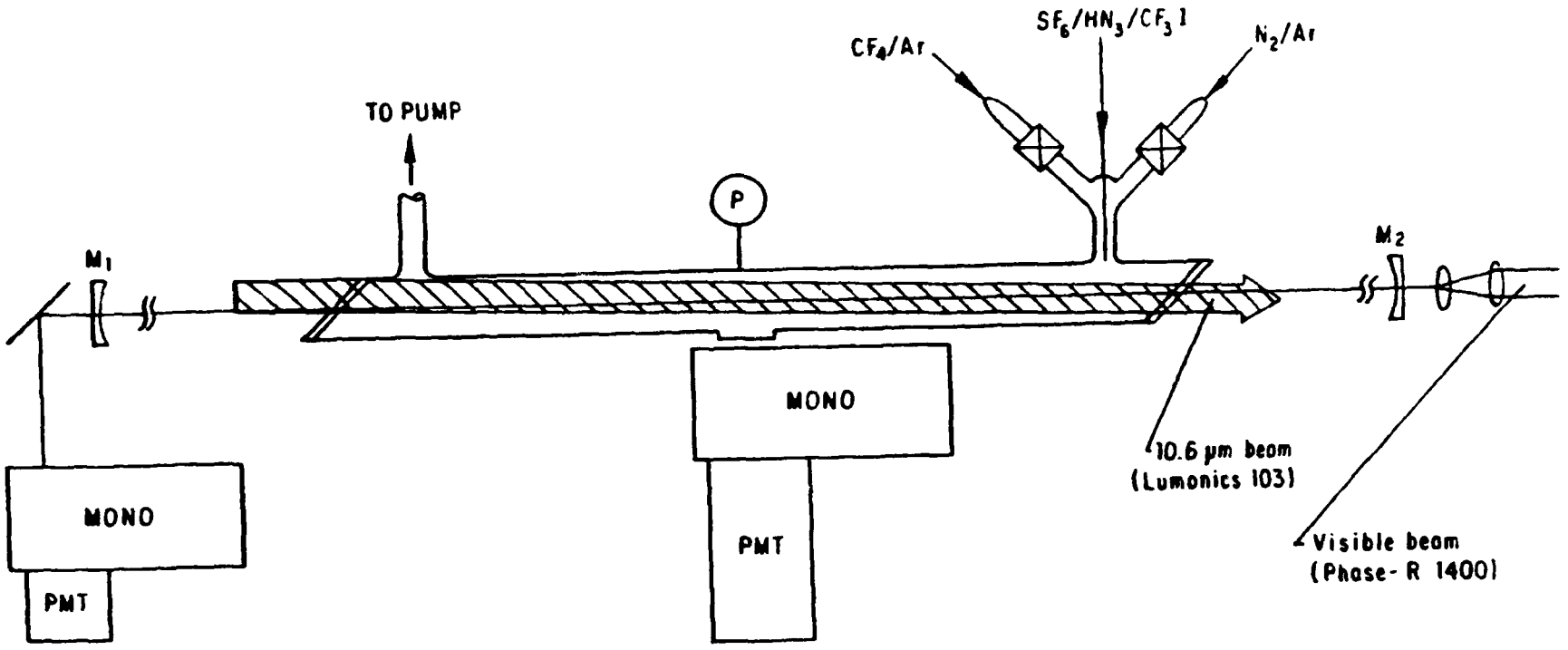

Figure 34. Apparatus to be used for gain determination in the $N_2(A)$-IF system.

used to condition the IR beam to produce a fluence in excess of 5 J/cm^2 over its pathlength in the reactor.

Although conceptually possible, actual gain experiments were never performed because of the failure to produce optically pumped IF B-X lasing under conditions appropriate for the chemical production of $N_2(A)$. The initial attempts at operating the optically pumped laser made use of the Phase-R 1200V dye laser. The laser was operated on Coumarin 504 dye and was tuned to the 3,0 band of the IF B→X transition near 496 nm with a grazing incidence grating. In later experiments, this laser was replaced by a Phase-R DL 1400 system which delivered considerably more output energy (up to ~75 mJ/pulse) and was tuned with a double prism assembly to give a broader-band output. In either case, bright IF B→X laser-induced fluorescence was readily obtained, but threshold operation of the system (with optics for the collisionally-pumped transitions) was not obtained for flow rates of F and CF_3I useful in the proposed gain experiment. To test the operation of the system and our technique, the system was easily lased on the B→X transition in I_2 vapor, with the dye laser tuned to I_2 transitions near 518 nm. The I_2 lasing was used to optimize alignment of the cavity mirrors. The IF lasing was still not observed from the $F+CF_3I$ system, however. Observation of the laser-induced fluorescence showed that its intensity continuously increased with the reagent flow rates. Indeed, it does seem likely that the flow rates (and hence IF density) were much smaller than those used in the lasers operated at AFWL, which used the F_2+I_2 reaction to produce IF. Hence, it was concluded that the conditions appropriate for operation of the chemically pumped IF system were not appropriate for optically pumped IF lasing, as the optically pumped system requires a large density of ground state IF. A dual reactor experiment

may, in fact, be more reasonable. In this case, the chemically pumped system would be operated in a separate reactor inside the cavity of the optically pumped IF laser, which would be based on $F_2 + I_2$ generation of IF.

VII. Interaction of Trifluorohalomethanes With Active Nitrogen

As part of the effort to couple the chemical generation of $N_2(A)$ by $N+N_3$ to collisional pumping of the IF molecule, a number of observations of the interaction of CF_3I (used to produce IF by reaction with fluorine atoms) with active nitrogen (used as a source of N atoms) were made. The rather unexpected results obtained led us to observe interactions between active nitrogen and the analogous species CF_3Br and CF_3Cl. Further, measurements of rate constants for the quenching of $N_2(A^3\Sigma_u^+)$ by collisions with CF_3I, CF_3Br, and CF_3Cl were made.

1. Chemiluminescence from CF_3X+ Active Nitrogen

Experiments in which CF_3X compounds were added to active nitrogen were performed with the Pyrex discharge flow apparatus. Active nitrogen was produced by N_2 diluted in argon through a microwave discharge located on one sidearm of the reactor. The CF_3X species were admitted to the flow via the movable injector.

Admission of a small flow of CF_3I to a flow of active nitrogen produced a bright yellow-green flame which extended down the full length of the flow reactor and into the pumping system. The spectrum of this flame is shown in Figure 35. All of the banded features shown in the spectrum are attributable to the $B^3\Pi_0^+ \rightarrow X^1\Sigma^+$ transition in IF. Emissions from vibrational levels as high as v' = 4 of the IF(B) state are evident. In view of the efficiency with which IF is pumped to its $B^3\Pi_0^+$ state by collisions with $N_2(A)$ metastables (Ref. 50), it is expected that this is the primary excitation mechanism operative in the system. Indeed, the slow production of $N_2(A)$ by N atom recombination in the active nitrogen flow

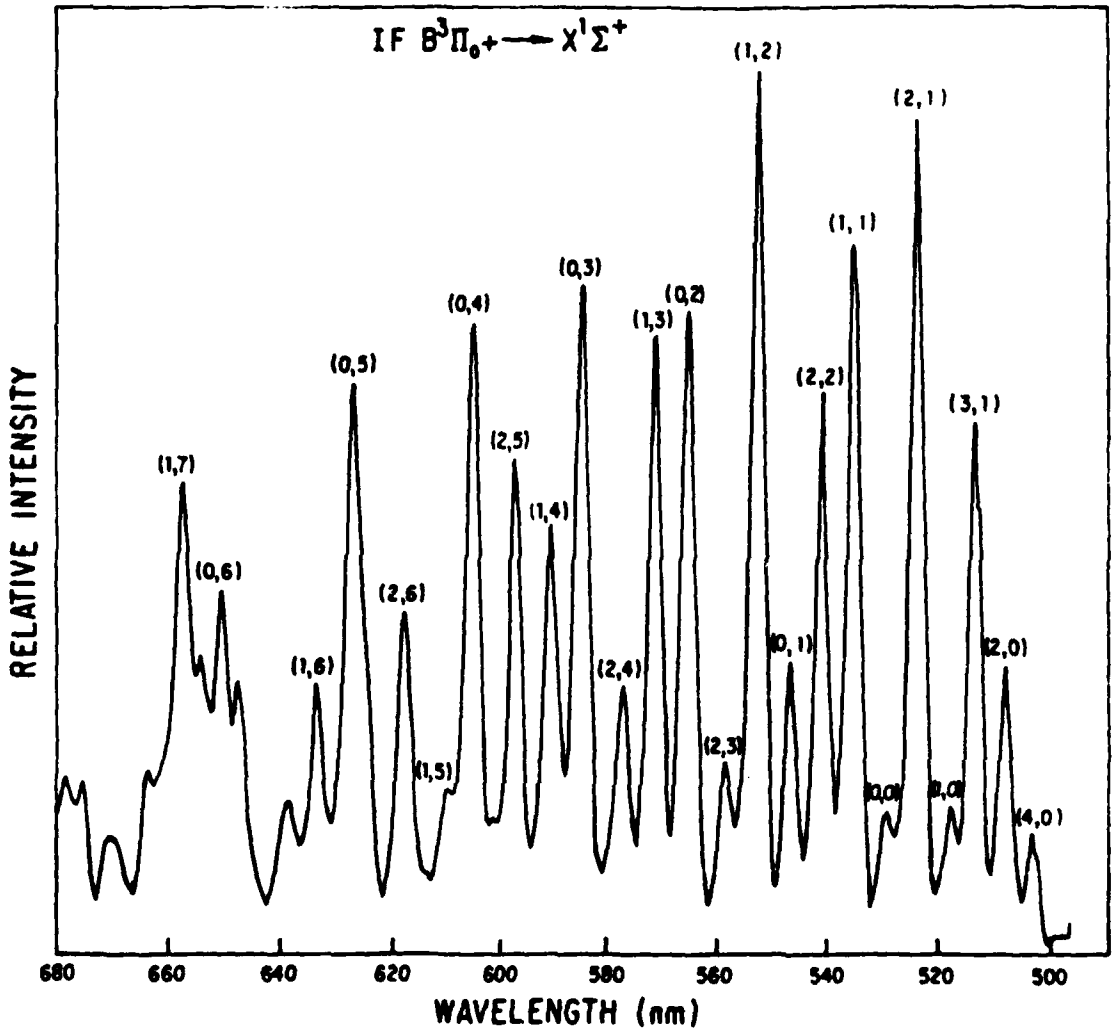

Figure 35. A portion of the spectrum of visible emission produced when CF_3I is added to active nitrogen. IF B-->X bands are labeled.

would account in part for the long duration of the IF flame. Since IF disproportionates rapidly (Ref. 55) on the Pyrex walls of the flow reactor, however, it seems likely that it must be continually produced during the time period of the flame. The primary issue is the mechanism by which IF is originally formed in the flow; presumably this mechanism involves interaction of CF_3I with excited species present in the active nitrogen. At least two collisional dissociation mechanisms are energetically feasible:

A. $N_2^* + CF_3I \rightarrow N_2(X) + CF_2 + I + F$ (42)

$F + CF_3I \rightarrow CF_3 + IF$ (41)

$IF + N_2^*(A) \rightarrow IF^*(B) + N_2(X)$ (40)

B. $N_2^* + CF_3I \rightarrow N_2(X) + CF_2 + IF(X)$ (43)

$IF(X) + N_2^*(A) \rightarrow IF^*(B) + N_2(X)$ (40)

where N_2^* represents a metastable excited species. The rate constants for reactions 41 and 40 are 1.6×10^{-10} and $1.0 \times 10^{-10} cm^3 s^{-1}$, respectively (Refs. 51 and 50). Mechanism B, in which IF is produced by collisional dissociation of CF_3I, was eliminated by an experiment in which H_2 was added to the flow to scavenge fluorine atoms. Admission of a flow of H_2 corresponding to a density of $5 \times 10^{13} cm^{-3}$ effectively titrated the IF flame, suggesting that this density of fluorine atoms is eventually produced by the dissociation of CF_3I (at an initial density of $2.5 \times 10^{14} cm^{-3}$) via mechanism A. Hence, it would appear that the dissociation to fluorine atoms (reaction 42) is a reasonably efficient process.

The choice of N_2 metastables (produced by N atom recombination) as the energy carrier responsible for the dissociation of CF_3I is based largely on the long duration of the flame, which argues against the action of excited

species created in the microwave discharge (e.g., $N(^2D)$ atoms). This point was specifically tested by an experiment in which a glass wool plug was inserted in the flow reactor downstream of the discharge zone, but upstream of the CF_3I injector. The plug, which should effectively remove $N(^2D)$ from the flow, had no observable effect on the production of the IF flame when CF_3I was admitted to the system.

It is well known that photolysis of CF_3I in the continium near 260 nm produces CF_3 radicals and excited $I(5^2P_{1/2})$ atoms (Ref.56). It is also known, however, that CF_3I photolysis in the region between 160 and 180 nm where the molecule has diffuse banded absorptions produces fluorine atoms (Ref.57). Hence, the present data suggest that reaction 42 may result from excitation of CF_3I to these same predissociated states ($\tilde{C}$ and $\tilde{D}$) by collisions with N_2* metastables. From the energies of these states (164 kcal $mole^{-1}$ for $\tilde{C}$ and 179 kcal $mole^{-1}$ for $\tilde{D}$), they cannot be accessed directly by collisions with vibrationally cold $N_2(A^3\Sigma_u^+)$ metastables. Hence, the energy carrier must be another metastable state produced by N atom recombination. Since CF_3I was present in the flow at densities on the order of $10^{14}cm^{-3}$, and the dissociation was reasonably efficient, we infer that the lifetime of the metastable energy carrier must be at least 100 μs. A number of excited states of N_2 satisfy both of these energy and lifetime criteria.

The admission of a flow of CF_3Br to a stream of active nitrogen produced a markedly different result. A bright red flame was generated in the mixing zone, extending for ~5 ms downstream. Figure 36 shows a spectrum of this emission, which is readily identified as NBr $b^1\Sigma^+ \rightarrow X^3\Sigma^-$ transitions. Downstream of the red emission, a dull yellow flame was found, extending down the length of the reactor. The spectrum of this

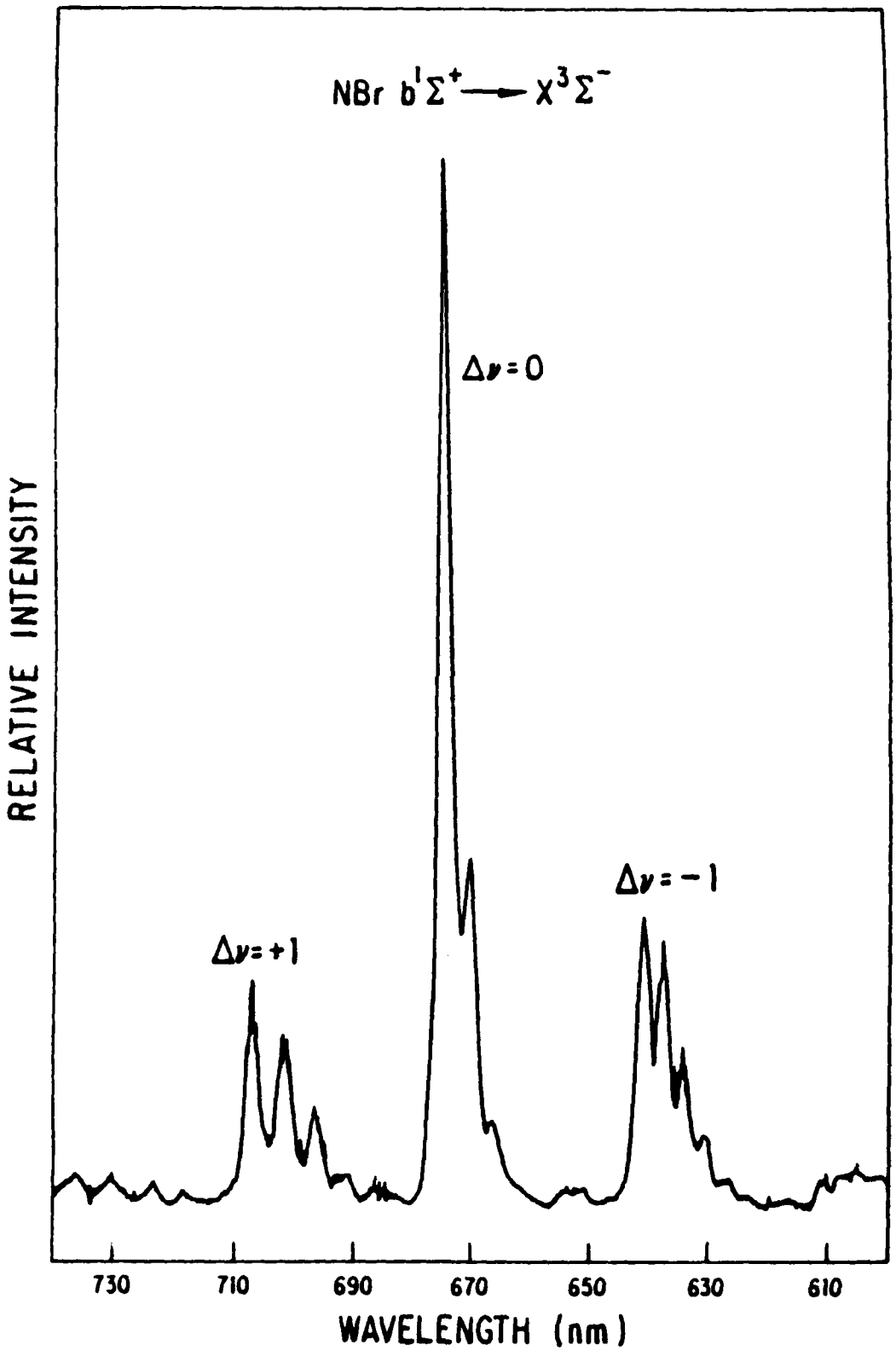

Figure 36. Spectrum of visible emission produced by admission of CF_3Br to active nitrogen. NBr b-->X sequences are labeled.

emission exhibited a regular series of bands, identified as the $A^2\Pi \rightarrow X^2\Sigma^+$ transition in CN.

These results for CF_3Br suggest a mechanism quite different from that postulated for the CF_3I case. In view of the short duration of the NBr $b \rightarrow X$ emission downstream of the discharge, an experiment with a glass wool plug (analogous to that previously described) was performed to ascertain the role of short-lived discharge products. With the plug in place, the NBr emission was completely quenched. This behavior suggests the following reaction as the source of excited NBr:

$$N(^2D) + CF_3Br \rightarrow NBr(b^1\Sigma^+) + CF_3 \qquad (43)$$

This reaction is feasible both energetically and from the point of view of angular momentum correlations, as $NBr(b^1\Sigma^+)$ correlates adiabatically to $N(^2D) + Br(^2P)$ (Ref.58). The absence of NI $b \rightarrow X$ emission when CF_3I was added to active nitrogen, along with the observation that the glass wool plug had no effect, argues that a reaction analogous to Eq. 43 is not important in that system. The CN emission has been observed from the addition of several different kinds of halomethanes to active nitrogen (Refs. 59 and 60). The mechanism in such cases is thought to involve initial formation of CN by reaction of $N(^2D)$ atoms with halomethyl or halomethylene radicals, followed by excitation to the $A^2\Pi$ state by collisions with N_2 metastables.

Admission of a flow of CF_3Cl to active nitrogen produced no new emission, nor did it perceptibly diminish the visible emission from the N_2 afterglow.

2. $N_2(A^3\Sigma_u^+)$ Quenching by CF_3X

Rate constants for quenching of $N_2(A)$ by CF_3I, CF_3Br, and CF_3Cl were measured with the apparatus and method described in Section V. In brief, $N_2(A)$ metastables were produced by energy transfer from $Ar(^3P_{0,2})$ metastables generated in a low current dc discharge, and were detected downstream by admission of NO to the flow. The CF_3X species (either pure or premixed with Ar) were added via a movable injector. The $N_2(A)$ decay was determined by measurement of the NO γ band intensity versus the position of the CF_3X injector, for various CF_3X flow rates. For the conditions of these experiments, the Reynolds number of the flowing gases was near 47, indicating that the time required for development of a parabolic $N_2(A)$ density profile was much smaller than the time frame of the measured decays. Hence, rate constants determined from these data were multiplied by a factor of 1.6 to account for the deviation from plug flow (Ref. 40.).

Argon (99.995%), CF_3I (99.8%), CF_3Br (99.7%), and CF_3Cl (99.7%) were obtained from commercial sources and were used without further purification.

For CF_3I and CF_3Br, the decay of the $N_2(A)$ density was measured as a function of time for a number of different pseudo-first order densities of these quenchers. Rate constants were determined from the slopes of plots of decay rate versus density. Quenching by CF_3Cl was found to be so slow as to preclude measurements of actual time decays, so the quenching rate constant was determined by using the fixed point method wherein the decline in the $N_2(A)$ density was measured for a single time interval Δt, for large flows of added CF_3Cl. Table I shows the measured quenching rates, along with the literature values (Ref. 50) for quenching by CF_4 and

CF_3I. CF_3Cl likely behaves much like CF_4; i.e., it acts only as a vibrational quencher of $N_2(A, v)$. The rate constants for quenching by CF_3I and CF_3Br are orders of magnitude greater than those for quenching by CF_3Cl and CF_4, indicating the accessibility of new channels for the energy transfer process. These channels are not likely to be those which produce fluorine atoms, but rather may be those which lead to dissociation to iodine or bromine atoms, respectively. No emission from IF, NBr, or CN was detected in the quenching experiments. The rate constants for $N_2(A)$ quenching by CH_3X species (X = halogen) have been measured (Ref.1). These values are approximately four times greater than those from the present work shown in Table I. The relative values of rate constants within the two series CH_3X and CF_3X are quite similar, however, suggesting analogous mechanisms.

Table I. $N_2(A^3\Sigma_u^+)$ Quenching by Trifluorohalomethanes

Quencher	Rate Constant (cm^3s^{-1})	Reference
CF_3I	$1.2 \pm 0.2 \times 10^{-10}$ 2.0×10^{-10}	This work (50)
CF_3Br	$5.0 \pm 0.8 \times 10^{-11}$	This work
CF_3Cl	5×10^{-14}	This work
CF_4	3×19^{-13}	(50)

The present data have shown that CF_3I, CF_3Br, and CF_3Cl each interact with active nitrogen in different ways. The production of fluorine atoms and excited IF in the CF_3I case may have relevance for the development of chemically pumped lasers operating on the $N_2(A)$-IF energy transfer mechanism. The CF_3I may be a special case in which the states responsible for dissociation to F atoms lie at energies accessible to energy transfer from metastable excited states of N_2 produced by atom recombination. These

states lie at considerably higher energies for CF_3Br and CF_3Cl, such that other mechanisms (e.g., reaction with $N(^2D)$ atoms as in Eq. 43) become dominant.

VIII. Conclusions

It has been suggested that the criteria for assessment of chemical sources of $N_2(A^3\Sigma_u^+)$ metastables for use in potential laser systems included (a) a rate competitive with energy loss from the $N_2(A,B,W)$ energy pool, and (b) compatibility of the chemical system with known laser candidates. From the data presented, it is clear that the $N(^4S) + NF(a^1\Delta)$ reaction does not meet the first of these criteria. The slow rate of this reaction likely results from the fact that the angular momentum constraints are strong, driving the reaction through a channel that requires nearly all of the energy released to be concentrated in electronic excitation of the product N_2.

On the other hand, the $N(^4S) + N_3(^2\Pi_g)$ reaction appears to be a good chemical source of N_2 metastables, from the point of view of both criteria. The reaction is controlled by both spin and orbital angular momentum correlations, and consequently produces excited $N_2(B,W)$ in high yield. The rate constant, $1.4 \times 10^{-10} cm^3 s^{-1}$, is such that the reaction competes well with both energy loss from the $N_2(A,B,W)$ pool and $N_2(A)$ quenching in collisions with N atoms. Further, $N + N_3$ appears to be quite compatible with known laser candidates such as NO, IF, and CN, as was demonstrated by both cw and pulsed pumping of IF(B) by $N_2(A)$ metastables generated from $N + N_3$. This compatibility is based largely on the facile generation of N_3 radicals by the $F + HN_3$ reaction, a process which has a near gas kinetic rate constant. The fluorine atoms used in this step can also be used for the generation of the laser candidate molecule, as was demonstrated in the IF experiments.

In summary, this program has succeeded in identifying and characterizing a chemical source of excited N_2 metastables useful for potential laser systems. The key issues to be addressed at present are related to scaling. These issues include the rates of deleterious second order processes which may remove N_3, and identification of an appropriate source of N atoms. Controlled dissociation of N_3 to N atoms may be the most straightforward approach to the latter problem.

REFERENCES

1. Clark, W. G., and D. W. Setser, J. Phys. Chem., 84, 2225 (1980).

2. Coombe, R. D., D. Patel, A. T. Pritt, Jr., and F. J. Wodarczyk, J. Chem. Phys., 75, 2177 (1981).

3. Coombe, R. D, J. Chem. Phys., 79, 254 (1983).

4. Deperasinska, I., J. A. Beswick, and A. Tramer, J. Chem. Phys., 71, 2477 (1979).

5. Nadler, I., and S. Rosenwaks, Chem. Phys. Lett., 69, 266 (1980).

6. Lofthus, A., and P. H. Krupenie, J. Phys. Chem. Ref. Data, 6, 288 (1977).

7. Hays, G. H., and H. J. Oksam, J. Chem. Phys., 59, 1507 (1973).

8. Nadler, I., D. W. Setser, and S. Rosenwaks, Chem. Phys. Lett., 72, 536 (1980).

9. Piper, L. G., unpublished results.

10. Sadeghi, N., and D. W. Setser, J. Chem. Phys., 79, 2710 (1983).

11. Walton, D. I., M. J. McEwan, and L. F. Phillips, Can. J. Chem., 43, 3095 (1965).

12. Phillips, L. F., Can. J. Chem., 46, 1429 (1968).

13. Coombe, R. D., A. T. Pritt, Jr., and D. Pilipovich, Electronic Transition Lasers, II (MIT Press, Wilson, Suchard, Steinfeld, Eds., 1977) pg. 107.

14. Clark, T. C., and M. A. A. Clyne, Trans. Faraday Soc., 66, 877 (1970).

15. Yamasaki, K., T. Fueno, and O. Kajimoto, Chem. Phys. Lett., 94, 425 (1983).

16. Shuler, K. E., J. Chem. Phys., 21, 624 (1953).

17. Douglas, A. E., and W. J. Jones, Can. J. Phys., 43, 2216 (1965).

18. Pritt, A. T., Jr., D. Patel, and R. D. Coombe, Int. J. Chem. Kinetics, 16, 977 (1984)

19. Ganguli, P. S., and M. Kaufman, Chem. Phys. Lett., 25, 221 (1974).

20. Clyne, M. A. A., Physical Chemistry of Fast Reactions, (Plenum Press, London, Levitt, ed.), 245.

21. Shemansky, D. E., and A. L. Broadfoot, J. Quant. Spectrosc. Rad. Trans., 11 1385 (1971).

22. Stedman, D. H., and D. W. Setser, Chem. Phys. Lett., 8, 542 (1968).

23. Meyer, J. A., D. W. Setser, and D. H. Stedman, J. Phys. Chem., 74, 2238 (1970).

24. Fontijn, A., C. B. Meyer, and H. I. Schiff, J. Chem. Phys., 40, 64 (1964).

25. Johnson, A. W., and R. G. Fowler, J. Chem. Phys., 53, 65 (1970).

26. Setser, D. W., D. H. Stedman, and J.A. Coxon, J. Chem. Phys., 53, 1004 (1970).

27. Coombe, R. D., and A. T. Pritt, Jr., Chem. Phys. Lett., 58, 606 (1978).

28. Pritt, A. T., Jr., and R. D. Coombe, Int. J. Chem. Kinetics, 12, 741 (1980).

29. Sloan, J. J., D. G. Watson, and J. S. Wright, Chem. Phys., 43, 1 (1979).

30. Clark, T. C., Thesis, Queen Mary College, London, 1969.

31. MacRobert, A. J., Thesis, Queen Mary College, London, 1981.

32. Piper, L. G., R. H. Krech, and R. L. Taylor, J. Chem. Phys., 71, 2099 (1979).

33. Jourdain, J. L., G. LeBras, G. Poulet, and J. Combourieu, Combust. Flame, 34, 13 (1979).

34. Coombe, R. D., D. Patel, A. T. Pritt, Jr., and F. J. Wodarczyk, Report No. AFWL-TR-81-211, Rockwell International Science Center, Thousand Oaks, CA, 1982.

35. Dyke, J. M., et.al., Mol. Phys., 47, 1231 (1982).

36. See, for example, Osgood, R. M., Jr., P. B. Sackett, and A. Javan, J. Chem. Phys., 60, 1446 (1974).

37. Grigor, M. R., and L. F. Phillips, Symp. Int. Combust. Proc., 11 1171 (1967).

38. Coombe, R. D., and C. H.-T. Lam, J. Chem. Phys., 80, 3106 (1984).

39. Love, R. M., J. M. Herrmann, R. W. Bickes, Jr., and R. B. Bernstein, J. Am. Chem. Soc., 99, 8316 (1977).

40. Fergusen, E. E, F. C. Fehsenfeld, and A. L. Schmeltekopf, Adv. At. Mol. Phys., 5, 1 (1969).

41. Piper, L. G., J. E. Valazco, and D. W. Setser, J. Chem. Phys., 74, 2888 (1981).

42. Piper, L. G., G. E. Caledonia, and J. P. Kennealy, J. Chem. Phys., 59, 3323 (1973).

43. Peyerimhoff, S. D., private communication.

44. Coombe, R. D., S. J. David, T. L. Henshaw, and D. J. May, Chem. Phys. Lett., 120, 433 (1985).

45. Cao, D.-Z, and D. W. Setser, Chem. Phys. Lett., 116, 363 (1985).

46. Patel, D., A. T. Pritt, Jr., and D. J. Benard, J. Phys. Chem., 90, 1931 (1986).

47. Coombe, R. D., and C. H.-T. Lam, J. Chem. Phys., 79, 3746 (1983).

48. Davis, S. J., L. Hanko, and R. F. Shea, J. Chem. Phys., 78, 172 (1983).

49. Davis, S. J., L. Hanko, and P. J. Wolf, J. Chem. Phys., 82, 4831 (1985).

50. Piper, L. G., W. J. Marinelli, W. T. Rawlins, and B. D. Green, J. Chem. Phys., 83, 5602 (1985).

51. Iyer, R. S., and F. S. Rowland, J. Phys. Chem., 85, 2493 (1981).

52. Sudbo, Aa. S., P. A. Schulz, E. R. Grant, Y. R. Shen, and Y. T. Lee, J. Chem. Phys., 68, 1306 (1978).

53. Hartford, A., Jr., Chem. Phys. Lett., 57, 352 (1978).

54. See, for example, MacDonald, M. A., S. J. David, and R. D. Coombe, J. Chem. Phys., 84, 5513 (1986).

55. Appelman, E. H., and M. A. A. Clyne, J. Chem. Soc. Faraday I, 71, 2072 (1975).

56. Sutcliffe, L. H., and A. D. Walsh, Trans. Faraday Soc., 57, 873 (1961).

57. Berry, M. J., Chem. Phys. Lett., 15, 269 (1972).

58. See, for example, Herbelin, J. M., Chem. Phys. Lett., 42, 367 (1976).

59. Thrush, B. A., and M. F. Golde, in Chemiluminescence and Bioluminescence (Plenum Press, New York, M. J. Cormier, D. M. Hercules, and J. Lee, eds., 1973).

60. Rabanos, V. Saez, F. Tabares, and A. Gonzalez Urena, J. Photochem., 18, 301 (1982).